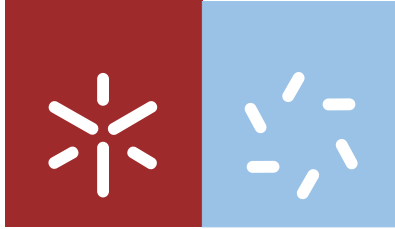


Universidade do Minho
Escola de Ciências

Fátima Alexandra Meira Machado

**Development of a Liposomal Formulation
for Peptide Delivery to Serve as Vaccine
against Chronic Myeloid Leukemia**



Universidade do Minho

Escola de Ciências

Fátima Alexandra Meira Machado

**Development of a Liposomal Formulation
for Peptide Delivery to Serve as Vaccine
against Chronic Myeloid Leukemia**

Mss Thesis

Master in Biophysics of Bionanosystems

Supervised by:

Prof. Doutora Maria Elisabete C. D. Real Oliveira

Prof. Doutora Andreia C. Gomes

Prof. Doutor Steffen Peterson

November 2013

DECLARAÇÃO

Nome: Fátima Alexandra Meira Machado

Endereço electrónico: pg19029@alunos.uminho.pt

Número do Bilhete de Identidade: 13441552

Título dissertação:

- Development of a liposome formulation for peptide delivery to serve as vaccine against chronic myeloid leukemia

Orientador(es): Professora Doutora Elisabete Oliveira,
Professora Doutora Andreia Gomes

Ano de conclusão: 2013

Designação do Mestrado: Mestrado em Biofísica e Bionanossistemas

É AUTORIZADA A REPRODUÇÃO INTEGRAL DESTA DISSERTAÇÃO APENAS PARA EFEITOS DE INVESTIGAÇÃO, MEDIANTE DECLARAÇÃO ESCRITA DO INTERESSADO, QUE A TAL SE COMPROMETE;

Universidade do Minho, ___/___/_____

Assinatura: _____

ACKNOWLEDGEMENTS

Agradeço a todos que de uma forma ou de outra colaboraram para a realização deste trabalho, em especial:

À Professora Doutora Maria Elisabete Real Oliveira e à Professora Doutora Andreia Gomes, pela orientação ao longo deste trabalho. Agradeço a constante disponibilidade, o incomensurável apoio e dedicação, a partilha de conhecimento e o estímulo transmitido durante a elaboração desta dissertação. Estou muito grata por me proporcionarem esta valiosa oportunidade de aprendizagem.

To Doctor Steffen Petersen and Doctor Teresa Petersen for sharing their knowledge. This was crucial for the elaboration of my thesis. Thank you for your interest and willingness to guide this work.

Ao João Neves, Artur Ribeiro e Raul Machado pela importante colaboração, pelas valiosas sugestões e muitos conhecimentos transmitidos durante a realização deste trabalho que permitiram ultrapassar muitos obstáculos. O seu apoio e boa vontade foram admiráveis. Um obrigado especial ao João Neves pelas imagens fornecidas para esta tese.

Aos meus colegas de laboratório pelo apoio constante, pelo seu espírito hospitaleiro, pela força e pela disponibilidade e grande paciência em ajudar no laboratório.

Aos colegas do Laboratório de Biologia Molecular, em especial ao André Costa, pela paciência e longos dias de apoio no laboratório, muito além do que o dever imporia.

Aos meus amigos e colegas que conheci neste longo percurso académico, Cátia Costa, Tiago Barbosa, Hugo Gonçalves e Juan Arroyo pelo enorme apoio, pelos momentos de descontração e entreajuda e por tornarem este percurso menos custoso.

Ao Rui Pinto, pela motivação, otimismo, elogios, ajuda e alegrias que me deu ao longo destes anos, e acima de tudo pela paciência nos momentos difíceis. Um grande obrigado por tudo.

Por último, mas não menos importante, à minha Mãe, ao meu Pai e à minha querida irmã por sempre terem acreditado que era possível chegar até aqui, e por estarem sempre ao meu lado. Por todo o amor, paciência e estrutura que sempre me proporcionaram não só durante este percurso, mas durante toda a minha vida. Não há palavras que possam expressar a minha gratidão.

(Page intentionally left blank)

ABSTRACT

The main goal of this work was to characterize and explore the potential of Dioctadecyldimethylammonium Chloride (DODAC) / Monoolein (MO) liposomes in a 1:2 proportion and identify the formulations that could be used in the development of an immunoprotective protocol for Chronic Myeloid Leukemia (CML).

CML has long been recognized as one of the most responsive leukemic disorder to immunotherapy. CML is potent model for immune therapy in humans because there is a specific gene rearrangement, BCR/ABL, which product, P210bcr/abl, can be the target antigen.

The loading of drugs into particles at the nanometer size range is a recognized technique for the optimization of controlled drug delivery. In its use in vaccines, liposomes have the advantage of being able to maintain antigens present in the organism for long enough to obtain an immune response.

Different methods of preparation and distinct peptide/lipid molar ratios were used to prepare P210bcr/abl / DODAC:MO (1:2) nanoparticles. This thesis describes results for biophysical characterization of the peptide/lipid system, encapsulation efficiency and exposure of THP-1 cells to the nanoparticles.

The lipid content was essential to achieve the desired nanoparticles. The highest lipid concentration showed higher encapsulation, however, a lower lipid content induced a more efficient cell response. The peptide/lipid system was capable of inducing a stronger cell response than the peptide by itself, emphasizing the potential of this system in vaccine development for the treatment of CML.

Key words: DODAC/MO (1:2), Chronic Myeloid Leukemia, BCR-ABL, vaccines.

(Page intentionally left blank)

RESUMO

O objetivo principal deste trabalho foi caracterizar e explorar o potencial dos lipossomas de cloreto de Dioctadecildimetilamónio (DODAC) / Monooleína (MO) numa proporção de 1:2 e identificar as formulações que poderão ser usadas no desenvolvimento de um tratamento imunoprotetor para a Leucemia Mieloide Crónica (LMC).

A LMC é desde há muito tempo conhecida como uma das desordens imunológicas mais responsivas à imunoterapia. A LMC é um poderoso modelo para imunoterapia em humanos devido à existência de um gene específico BCR/ABL, cujo produto, P210bcr/abl, pode ser usado como antígeno-alvo.

A incorporação de fármacos em partículas a uma escala nanométrica é uma técnica reconhecida para a optimização da entrega controlada de fármacos. No seu uso em vacinas, os lipossomas possuem a vantagem de ser capazes de manter os antígenos presentes no organismo o tempo suficiente para se obter uma resposta imune.

Diferentes métodos de preparação e várias razões molares de péptido/lípido foram usadas para preparar nanopartículas de P210bcr/abl / DODAC:MO(1:2). Esta tese descreve os resultados obtidos da caracterização biofísica do sistema péptido/lípido, eficiência de encapsulação e exposição das células THP-1 às nanopartículas.

O conteúdo lipídico foi essencial para obter nanopartículas desejáveis. A concentração mais alta de lípido demonstrou maior eficiência de encapsulação, no entanto, uma concentração de lípido mais baixa mostrou-se mais eficiente em induzir uma resposta por parte das células. O sistema péptido/lípido foi capaz de induzir uma resposta mais forte do que o péptido por si só, enfatizando o seu potencial no desenvolvimento de uma vacina para o tratamento da LMC.

Palavras-chave: DODAC/MO (1:2), Leucemia Mielóide Crónica, BCR/ABL, vacinas.

(Page intentionally left blank)

CONTENTS

LIST OF FIGURES	xi
LIST OF TABLES	xvii
SYMBOLS AND ABBREVIATIONS	xix
1. CHAPTER 1 BACKGROUND	1
1.1. Goals	1
1.2. Research motivation and contribution	1
1.3. Dissertation organization	2
2. CHAPTER 2 STATE OF THE ART	5
2.1. Liposomes	5
2.1.1. Particle Size.....	6
2.1.2. Liposome preparation.....	7
2.1.3. Liposome-based delivery systems.....	11
2.1.4. DODAC:MO-based liposomes	16
2.2. Chronic Myeloid Leukemia	19
2.2.1. Vaccination with BCR-ABL	20
2.2.2. The b2a2 breakpoint derived peptide	21
2.3. Liposomal vaccines.....	26
2.3.1. Role of adjuvants in vaccine development.....	30
3. CHAPTER 3 METHODOLOGIES	35
3.1. Materials	35
3.2. BCR-ABL peptide analyses.....	35
3.3. Nanoparticles preparation	36
3.3.1. Preparation of liposomes for hydration and injection method	37
3.3.2. Preparation of nanoparticles by post-insertion and direct-insertion.....	38
3.4. Biophysical Characterization	40
3.4.1. Dynamic Light Scattering assays	40
3.4.2. Zeta (ζ) Potential assays	42
3.4.3. Electrophoresis and Electrophoretic Mobility.....	44
3.4.4. Mean diameter and zeta potential measurements.....	45
3.5. Encapsulation Efficiency	46
3.6. Delivery of antigenic BCR-ABL junctional peptide	47
3.6.1. Cell Culture	48

3.6.2.	LPS Extraction assay	48
3.6.3.	LPS Activation assay	48
3.6.4.	Peptide and Peptide/DODAC:MO(1:2) Activation assay	49
3.6.5.	ELISA assay procedure	49
3.6.5.1.	Experimental work	50
4.	CHAPTER 4 RESULTS AND DISCUSSION.....	54
4.1.	Effect of pH, peptide concentration and sonication	55
4.2.	Incorporation of BCR_ABL peptide into DODAC:MO(1:2) liposomes	64
4.2.1.	Citrate-phosphate versus HEPES	64
4.2.2.	Incubation time	66
4.2.3.	Effect of the preparation methods on nanoparticles behavior in solution	68
4.2.4.	Effect of MLV liposomes and LUV liposomes in the final nanoparticle – Method A versus method E.	83
4.3.	Encapsulation efficiency	90
4.4.	Delivery of antigenic BCR-ABL junctional peptide	98
4.4.1.	Optimization of the control LPS Activation	98
4.4.2.	Peptide Activation assay	99
4.4.3.	Peptide/DODAC:MO(1:2) Activation assay	101
5.	CHAPTER 5 CONCLUSIONS AND FUTURE DIRECTION	108
5.1.	Conclusions	108
5.2.	Future work	110
	REFERENCES.....	113
	APPENDIX I	123
	APPENDIX II.....	127
	APPENDIX III	133

LIST OF FIGURES

Figure 2.1 – Representation of the steric organization of a liposome (up) and lipid bilayer (bottom) (adapted from (Bitounis, Fanciullino, Iliadis, & Ciccolini, 2012)).	5
Figure 2.2 – Liposomes classification based on size and lamellarity (Laouini et al., 2012).	7
Figure 2.3 – Different types of liposomes produced by ethanol injection, lipid film hydration and extrusion: Small Uni-lamellar Vesicles (SUV); Large Uni-lamellar Vesicles (LUV); Multi-vesicular Vesicles (MVV); Multi-lamellar Vesicles (MLV).	8
Figure 2.4 – Representation of MLV preparation by lipid hydration method (adapted from Lopes et al., 2013).	9
Figure 2.5 – Representation of the extrusion process (Zhua, Xueb, Guob, & Marchant, 2007).	11
Figure 2.6 – Multi-functions of liposomes as nanocarriers.	13
Figure 2.7 – Liposome-cell interaction processes.	14
Figure 2.8 – Membrane destabilization of liposomes and endosomes.	15
Figure 2.9 – Chemical structure of DODAC (Thiele, Merkle, & Walter, 2003).	17
Figure 2.10 – Chemical structure of monoolein (Kulkarni, Wachter, Iglesias-Salto, Engelskirchen, & Ahualli, 2011).	18
Figure 2.11 – Representation of CMLb2a2-25mer peptide: A – Chemical bonds are denoted for Carbon (grey), Nitrogen (blue), Oxygen (red) and Hydrogen (white); B – molecule's solvation area. The molecular properties of this peptide were attained by ChemBioOffice 13 program, developed by Cambridge Software.	22
Figure 2.12 – Amino acid structure (adapted from Hambly, 2013).	22
Figure 2.13 – Representation of the molecular mechanism of peptide-conjugated liposomes on cancer therapy (Wu & Chang, 2010).	29

Figure 3.1 – Representation of the different methodologies applied in this work to attach peptide molecules to lipid vesicles: A - Preparation of liposomes by lipid film hydration before adding peptide solution; B - Preparation of liposomes by lipid film hydration with peptide solution being added before lipid vesicles are formed; C - Preparation of liposomes by ethanolic injection before adding peptide solution; D - Preparation of liposomes by ethanolic injection hydration with peptide solution being added before lipid vesicles are formed. 38

Figure 3.2 – Schematic representation of methods: A (left), preparation of liposomes by lipid film hydration (1st) before adding peptide solution (2nd) followed by extrusion (3rd); and method E (right), preparation of liposomes by lipid film hydration (1st) followed by extrusion (2nd) before adding peptide solution (3rd)..... 39

Figure 3.3 – Optical configurations of the Zetasizer Nano series for dynamic light scattering measurements (Malvern, 2005)..... 42

Figure 3.4 – Schematic representation of the double layer surrounding a particle in suspension (Malvern, 2005). 43

Figure 3.5 – The technique used to measure this velocity in Malvern’s Zetasizer Nano series(Malvern, 2005). 45

Figure 3.6 – The ELISA technique illustrated (“Mabtech,” 2013)..... 50

Figure 4.1 – Results of weighted mean size (nm) (bars - left axis) and z-potential (mV) (—■— - right axis) for preparations of 10 µg/mL, 20 µg/mL and 40 µg/mL of BCR-ABL peptide, in citrate-phosphate buffer at pH=4, 7.2 and 9, before and after sonication..... 56

Figure 4.2 – Results of weighted mean size (nm) (bars - left axis) and z-potential (mV) (—■— - right axis) for preparations of 10 µg/mL, 20 µg/mL and 40 µg/mL of BCR-ABL peptide, in HEPES buffer and citrate-phosphate buffer at pH=7.2, before and after sonication. 62

Figure 4.3 – Photography of DODAC:MO (1:2) liposomes prepared by ethanolic injection in citrate-phosphate buffer at pH=9. 64

Figure 4.4 – At the left side are presented results of weighted mean size (nm) (bars - left axis) and z-potential (mV) (—■— - right axis) for lipid vesicles (control) and peptide/DODAC:MO nanoparticles prepared by method A at 1/500 molar ratio. At the right side are presented the distribution of intensity profiles of the respective mean size and z-potential. 66

Figure 4.5 – At the left side are presented results of weighted mean size (nm) (bars - left axis) and z-potential (mV) (—■— - right axis) for lipid vesicles (control) and peptide/DODAC:MO nanoparticles prepared by method C at 1/500 molar ratio. At the right side are presented the distribution of intensity profiles of the respective mean size and z-potential. 67

Figure 4.6 – At the left side are presented results of weighted mean size (nm) (bars - left axis) and z-potential (mV) (—■— - right axis) for peptide/DODAC:MO nanoparticles prepared by method A and B at 1/100 molar ratio, after extrusion. At the right side are presented the distribution of intensity profiles of the respective mean size and z-potential. 69

Figure 4.7 – At the left side are presented results of weighted mean size (nm) (bars -left axis) and z-potential (mV) (—■— - right axis) for peptide/DODAC:MO nanoparticles prepared by method A and B at 1/200 molar ratio, after extrusion. At the right side are presented the distribution of intensity profiles of the respective mean size and z-potential. 70

Figure 4.8 – At the left side are presented results of weighted mean size (nm) (bars - left axis) and z-potential (mV) (—■— - right axis) for peptide/DODAC:MO nanoparticles prepared by method A and B at 1/300 molar ratio, after extrusion. At the right side are presented the distribution of intensity profiles of the respective mean size and z-potential. 71

Figure 4.9 – At the left side are presented results of weighted mean size (nm) (bars - left axis) and z-potential (mV) (—■— - right axis) for peptide/DODAC:MO nanoparticles prepared by method A and B at 1/500 molar ratio, after extrusion. At the right side are presented the distribution of intensity profiles of the respective mean size and z-potential. 72

Figure 4.10 – At the left side are presented results of weighted mean size (nm) (bars - left axis) and z-potential (mV) (—■— - right axis) for peptide/DODAC:MO nanoparticles prepared by method C and D at 1/100 molar ratio, after extrusion. At the right side are presented the distribution of intensity profiles of the respective mean size and z-potential.... 75

Figure 4.11 – At the left side are presented results of weighted mean size (nm) (bars - left axis) and z-potential (mV) (—■— - right axis) for peptide/DODAC:MO nanoparticles prepared by method C and D at 1/200 molar ratio, after extrusion. At the right side are presented the distribution of intensity profiles of the respective mean size and z-potential. .. 76

Figure 4.12 – At the left side are presented results of weighted mean size (nm) (bars - left axis) and z-potential (mV) (—■— - right axis) for peptide/DODAC:MO nanoparticles prepared by method C and D at 1/300 molar ratio, after extrusion. At the right side are presented the distribution of intensity profiles of the respective mean size and z-potential. .. 77

Figure 4.13 – At the left side are presented results of weighted mean size (nm) (bars - left axis) and z-potential (mV) (—■— - right axis) for peptide/DODAC:MO nanoparticles prepared by method C and D at 1/500 molar ratio, after extrusion. At the right side are presented the distribution of intensity profiles of the respective mean size and z-potential. .. 78

Figure 4.14 – At the left side are presented results of weighted mean size (nm) (bars - left axis) and z-potential (mV) (—■— - right axis) for nanoparticles prepared by method A and E at 1/100 (up) and 1/200 (bottom) molar ratio. At the right side are presented the distribution of intensity profiles of the respective mean size and z-potential. 84

Figure 4.15 – At the left side are presented results of weighted mean size (nm) (bars - left axis) and z-potential (mV) (—■— - right axis) for nanoparticles prepared by method A and E at 1/300 (up) and 1/500 (bottom) molar ratio. At the right side are presented the distribution of intensity profiles of the respective mean size and z-potential. 86

Figure 4.16 – Distribution of intensity profiles of the respective mean size (nm) and z-potential (mV) for peptide/DODAC:MO nanoparticles prepared by method E at 1/500 (left) and 1/250 (right) molar ratio. 89

Figure 4.17 – Photography of sample tubes after lyophilization, containing: free peptide fraction (1) and peptide encapsulated fraction in which it lipid was not separated from peptide (2) – first experiment; free peptide fraction (3) and peptide encapsulated fraction after separation from lipid (4) – second experiment. 92

Figure 4.18 – Gel stained with silver. Samples showed are relative to method E and method C and to peptide/lipid molar ratios of 1/300 and 1/500. 93

Figure 4.19 – Gels stained with silver. Samples showed are relative to method E and method C and to peptide/lipid molar ratios of 1/300 and 1/500.....	94
Figure 4.20 – Gels with comassie blue staining. Samples showed are relative to method E and method C and to peptide/lipid molar ratios of 1/300 and 1/500.....	96
Figure 4.21 – Quantitative results for TNF- α (pg/mL) produced in response to 4h, 12h and 24h of incubation with four LPS conditions: 0%, 25%, 50% and 100%.	98
Figure 4.22 – Quantitative results for TNF- α (pg/mL) produced by THP-1 cells in response to 4h of incubation with increasing peptide concentrations: 0 (cells control), 0 (HEPES control), 5, 10, 20, 50, 80 and 100 μ g/mL.	100
Figure 4.23 – Quantitative results for TNF- α (pg/mL) produced by THP-1 cells in response to 4h of incubation with DODAC:MO (1:2) vesicles and peptide/DODAC:MO(1:2) nanoparticles. Cells without any treatment, HEPES at 10 mM, LPS at 100% and peptide at 23.8 μ g/mL were used as controls.....	102
Figure 4.24 – THP-1 cells after 4h, without any treatment (40x magnification).	103
Figure 4.25 – THP-1 cells after 4h of incubation with a peptide concentration of 100 μ g/mL (40x magnification).	104

(Page intentionally left blank)

LIST OF TABLES

Table 2.1 – Amino acids properties.....	23
Table 2.2 – Buried and surface amino acids, and the respective pK_a and pI , included in the peptide CMLb2a2 peptide.	24
Table 2.3 – Positively and negatively charged amino acids for CMLb2a2 peptide at acidic (pH=4), neutral (pH=7) and alkaline (pH=9) pH conditions, according to pK_a . Amino and carboxyl groups placed at the two extremes of the peptide are also considered.	26
Table 3.1 – Total lipid concentration (mM) peptide/lipid molar ratios, for 10 $\mu\text{g/mL}$ and 20 $\mu\text{g/mL}$ of peptide concentration.	40

(Page intentionally left blank)

SYMBOLS AND ABBREVIATIONS

AP – Accelerated phase

APC – Antigen Presenting Cell

BP – Blast phase

CML – Chronic myeloid leukemia

CP – Chronic phase

CTL – Cytotoxic T-lymphocyte

DC – Dendritic Cell

DLS – Dynamic Light Scattering

DODAC – Dioctadecyldimethylammonium Chloride

EPR – Enhanced Permeability and Retention

EPR – Enhanced Permeability and Retention

FBS – Fetal Bovine Serum

HEPES – 4-(2-hydroxyethyl)-1-piperazineethanesulfonic acid

HLA – Human Leukocyte Antigen

LAA – Leukemia-associated Antigens

LMC – Leucemia Mielóide Crónica

LPS – Lipopolysaccharide

LUV – Large Uni-lamellar Vesicles

MHC – Major histocompatibility Complex

MLV – Multi-lamellar Vesicles

MO – 1-monooleoyl-rac-glycerol (Monoolein)

MVV – Multi-vesicular Vesicles

OLV – Oligo-lamellar Vesicles

PDI – Polydispersity index

Ph – Philadelphia chromosome

pI – Isoelectric point

RES – Reticulum-endothelial System

SUV – Small Uni-lamellar Vesicles.

T_m – Transition temperature

TNF- α – Tumor Necrosis Factor-alpha

ζ – Zeta Potential

Chapter 1

Background

(Page intentionally left blank)

1. CHAPTER 1 BACKGROUND

Nowadays, knowledge about the properties of nanoparticles and how to handle them is still limited, opening a wide field of work and scientific research in nanotechnology to be explored. New technology related to the treatment of cancer has become a major focus in the world and new systems that could not have been developed before are now being accomplished. Nanobiotechnology permits bringing together, targeting, therapeutic and imaging compounds condensed in single liposome-based delivery systems. Liposomes provide several benefits, and therefore, are ideal candidates for controlled drug release in the affected region.

1.1. Goals

The use of liposomes as carriers of biomolecules has been widely reported in the international literature as an important step in the production of vaccines or drug-delivery systems. The main goal of this work is to characterize and explore the potential of the system DODAC/MO (1:2) for peptide delivery, enhancing the immunopotentiating action of a CML specific peptide. This increased antigen immunization will activate tumor-specific T cells and consequently increase the therapeutic action of the molecule.

For this purpose distinct approaches have been used throughout this work in order to fulfill three main stages: (i) inclusion of junctional peptide p210 from CML-specific oncoprotein BCR-ABL into liposomes (ii) encapsulation efficiency (iii) delivery of antigenic BCR-ABL junctional peptide to cells *in vitro*.

1.2. Research motivation and contribution

With the new nanotechnology instruments developed in the latest years and understanding the pathology involved, it is absolutely possible to develop an innovative strategy that could be extrapolated to other treatments. Indeed, considering the possibility of building combined systems with nano-sized particles and bioactive molecules, conditions are gathered to develop new vaccines with important therapeutic action. Furthermore, the interaction between

DODAC and MO is still poorly investigated, in spite of the potential application of such DODAC/MO mixture, which has also motivated the present investigation.

Moreover, the possibility of benefiting from the interaction between the Centers of Physics and Environmental Biology from University of Minho, as well as with the BioPhotonics Group from the International Iberian Nanotechnology Laboratory (INL), makes this project a gratifying multidisciplinary experience.

1.3. Dissertation organization

This dissertation encompasses all the stages of the experimental work, beginning with the finding of the most suitable formulation of lipid/peptide in order to test its capability on triggering immunological responses. The work has been organized into five main chapters.

Chapter 1 describes the main goals of this work. It also explains the research motivation and contribution as well as the dissertation organization.

Chapter 2 provides a general overview on key factors related to physicochemical and biological parameters of liposome-based delivery systems for drug delivery and vaccine development. Detailed information about liposomes preparation is also presented. Moreover, principles and current status concerning treatment options for CML are discussed.

Chapter 3 presents a detailed description of the methodology used to create an innovative system to treat CML patients.

Chapter 4 presents data analysis that characterizes the peptide incorporation into the nano-delivery system. Furthermore, data analysis regarding the system's ability to induce an immune response is also discussed.

In Chapter 5 conclusions and future directions are presented.

Bibliography referenced in the text is listed at the end of the work.

Chapter 2

State of the art

"There are known knowns. There are things we know we know. We also know there are known unknowns. That is to say we know there are some things we do not know. There are also unknown unknowns, the ones we don't know we don't know."

Donald Rumsfeld (2002)

(Page intentionally left blank)

2. CHAPTER 2 STATE OF THE ART

2.1. Liposomes

Liposomes are nano-sized artificial vesicles of spherical shape in which an aqueous volume is entirely enclosed by a membrane composed of lipid molecules, usually phospholipids (Vemuri & Rhodes, 1995). These structural units are amphipathic molecules that have a polar or hydrophilic head group (has affinity for water molecules) and a nonpolar hydrophobic tail consisting of fatty acid chains (that repels water molecules), as shown in Figure 2.1. Phospholipids are characterized by its solubility in organic solvents and low solubility in water.

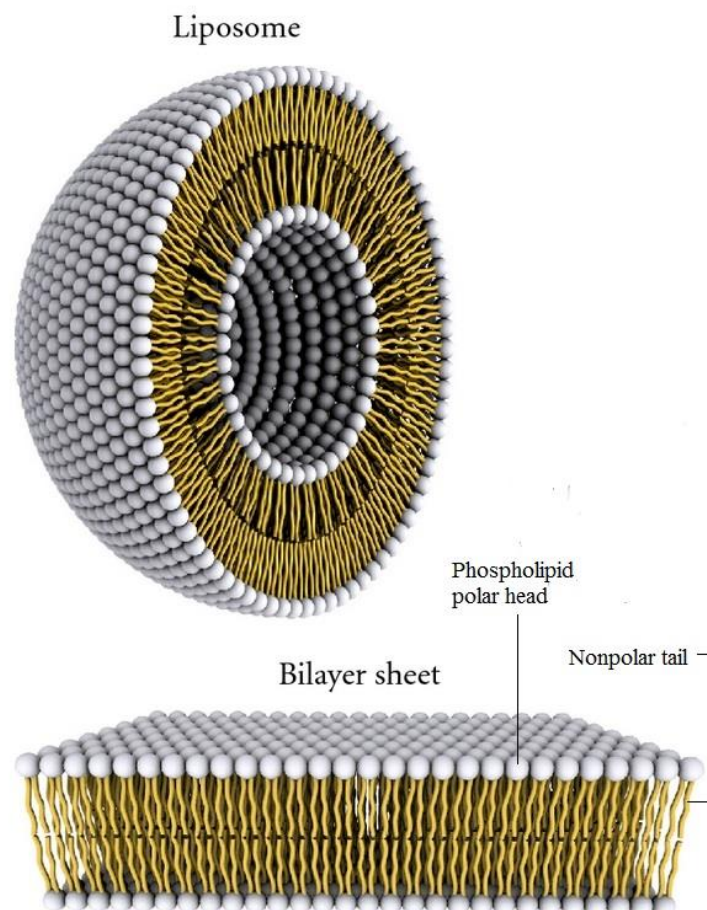


Figure 2.1 – Representation of the steric organization of a liposome (up) and lipid bilayer (bottom) (adapted from (Bitounis, Fanciullino, Iliadis, & Ciccolini, 2012)).

Liposomes were first introduced in the 60's when Alec Bangham observed that phospholipids in aqueous solutions could form closed bilayer structures (Bangham, Standish, & Watkins, 1965). In fact, when phospholipids are combined with water they immediately form a bilayered sphere, a process commonly referred as “self-assembly” by which a disordered system forms an organized structure due to the local interactions between the system units (monomers). Thus, they can be prepared so that they entrap materials both within their aqueous compartment and/or within the membrane.

A model referred to as “fluidic mosaic” introduced in 1972 by Singer and Nicholson, proposes that biological membranes are composed of lipids, proteins and carbohydrates (Singer & Nicholson, 1972). Their biological structure is very similar to that of normal human cellular membranes. Therefore, liposomes are good study models for biological membranes.

The properties and structure of the lipid bilayer can be affected by the gel or fluid state (Ryhänen, 2006). With increasing temperature, lipid vesicles constituted by one type of phospholipid goes through a transition from a gel state into a fluid “liquid crystalline” state. Each lipid has its own transition temperature (T_m) point, above which, in liquid crystalline state, lipid bilayer becomes more fluid and elastic with increasing diffusion of the individual lipid molecules (Ryhänen, 2006). The fluid state of lipids facilitates liposome production and manipulation.

2.1.1. Particle Size

Particle size affects drug release. Smaller particles have larger surface area, therefore, most of the drug associated would be at or near the particle surface, leading to fast drug release. However, smaller particles also have higher risk of aggregation. On the other hand, larger particles have larger cores which allow higher quantity of drug to be encapsulated and slowly diffuse out. The ability to produce nanoparticles of desired size with great precision (narrow size distribution and small variation) is the key factor of producing the nano-suspensions (Silva, Little, Ferreira, & Cavaco-Paulo, 2008).

Liposomes are classified on the basis of different structural parameters and they are produced according to the purpose for which they are more suitable. Figure 2.2 presents different types of liposomes according to size and lamellarity. Multi-lamellar vesicles (MLV) are particles

that are usually up to 0,5 μm . The liposomes containing encapsulated vesicles are called multi-vesicular vesicles (MVV) and their size is up to 1 μm . Uni-lamellar vesicles ranging from 20-100 nm are referred to as SUV, whereas LUV are uni-lamellar vesicles bigger than 100 nm. There are also liposomes of very large size that are called giant liposomes ($>1\mu\text{m}$) which can be either uni-lamellar or multi-lamellar. OLV are oligo-lamellar vesicles ranging from 100-500 nm.

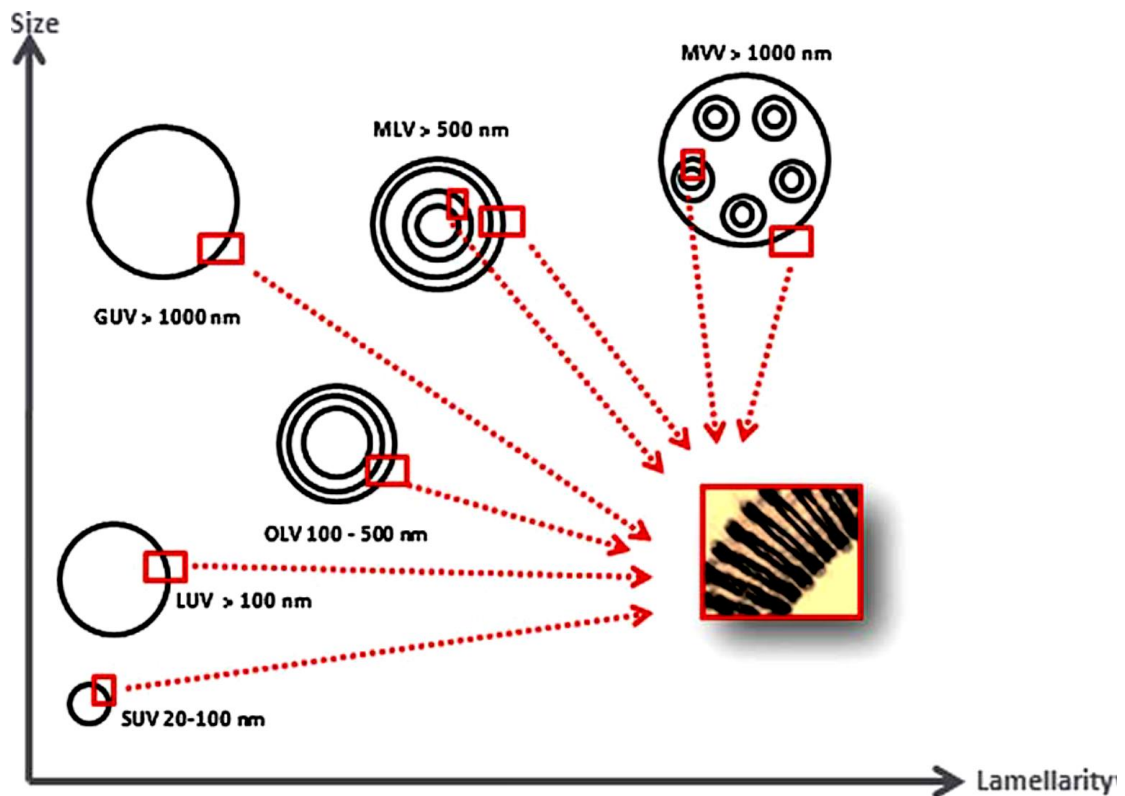


Figure 2.2 – Liposomes classification based on size and lamellarity (Laouini et al., 2012).

2.1.2. Liposome preparation

Different methods of liposome preparation allow the production of lipid vesicles with distinct structural parameters (Dua et al., 2012), as Figure 2.3 illustrates.

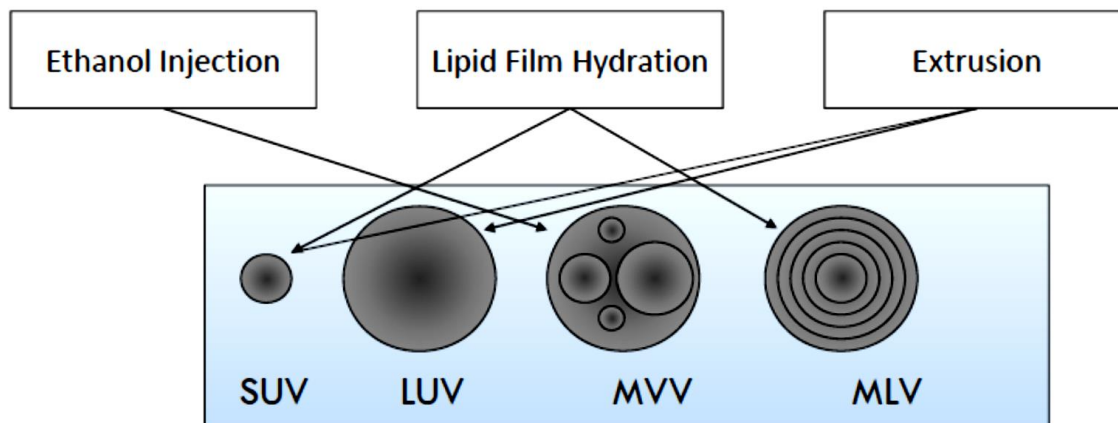


Figure 2.3 – Different types of liposomes produced by ethanol injection, lipid film hydration and extrusion: Small Uni-lamellar Vesicles (SUV); Large Uni-lamellar Vesicles (LUV); Multi-vesicular Vesicles (MVV); Multi-lamellar Vesicles (MLV) (courtesy from João Neves).

Liposomes self-close to form large, multi-lamellar vesicles (MLV) which prevents interaction of water with the hydrocarbon core of the bilayer. Once these particles have formed, reducing the size of the particle requires the use of mechanical treatments such as extrusion through polycarbonate membranes that can transform the MLV suspension into LUV or SUV. Sonication is another alternative to reduce liposome size and produces SUV, and it can be applied to the other methods of preparation.

Methods to prepare liposomes used in this work will be described in the following paragraphs. For further information, there are several reviewed methods (Dua et al., 2012; Laouini et al., 2012; Ulrich, 2002).

A) Multi-lamellar Liposomes (MLV)

Lipid hydration method

First the lipids are thoroughly mixed in the organic solvent. After drying the lipid a thin film is formed at the bottom of round bottom flask. A suspension of MLV is readily obtained by hydrating the thin film with aqueous buffer dispersion. For larger volumes, the organic solvent should be removed by rotary evaporation. After adding aqueous buffer, the solution should be under agitation for some time above the lipid phase transition temperature T_m of the

lipid or above the T_m of the highest melting component in the lipid mixture. The compounds to be encapsulated are added either to aqueous buffer or to organic solvent containing lipids depending upon their solubility. Spinning the round bottom flask in the warm water bath maintained at a temperature above the T_m of the lipid suspension allows the lipid to hydrate in its fluid phase.

This is the most widely used method for the preparation of MLV (Figure 2.4), making it simple to prepare and a variety of substances can be encapsulated in these liposomes. As for a disadvantage of this method, the resulting size distribution and lamellarity of the MLV is very heterogeneous. Still, sophisticated procedures have been developed to produce uniformly sized liposomes (Frézard, 1999; Lasic, 1997; New, 1994).

Alternatively, for small volumes of organic solvent (<1mL), the solvent may be evaporated using a nitrogen gas or argon stream over the mixture in a fume hood. After the removal of organic solvent an aqueous solution is added to hydrate and MLV are formed immediately in this aqueous phase. The content is then emulsified by vigorous vortexing and/or sonication.

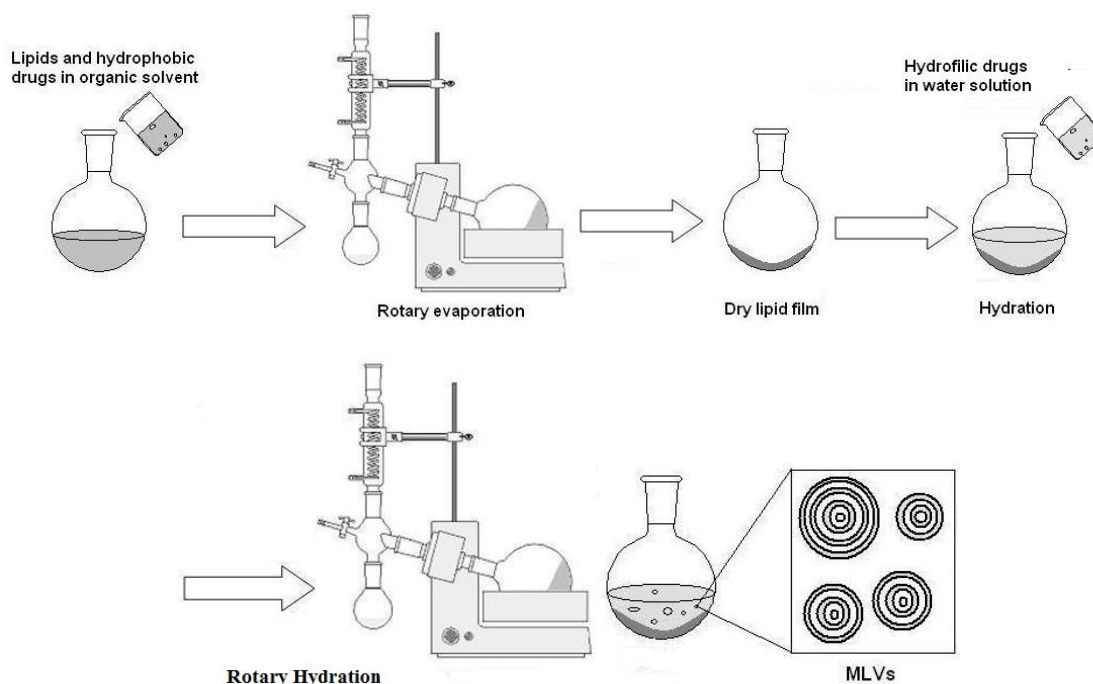


Figure 2.4 – Representation of MLV preparation by lipid hydration method (adapted from Lopes et al., 2013).

B) Multi-vesicular Liposomes (MVV)***Ethanol injection method***

Another approach relies on injecting, drop by drop, the lipid dissolved in the organic solvent to a vast excess of buffer pre-heated to the T_m of the lipids, under vigorous vortexing. A heterogeneous mixture of SUV, LUV or MLV is immediately formed. Therefore, one of the drawbacks of the method is that the population is heterogeneous. Furthermore, liposomes are very diluted, it is difficult to remove all ethanol because it forms an azeotrope with water, and various biologically active macromolecules may be inactivated in the presence of even low amounts of ethanol (Batzri & Korn, 1973).

C) Large Uni-lamellar Liposomes (LUV) and Small Uni-lamellar Liposomes (SUV)***(i) Sonication method***

Disruption of MLV suspensions (produced by lipid film hydration method) using ultra-sonic energy (sonication) typically produces SUV. The most widely used instrumentation for preparation of SUV is a bath sonicator. Sonication of MLV dispersion is accomplished by placing a test tube containing the suspension in a bath sonicator for a certain amount of time. Sonication can be applied to the other methods to increase efficiency in the formation of hydrated lipid vesicles of the smallest size.

Mean size and its distribution are influenced by temperature, sonication time and power, volume, composition and concentration, and sonicator tuning. Thus, it is understandable that it is nearly impossible to reproduce the conditions of sonication, meaning that size variation between samples produced at different times is common. Moreover, due to the high degree of curvature of these membranes, SUV are unstable and have a tendency to undergo aggregation and fusion, forming larger vesicles when stored below their phase transition temperature.

(ii) Extrusion method

This process, showed in Figure 2.5 consists in submitting a suspension of liposomes through a small orifice, repeatedly and sequentially, through polycarbonate membranes filter of well-defined pore-size, under conditions of elevated pressure and temperature above the transition temperature of the lipid. LUV with a diameter near the pore size of the filter used, are

produced. Attempts to extrude below the T_m will be unsuccessful as the rigid membranes cannot pass through the pores. Interestingly, extruded vesicles have been reported to retain significantly elongated elliptical shapes, which have to be taken in to account when evaluating their size and entrapped volume (Jin, Huster, Gawrisch, & Nossal, 1999). The method has some advantages over sonication method, being simple and rapid, reproducible and involving gentle handling of unstable materials. The resulting vesicles are somewhat larger than sonicated SUV.

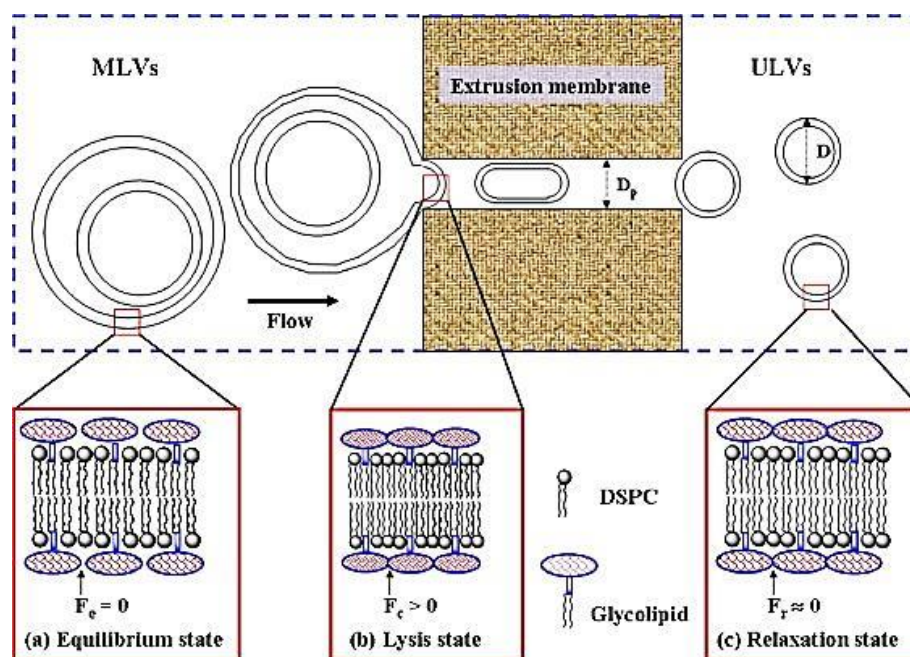


Figure 2.5 – Representation of the extrusion process (Zhua, Xueb, Guob, & Marchant, 2007).

2.1.3. Liposome-based delivery systems

Soon after Alec Bangham observed that phospholipids in aqueous solutions could form closed bilayer structures (Bangham, Standish, & Watkins, 1965), the capture of liposomes by macrophages was recognized as the main mechanism by which liposomes potentiate immune responses to entrapped antigens, which was followed by many immunization studies (Alving, 1991; Gregory Gregoriadis, 1990; Kersten & Crommelin, 1995; V. Torchilin, 2003). Liposomes were first proposed as drug delivery system more than 30 years ago (Gregoriadis, 1973).

Since then, they have been extensively investigated for their potential as drug carriers. Advances in our understanding of the behavior of liposomes at the cellular and subcellular level have allowed the construction of bionanodevices for use in the treatment and prevention of a number of diseases.

Allison and Gregoriadis (Allison & Gregoriadis, 1974), conducted a pioneer work that demonstrated the immunoadjuvant properties of liposomes. In the early 80s, the involvement and investment of several companies, parallel to great achievements in liposome technology, led to the design and licensing of liposome formulations for the treatment of certain cancers, and the first liposome-based vaccine for use in humans. Finally, liposomes as adjuvants became an important attraction with the first liposome-based vaccine (against hepatitis A) having been licensed for use in humans (Gregoriadis, 1995).

However, the first results demonstrated that liposomes were physico-chemically and biologically unstable and drug encapsulation was not efficient. Fortunately, great advances in liposome technology allowed researchers to make significant improvements in its stability, as well as in the understanding of its characteristics and how they interact with biological fluids. Several factors have shown direct influence on the behavior of liposomes in a biological environment, such as preparation, vesicle size, composition, rate stability and drug encapsulation (Lasic, 1998). Thus, methods of characterization and controlling these factors became of extreme importance to produce these nanocarriers for drug delivery purposes.

Similarities between the lipid bilayer structure and the cell membrane, make liposomes capable of interacting with the cells, allowing the targeting of the drug to reach the specific site, and therefore, with less toxicity than free drugs (McPhail, Tetley, Dufes, & Uchegbu, 2000).

Various peptides are used as highly specific and effective therapeutic agents. However, their use is complicated by their instability and side effects. Several peptide drugs have their therapeutic targets inside cells. Thus, it is important to bring these drugs into target cells without subjecting them to lysosomal degradation.

The use of liposomes as carriers of biomolecules is presented as an important step in the production of vaccines or drug-delivery systems, used for controlled delivery of drugs, markers for diagnosis, among other applications. In its use in vaccines, liposomes have the advantage of being able to maintain antigens (e.g. nucleic material, or small peptides) present

in the organism for long enough to obtain an immune response. Otherwise, these biomolecules easily degrade, or are rapidly removed from the circulatory system through the phagocytic cells of the reticulum-endothelial system (RES) (Takeuchi, Kojima, Yamamoto, & Kawashima, 2000), and there is not enough time to obtain an immune response. The antigenic materials can be retained on the surface of liposomes, or else could be encapsulated or embedded within the membrane.

Technology related to controlled release of drugs represents one of the frontiers of science. Nanocarriers are multifunctional and can contribute significantly to the improvement of human health. Drug delivery systems offer a number of advantages when compared to other conventional dosage forms. Various applications of nanocarriers have shown positive results. Figure 2.6 highlights the major functions of nanocarriers in general and, in particular, advantages of liposome-based delivery systems are summarized, to understand why they are candidates to this study (Mohanraj & Chen, 2006; Rawat, Singh, Saraf, & Saraf, 2006; Solaro, Chiellini, & Battisti, 2010).

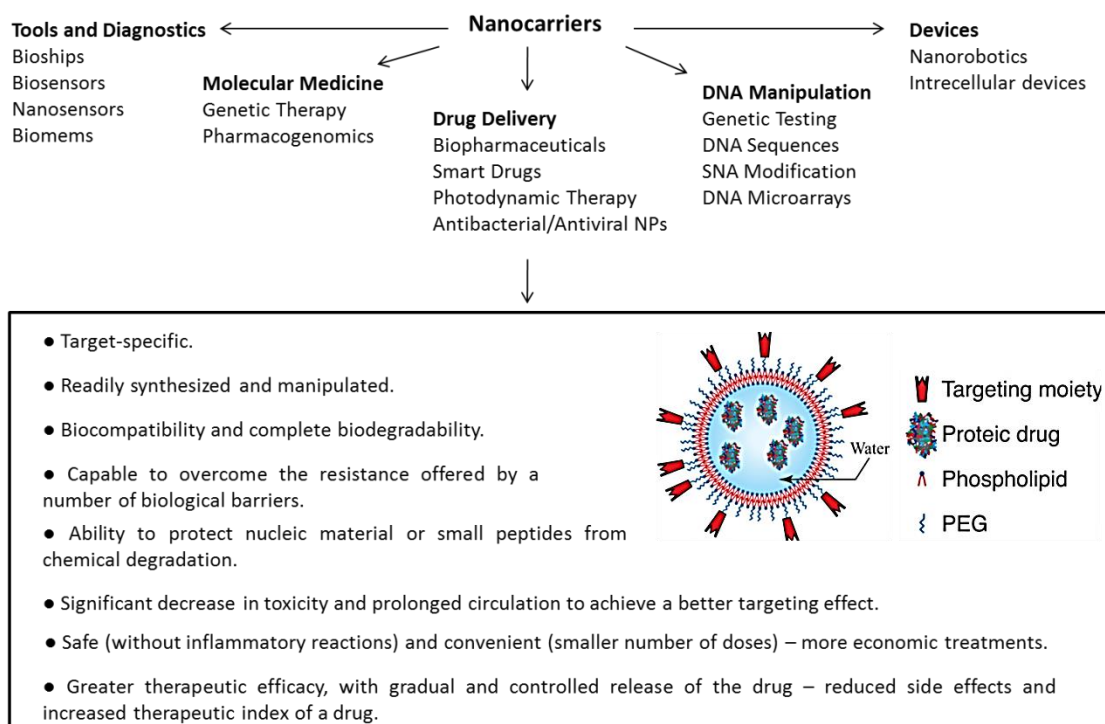


Figure 2.6 – Multi-functions of liposomes as nanocarriers (adapted from Mohanraj & Chen, 2006; Rawat, Singh, Saraf, & Saraf, 2006; Solaro, Chiellini, & Battisti, 2010).

Understanding liposome-cell interaction processes may facilitate potentiating the desired effect of a drug. Many liposomes are made of certain components (e.g. pH-sensitive components) so that drug release can occur only in the target site. Figure 2.7 highlights some liposome-cell interaction processes already known (Torchilin, 2005).

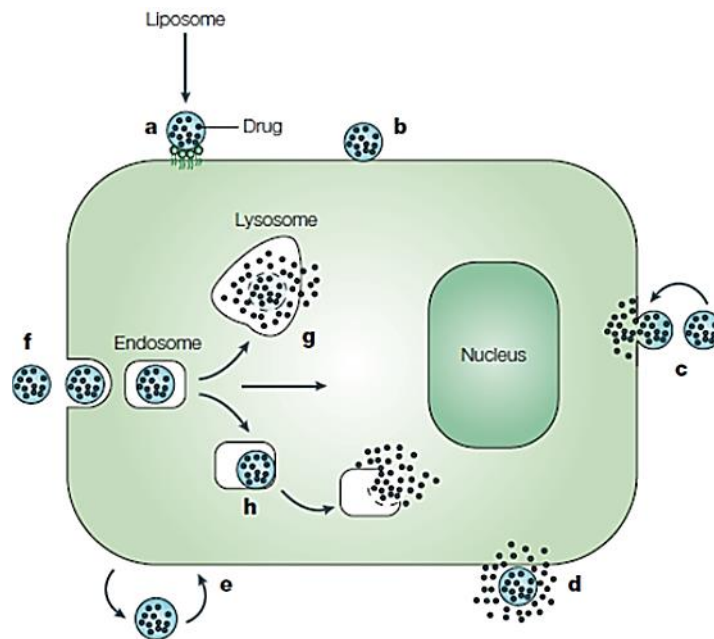


Figure 2.7 – Liposome-cell interaction processes (Torchilin, 2005).

Liposomes can be specifically (a) or nonspecifically adsorbed onto the cell surface. Alternatively, they also fuse with the cell membrane (c), and release their content into the cell cytoplasm, or can be destabilized by certain cell membrane components when adsorbed on the surface (d) so that the released drug can enter cell via micropinocytosis. Direct or transfer-protein-mediated exchange of lipid components with the cell membrane is another process that liposomes can undergo (e) or, instead, be subjected to a specific or nonspecific endocytosis (f). In the case of endocytosis, a liposome can be delivered by the endosome into the lysosome (g) or, en route to the lysosome, the liposome can provoke endosome destabilization (h), which results in drug liberation into the cell cytoplasm (Figure 2.7).

Figure 2.8 highlights membrane destabilization of liposomes and endosomes (Torchilin, 2005).

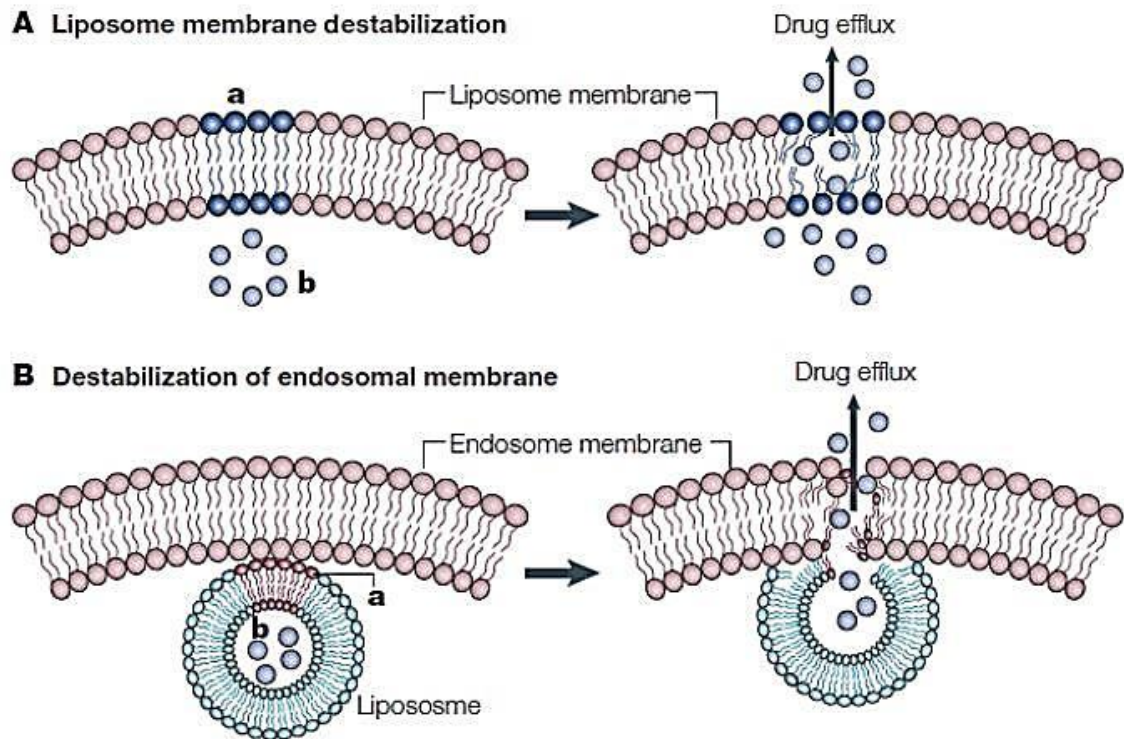


Figure 2.8 – Membrane destabilization of liposomes and endosomes (Torchilin, 2005).

After accumulation in required sites in the body, liposomes containing stimuli sensitive components, such as lipids (a) in the membrane and drug (b) inside, after being subjected to a certain stimulus (such as pH or temperature), liposomes undergo local membrane destabilization, consequently drug efflux occurs from the liposome into surroundings (A). Destabilization of endosomal membrane (B) occurs after being endocytosed by the cell and taken inside the endosome, the liposome containing stimuli (pH)-sensitive components, such as lipids (a) in the membrane and drug (b) inside, can undergo pH-dependent membrane destabilization and initiate the destabilization (Figure 2.8) of the lysosomal membrane, and consequently drug efflux occurs into the cell cytoplasm.

Besides being prepared entirely synthetically, liposomes have also the benefit of being biodegradable, nontoxic and can be administrated in several forms. When immunostimulants are incorporated within these tiny particles, the effect of the resulting system will not only be an increase of their immunological action, but also a reduction of their toxic side effects. Liposomes effect is not only to improve drug action. In fact, many drugs and current classes

of therapeutics cannot even cross cell membranes to gain access to their intracellular site of action. Liposomes can easily overcome this obstacle.

Liposomes are versatile structures, in which many characteristics can be manipulated with high level of accuracy. Consequently, their immunoadjuvant properties can be handled as well. To name some structural characteristics, vesicle size, surface charge, the lipid to antigen mass ratio, bilayer fluidity, and the mode of antigen association with lipid vesicles, are all factors that can significantly influence adjuvanticity. Marketed liposomal and lipid-based products, plus a selection of products in clinical development have been recently reviewed (Allen & Cullis, 2013).

2.1.4. DODAC:MO-based liposomes

There is a class of surfactants suitable to form vesicles in aqueous solutions, and DODAC (Figure 2.9) is one example. Dioctadecyldimethylammonium chloride is a synthetic cationic surfactant suitable to form vesicles in aqueous solutions. Surfactant concentration, vesicle preparation method and solvent condition are aspects to take into account. Optically clear dispersions of dioctadecyldimethylammonium chloride are capable of forming LUV by simply warming the aqueous surfactant solution (typically 1mM) to 50 °C, above the gel to liquid crystalline phase transition temperature, $T_m = 48.9$ °C (Feitosa, Barreleirob, & Olofsson, 2000), and gently shaking it. Cryo-transmission electron microscopy micrographs show that DODAX vesicles are unilamellar and polydisperse (Feitosa, Karlsson, & Edwards, 2006). Feitosa et al, also demonstrated that these vesicles are stable for at least 1 month according to the ageing time-dependence of the turbidity and molar absorption coefficient. Figure 2.9 shows the structure of DODAC (Eloi Feitosa & Alves, 2008).

The cationic nature of certain liposomes is an attractive characteristic for drug-delivery and gene delivery (Zuhorn, Engberts, & Hoekstra, 2007). Cationic liposomes remain for a longer time in circulatory system than negative and neutral liposomes, because cationic formulations are able to escape phagocytosis. This ability of cationic liposomes is related to their interaction with blood cells (Aoki, Tottori, Sakurai, Fujib, & Miyajima, 1997). The positive charge of cationic liposomes exhibit high affinity for the negative charge of cell membrane, which facilitates cell uptake (Wiethoff, Smith, Koe, & Middaugh, 2001), and may be used for the release of exogenous genetic material intracellularly (Sharma & Sharma, 1997).

Apparently, cationic microparticles are optimal for uptake into macrophages and dendritic cells (DC) (Thiele, Merkle, & Walter, 2003).



Figure 2.9 – Chemical structure of DODAC (Thiele, Merkle, & Walter, 2003).

Despite promising candidates to effectively enhance immune responses (Christensen et al., 2007; Nakanishi et al., 1999), cationic liposomes may have an immunotoxic effect (Kedmi, Ben-Arie, & Peer, 2010; Lv, Zhang, Wang, Cui, & Yan, 2006), limiting their safety for clinical use. This brings to mind the importance of an ideal liposome/antigen formulation, with characteristics that have to be tuned to reach the most effective and harmless formulation as possible.

Monoolein, 1-monooleoil-rac-glycerol (MO), is a natural amphiphilic neutral single tail unsaturated lipid that assembles in water, as it has the particularity to form two non-lamellar inverted bicontinuous cubic phases (Q_{II}^G and Q_{II}^D) even in excess H_2O (Ericsson, Larsson, & Fontell, 1983; Geil et al., 2000). Since the 1960s there has been a steady increase in publications, industrial applications and related patents (Kulkarni, Wachter, Iglesias-Salto, Engelskirchen, & Ahualli, 2011).

From the molecular point of view, despite being a simple molecule, it shows amphiphilic properties as it contains a polar head group and a nonpolar hydrocarbon chain. It is composed of a hydrocarbon chain, which is attached to a glycerol backbone by an ester bond. The remaining two hydroxyl groups of the glycerol moiety confer polar characteristics to this part of the molecule commonly referred as the head group. Thus, they may form hydrogen bonds with water in aqueous solutions. In contrast, the C_{18} hydrocarbon chain (usually referred as the ‘tail’), featuring a *cis* double bond at the 9, 10 position, is strongly hydrophobic (Kulkarni et al., 2011). Consequently, this allows monoolein molecules to self-assemble into different liquid crystalline structures under varying conditions of temperature and solvent composition (Ganem-Quintanar, Quintanar-Guerrero, & Buri, 2000).

Figure 2.10 shows the chemical structure of monoolein.

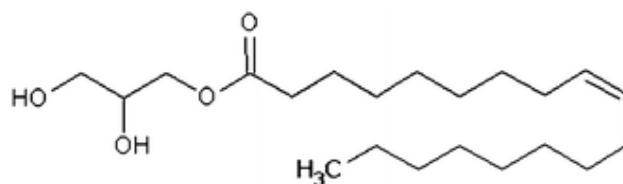


Figure 2.10 – Chemical structure of monoolein (Kulkarni, Wachter, Iglesias-Salto, Engelskirchen, & Ahualli, 2011)

Cubic phases are known to play an important role in many cell processes, such as membrane fusion (Luzzati, 1997), protein function (Epanand, 1998) and ultra-structural organization (Lipowsky & Sackmann, 2004), and DNA condensation in lipoplexes (Silva, Coutinho, & Oliveira, 2008, 2011).

Therefore, MO has become a preferential model for the study of a broad range of applications. MO is a non-bilayer-forming surfactant that favors vesicle formation. New reported results on this subject indicate that both temperature and MO tendency to form non-bilayer structures largely influence the self-assembly process, affecting the structure of the final aggregates (Oliveira et al., 2012).

Overall, this study may provide further insight on the relationship between delivery efficiency and structural organization of peptide/DODAC:MO complexes. Different formulations of peptide/DODAC:MO will certainly affect the structural organization of the final particle. This will all be extensively studied. The potential of the system DODAC/MO has motivated this investigation. Monoolein is a nontoxic, biodegradable, and biocompatible material classified as GRAS (generally recognized as safe). Its biodegradability is due to the fact that monoolein is subject to lipolysis because of different kinds of esterase activity in different tissues. This remarkable molecule is particularly interesting due to its nature and physicochemical behavior, which makes it an attractive alternative in relation to other conventionally used materials. The most significant advantages of monoolein are probably its solubilizing capability, rheological behavior, and low toxicity. Furthermore, the versatility of monoolein makes possible to include it in very different systems and cubic phase reveals great flexibility since drugs of very different polarity and size may be accommodated within it.

2.2. Chronic Myeloid Leukemia

Chronic myeloid leukemia (CML) is a malignant disorder that originates in a single abnormal hematopoietic stem cell. The anomalous clone originated from this cell expands and infiltrates the medullar parenchyma, slowly but progressively, over the proliferation of normal cells. The disease is associated with a specific cytogenetic abnormality, the Philadelphia chromosome (Ph), resulting from a reciprocal translocation between the long arms of chromosomes 9 and 22 $t(9;22)(q34;q11)$ that leads to the formation of a new leukemia-specific gene, BCR-ABL, generated by the fusion of the *c-abl* oncogene 1 (ABL1, from chromosome 9) with the breakpoint cluster region gene (BCR, from chromosome 22). In CML, the second or third exon of the BCR gene is usually spliced into the second exon of the ABL gene, creating B2A2 or B3A2 transcripts. Once translated, each B2A2 or B3A2 mRNA generate a 210-kDa BCR-ABL protein. The BCR-ABL fusion protein shows tyrosine kinase activity and is essential and sufficient for leukemia transformation and progression. In fact, the junctional sequences of BCR-ABL are only expressed in leukemia cells (Pinilla-Ibarz et al., 2000). This constitutively up regulated tyrosine kinase activity of the chimeric BCR-ABL1 protein affects several intracellular signaling pathways that promote proliferation and survival of cells and thus contribute to their malignant transformation (Guilhot et al., 2008; Quintás-Cardama & Cortes, 2009; Smahel, 2011). Under normal conditions, the BCR gene expressed on chromosome 22 encodes a protein whose function is related to cell cycle regulation, whereas gene ABL expressed on chromosome 9 encodes a protein tyrosine quinase (Druker et al., 2001). The reciprocal gene resulting from translocation ABL-BCR on chromosome 9q+, though active, plays no role in any kind of disease. The hybrid gene BCR-ABL produces a chimeric protein with elevated tyrosine kinase activity. The disease begins with a chronic phase (CP) that can last for 3 to 5 years, and if untreated, it progresses into accelerated phase (AP) and within a year, blast phase (BP). Survival at this point is less than 1 year.

CML patients were once regarded as incurable, but more recent understanding of the molecular anatomy and pathophysiology of the disease provides important insights into the targeting of treatment to a specific molecular abnormality. CML has been recognized as a potent model for immune therapy in humans because there is a specific gene rearrangement, BCR/ABL, which product, P210bcr/abl can be the target antigen for immune therapy. Peptides spanning the junction between BCR and ABL in P210bcr/abl are specific to CML

cells; they are not present in other normal cells neither in CML patients nor in cells in normal individuals without CML (Guilhot et al., 2008).

Despite the therapeutic advances that made possible the significant increase in the perspective of life in patients with CML, several biological mechanisms that favor the selection of malignant cells over normal cells have been responsible for treatment failure in many cases (Bergantini, Castro, Souza, & Fett-conte, 2005).

Because the preeminent mutation driving CML is BCR-ABL, therapies targeting this gene are the logical choice for disease-specific therapy directed at the BCR-ABL tyrosine kinase. However, even in the best responders residual leukemic cells may persist. Since these therapies fail to eradicate the CML stem cells, much work still has to be done and improvement or development of new and more effective strategies would be useful.

2.2.1. Vaccination with BCR-ABL

The breakpoint in the bcr gene occurs either between bcr exon 2 (b2) and 3 (b3) or between bcr exon 3 (b3) and 4 (b4). Hence, 2 alternative chimeric p210 bcr-abl proteins, comprising either a b3a2 or a b2a2 junction, can result from this fusion gene (Shtivelman, Lifshitz, Gale, Roe, & Canaani, 1986). The cellular processing of the products of these two fusion proteins can originate peptides capable of being presented in the cell surface, and can be recognized by cytotoxic T-lymphocytes (CTL) in the context of human leukocyte antigen (HLA) class I molecules (Falkenburg, Smit, & Willemze, 1997; Melief & Kast, 1995). Thus, despite the intracellular location of p210, those peptides can be recognized by T cells within the cleft of HLA. For this reason, and considering that the junction between the fused BCR and ABL genes produces a novel peptide sequence that is unique to leukemic cells, it is a reasonable target for leukemia specific immunotherapy. A list of BCR-ABL peptides used in vaccine trials in patients with chronic myeloid leukemia has been reviewed (Dao & Scheinberg, 2008). Furthermore, there are three different forms of the Bcr-Abl oncogene p185, p210, and p230 (Melo, 1996), which may represent alternative potential targets for immunotherapy approaches (Volpe et al., 2007).

In Bocchia *et al.* (2010) documented clinical trial, one patient was treated with a target immune approach receiving a therapeutic vaccine. This vaccine consisted of a 25-mer b2a2

breakpoint derived peptide (CMLb2a2-25) with binding properties for several HLA-DR molecules and was able to elicit a consistent peptide-specific CD4⁺ T-cell response. This study shows, for the first time, that these peptide vaccinations were able to reduce and even eradicate minimal residual disease in a patient with CML.

Hereupon, the present work emerges in an attempt to find an alternative target approach that can be added to CML currently used therapy to eradicate minimal residual disease through immunotherapy. The approach described in this thesis consists of a liposomal peptide vaccine. Because several peptides can be encapsulated in lipid vesicles, one day this strategy may be used as a multitherapeutic therapy. This concept provides a new paradigm for the treatment of CML, and CMLb2a2-25 peptide used in Bocchia *et al.* (2010) trial will be studied in the present work.

2.2.2. The b2a2 breakpoint derived peptide

A therapeutic vaccine consisted of a 25-mer b2a2 breakpoint derived peptide (CMLb2a2-25) tested in a 63-year old woman with chronic myeloid leukemia was able to elicit a consistent peptide-specific CD4⁺ T-cell response (Bocchia, Defina, & Aprile, 2010). This resulted in a reduction and even eradication of minimal residual disease.

CMLb2a2 peptide has sequence of 25 amino acids (3-letter code), Thr-Val-His-Ser-Ile-Pro-Leu-Thr-Ile-Asn-Lys-Glu-Glu-Ala-Leu-Gln-Arg-Pro-Val-Ala-Ser-Asp-Phe-Glu-Pro-NH₂, whose properties can be seen in Table 2.1 and Table 2.2. Figure 2.11 shows a representation of the CMLb2a2-25-25mer peptide that is going to be used in the present study.

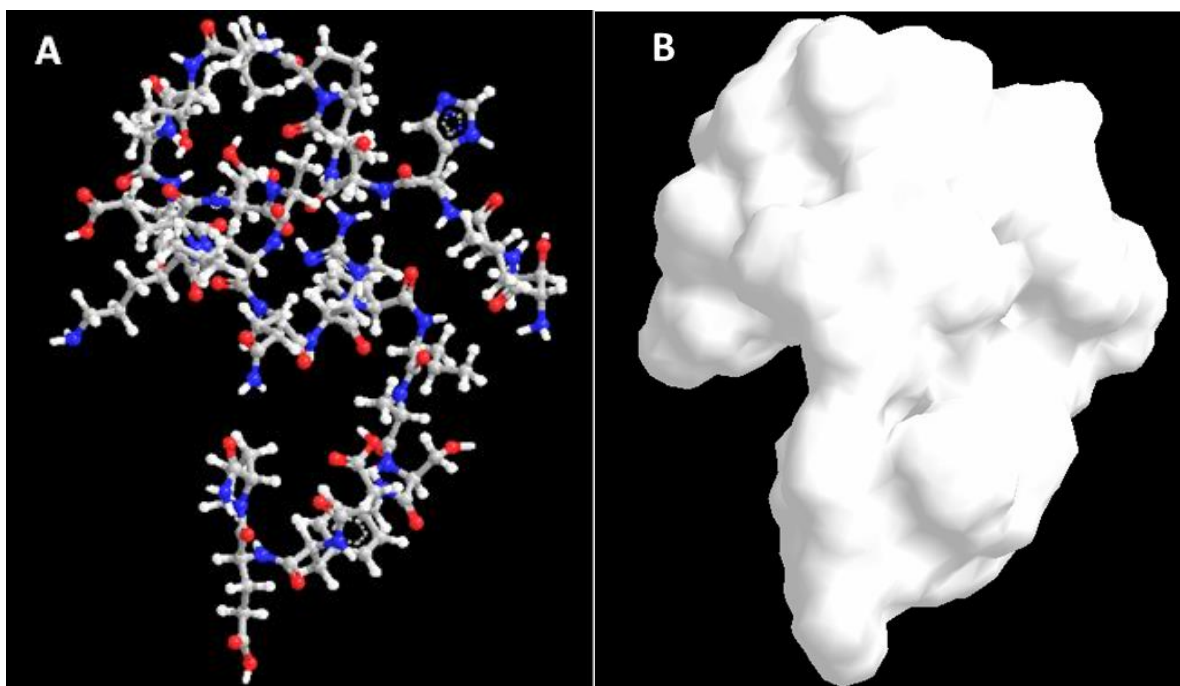


Figure 2.11 – Representation of CMLb2a2-25mer peptide: A – Chemical bonds are denoted for Carbon (grey), Nitrogen (blue), Oxygen (red) and Hydrogen (white); B – molecule's solvation area. The molecular properties of this peptide were attained by ChemBioOffice 13 program, developed by Cambridge Software.

The present thesis comprises a study of this peptide in different pH conditions. In order to support and interpret results, few properties as charge, hydrophobicity, pK_a and isoelectric point (pI) should be elucidated (HubPages, 2013; Publishing, 2013). First we must know the amino acid structure. Figure 2.12 shows a representation of an amino acid.

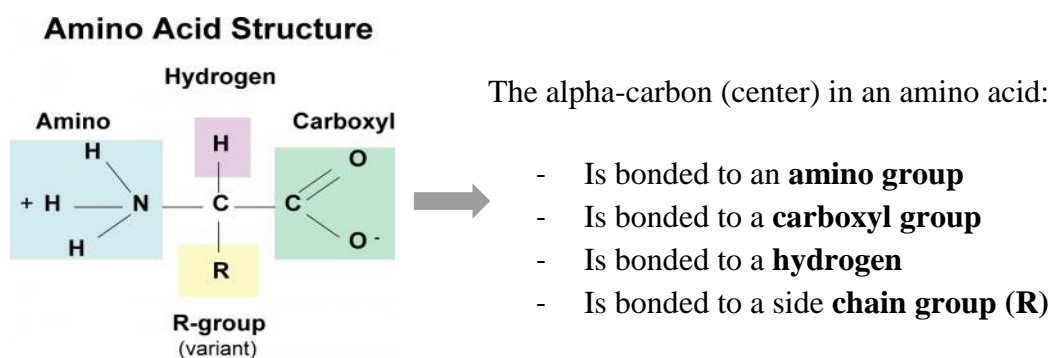


Figure 2.12 – Amino acid structure (adapted from Hambly, 2013).

Peptide bonds allow amino acids to be linked, consequently forming peptides. This peptide bond consists of a carbonyl group's carbon atom directly bound to the nitrogen atom of a secondary amine. After the peptide formation, the peptide chain will have an unbound amino group free at one end, called the N-terminus, and a single free carboxylate group at the other end, named the C-terminus.

Amino acids can be classified, among other aspects, according to the side chain group (R). Since amino acids, peptides, and proteins have different pK_a values, there is the possibility that they can have different charges at a given pH.

Table 2.1 shows the properties of the amino acids included in CMLb2a2 peptide, and the respective pK_a and pI are shown in Table 2.2.

Table 2.1 – Amino acids properties.

Amino Acid	3-letter code	Properties	Amino Acid	3-letter code	Properties
Alanine	Ala	aliphatic hydrophobic neutral	Leucine	Leu	aliphatic hydrophobic neutral
Arginine	Arg	polar hydrophilic charged (+)	Lysine	Lys	polar hydrophilic charged (+)
Asparagine	Asn	polar hydrophilic neutral	Phenylalanine	Phe	aromatic hydrophobic neutral
Aspartate	Asp	polar hydrophilic charged (-)	Proline	Pro	hydrophobic neutral
Glutamine	Gln	polar hydrophilic neutral	Serine	Ser	polar hydrophilic neutral
Glutamate	Glu	polar hydrophilic charged (-)	Threonine	Thr	polar hydrophilic neutral
Histidine	His	aromatic polar hydrophilic charged (+)	Valine	Val	aliphatic hydrophobic neutral
Isoleucine	Ile	aliphatic hydrophobic neutral			

Table 2.2 – Buried and surface amino acids, and the respective pK_a and pI , included in the peptide CMLb2a2 peptide.

Buried			Surface		
Amino Acid	pK_a	pI	Amino Acid	pK_a	pI
Alanine	-	6.0	Glutamate	4.3	3.22
Valine	-	5.96	Lysine	10.5	9.74
Phenylalanine	-	5.48	Glutamine	-	5.65
Leucine	-	5.98	Proline	-	6.30
Isoleucine	-	6.02	Serine	-	5.58
-			Threonine	-	5.60
-			Aspartate	3.7	2.77
-			Histidine	6.0	7.59
-			Arginine	12.5	10.76
-			Asparagine	-	5.41

An atom group in a molecule may lose or gain a proton when the molecule is placed in an aqueous solution. The exact probability that a molecule will be protonated or deprotonated depends on the pK_a of the molecule and the pH of the solution. Half of molecules will lose protons if they are in a solution with $pH = pK_a$. The higher the pH value, the more likely a molecule will lose a proton (Publishing, 2013). Furthermore, from the definition of pH, a high concentration of HO^- ions is present at higher pH, thereby being capable of accepting more protons which results in the neutralization of positive charges.

As for the isoelectric point, when the pH is lowered far below the pI , the protein will lose its negative charge and will contain only positive charges, but if the pH is adjusted to the isoelectric point of the protein, its net charge will be zero. Most proteins at physiological pH are above their pI , thereby having an overall negative charge. This information, along with table 2, suggests that at neutral pH, BCR-ABL peptide has a net negative charge.

By observing table 2 it can be noted that pK_a is not shown for certain amino acids. The pK_a essentially refers to the tendency for H^+ to dissociate from a molecule, and thus is a measure of the extent of H^+ dissociation under equilibrium conditions. So, if a molecule's hydrogen has no tendency to dissociate, then it will not have a pK_a . The R groups of such amino acids have no dissociable hydrogens - these groups are neither acids nor bases. It should be noted that we are referring strictly to the R-groups, because even the neutral amino acids still have a pK_a for

the backbone of amino and carboxyl groups. The carboxyl group has a pK_a ranging from 1.8 to 2.4 and is most likely negatively charged at neutral pH, whereas the amino group has a pK_a ranging from 8 to 11 and is most likely positively charged.

From Table 2.2 we can also infer that the peptide charged amino acids are characterized as being surface amino acids. Therefore, all these charges will be considered when predicting and analyzing the surface charge of the BCR-ABL peptide at different pH conditions.

From Table 2.1 and Table 2.2 we can observe that four negatively charged (Glu (3x) and Asp) and three positively charged (Lys, Arg and His) amino acids are included in this peptide. Thus, it is expected that this peptide will exhibit a negative overall charge which will be attracted for the positively charged membranes of liposomes (Friede, Vanregenmortel, & Schuber, 1993; Gregory Gregoriadis, 2007a). Additionally, the amphipathic character of this peptide may increase its affinity for biological membranes (Bessalle et al., 1993; Wimmer et al., 2006).

CMLb2a2 peptide contains two amino acids with beta strands, Val and Ile, and two amino acids with alpha helix, Ala and Leu. The special conformation of these amino acids may play an important role in the interaction with lipid membranes and affect peptide incorporation into liposomes. However, the interaction with liposomes can stabilize the alpha helix structure (Bessalle et al., 1993; Wimmer et al., 2006).

This peptide has a preference for secondary structures and contains 48% of hydrophobic amino acids, 16%, 12% and 24% of acidic, basic and neutral amino acids, respectively. Peptide molecular formula is $C_{124}H_{200}N_{34}O_{39}$, has a molecular weight of 2790,47 g/mol and a molecular volume of $3377,307 \text{ \AA}^3$.

From the information above we can predict the amino acids charge and, consequently, the overall surface charge of BCR-ABL peptide at acidic, neutral and alkaline pH (Table 2.3). It should be noted that histidine (His) is very sensitive to pH change in the physiological range. The R group of histidine ($pK_a = 6.0$) has only 10% probability to become positively charged at pH = 7, but the probability increases to 50% at pH = 6. Therefore, histidine will not be considered as positively charged at neutral and alkaline pH.

Table 2.3 – Positively and negatively charged amino acids for CMLb2a2 peptide at acidic (pH=4), neutral (pH=7) and alkaline (pH=9) pH conditions, according to pK_a . Amino and carboxyl groups placed at the two extremes of the peptide are also considered.

pH condition	4		7		9	
Charge	Negative	Positive	Negative	Positive	Negative	Positive
Amino Acids	-	Lys	Glu	Lys	Glu	Lys
	-	Arg	Glu	Arg	Glu	Arg
	-	His	Glu	-	Glu	-
	Asp	-	Asp	-	Asp	-
Carboxyl/Amino groups	carboxyl	-	carboxyl	Amino	carboxyl	-
Total	2	3	5	3	5	2

Considering the information from table 3, and considering that at acid pH the excess of H^+ ions is capable of neutralizing peptide negative charges and that at alkaline pH the excess of HO^- is capable of neutralizing peptide positive charges, we can expect that the peptide negative surface charge will be stronger at pH 7 and 9, than at pH 4.

Amino acids properties described above are of major importance since factors affecting peptide–liposome membrane interactions include effects of peptide length, charge, hydrophobicity, secondary structure, and topology (Strömstedt, Ringstad, Schmidtchen, & Malmsten, 2010).

CMLb2a2 peptide incorporation into liposomes will be analyzed using specific techniques described in chapter 3.

2.3. Liposomal vaccines

Extensive information about the use of liposomes as immunological adjuvants for protein and peptide antigens is available since the early 90s (G. Gregoriadis, Florence, & Patel, 1993; Philippot & Schuber, 1995). When peptide antigens are encapsulated in lipid vesicles, the liposome-peptide complexes formed are phagocytosed by macrophages. Eventually, liposome-peptide systems accumulate in lysosomes, where the encapsulated peptides are presented to the MHC class II complex. At this stage, the system is capable of stimulating

specific T-helper cells (Philippot & Schuber, 1995). This constitutes the basis for the use of lipid vesicles as adjuvants in vaccine development. Among many other reports, Maiko Taneichi *et al* (Taneichi et al., 2006) conducted a study in which liposomes were presented to both CD4⁺ and CD8⁺ T cells, and potent antitumor immunity was induced.

Although a similar approach is not apparently available for CML, liposomes have been successfully used in peptide vaccines, as they were capable of protecting and delivering the peptide in the proper target and elicit strong antigen-specific T- responses (Chikh, Kong, Bally, Meunier, & Schutze-Redelmeier, 2001; Copland et al., 2003; Guan et al., 1998; Ludewig et al., 2000; Masuda, Horie, Suzuki, Yoshikawa, & Hirano, 2002; Rao & Alving, 2000).

Other important aspect to take into account is that the adjuvant effect of cationic liposomes depends on administration route. Han-Chung Wu and De-Kuan Chang's (Wu & Chang, 2010) work elucidates the molecular mechanism of peptide-conjugated liposomes on cancer therapy. In the intravenous route, the immune system can easily recognize lipid vesicles, which are then cleared from circulation by phagocytes. Furthermore, the desired concentration of a drug in blood is obtained with an accuracy and speed that are not possible with other procedures. This is of major importance since in CML malignant cells are not localized in a specific region, instead, they are scattered throughout the organism. Therefore, this is an important aspect to be taken into account when developing the nano-system, and intravenous administration should be the proper approach to the aim of this thesis.

High doses of a drug may be severely detrimental to the patient, whereas small doses may be insufficient to eradicate the tumor. This is the main reason why most cancer drugs are ineffective in killing cancer cells. In this context, liposomes emerge as a successful alternative to overcome the problem. A clinical study in which a drug was encapsulated in liposomes reported that these lipid vesicles were able to retain the drug within it while circulating in blood stream (Orlowski et al., 2007). This makes possible to deliver the drug to the target without leakage from the liposomes, dramatically reducing side effects during its journey to the tumor tissues, and improving the index of a drug.

When producing liposome-delivery chemotherapy agents, the hyper permeability of tumor vasculature should be taken into account. The size of the liposome is a key-factor to succeed when developing a treatment strategy (Fifis et al., 2004; Mottram et al., 2007). Gap junction

found in normal endothelium are typically <6nm wide (Drummond, Meyer, Hong, Kirpotin, & Papahadjopoulos, 1999), and liposomes with 65-75nm diameters were found to be large enough to be excluded from normal endothelium and at the same time small enough to infiltrate tumor endothelium (T. Lee, Wu, Tseng, & Lin, 2004; T.-Y. Lee, Lin, Kuo, Chang, & Wu, 2007; Lo, Lin, & Wu, 2008). On the other hand, angiogenic tumor vasculature is estimated to have an average pore size of 100 – 600 nm (Hashizume et al., 2000), which is significantly larger than the normal endothelium. Thus, the proper size of the liposome is crucial to protect normal cells and tissues, and to deliver the drug to the target as they selectively reach the tumor interstitial space.

The advantage of liposomes to protect the drug from the body and to protect the body from the drug, retaining it during a period of time, associated with the advantage of the tumor vasculature's high permeability, turns this approach into a potential treatment for various cancers. Furthermore, liposomes may be retained longer in tumor tissues as it frequently lacks effective lymphatic drainage (Jain, 1987). In this respect, a new term known as “enhanced permeability and retention (EPR) effect” was first adopted by Matsumura & Maeda (1986), consisting in higher accumulation of a certain drug within the tumor. This becomes much more important when results concerning liposome delivery systems show a ten times higher effect, compared to free drugs (Northfelt et al., 1996).

To further enhance the selectivity and concentration of liposomes within the tumor region, peptides can be previously attached to the lipid vesicles. After intravenous administration, liposomes arrive to the tumor tissues where they are internalized by tumor cells through receptor-mediated endocytosis. Eventually, liposomes are broken down so that the encapsulated drug is released within the intracellular space of the cells. Diagram presented in Figure 2.13 may clarify the molecular mechanism of peptide-conjugated liposomes on cancer therapy.

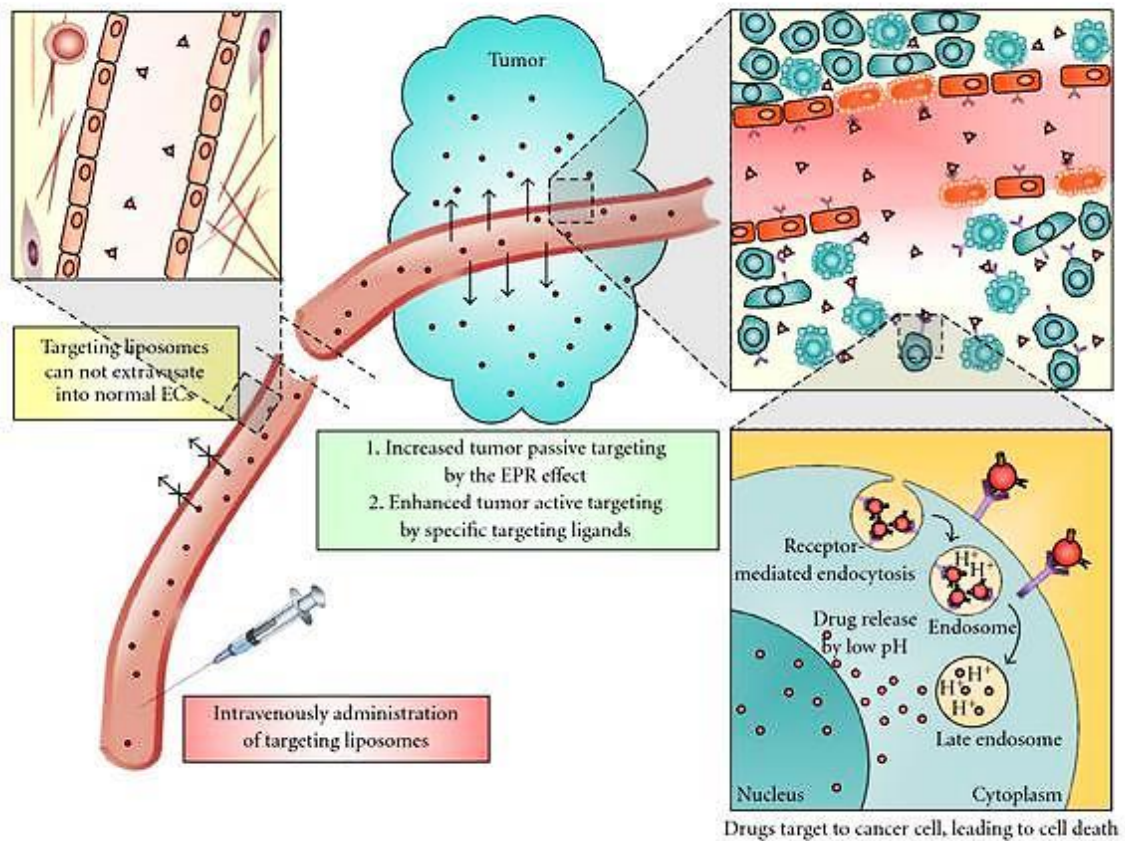


Figure 2.13 – Representation of the molecular mechanism of peptide-conjugated liposomes on cancer therapy (Wu & Chang, 2010).

The development of ‘pharmaceutical’ liposome-based delivery systems is an area of intense research currently, as new promising treatments may arise from it. The increasing variety of encouraging results reported in numerous clinical trials concerning many different diseases supports the revolutionary role of lipid vesicles in modern medicine.

2.3.1. Role of adjuvants in vaccine development

The first definition of immunological adjuvants was first reported in the 20th century (Ramon, 1924) as "substances used in combination with a specific antigen that produced a more robust immune response than the antigen alone." In other words, immunological adjuvants are molecules or substances capable of amplifying or enhance the cascade of immunological events that comprise the immune response (Schijns, 2000). Moreover, it should also induce antigens to elicit an early, high and long-lasting immune response with a smaller amount of antigen, by modulating the immune system (Audibert, 2003), and direct this immune response to a protective response, preventing the disease reappearance (Morein, Villacrés-Eriksson, Sjölander, & Bengtsson, 1996). In other words, adjuvants are molecules that accelerate and increase antigen-specific immune responses.

Peptide-liposomal vaccines are often poorly immunogenic and effective vaccines are not available against a number of important diseases at the present time. To be successful against the most difficult pathogens, vaccines must induce more potent immune responses. Specifically, cellular immune responses include induction of cytokines from CD4⁺ T helper cells and CD8⁺ cytotoxic T lymphocytes.

As traditional vaccines may not be successful as it is desired to, vaccine adjuvants may be required to achieve significant improvements, so that these new-generation vaccines can be effective against the most difficult diseases. Novel adjuvants together with vaccine delivery systems will enable the development of new-generation vaccines against diseases thought incurable today.

Nevertheless, adjuvant safety remains a significant concern. The level of adjuvant toxicity is a key issue in adjuvant development, since adjuvants that induce a certain degree of adverse effects will not prove acceptable. The potential use of an adjuvant will be based on its safety - if it induces minimal adverse effects - and on its strength, when in association with a certain molecule. In fact, most adjuvants that have proceeded to clinical trials have proven to be too toxic for clinical use. Other important characteristics to consider include stability, biodegradability, cost, ease of manufacture, and applicability to a wide range of vaccines.

In its use in antigen vaccines, adjuvants are useful to improve immune response to vaccine antigens in various different ways (Schinjs & T.O'Hagan, 2006), including: (i) enhancing the speed and duration of the immune response; (ii) stimulating cellular immunity, including the

desired cytokine profile; (iii) increasing the immunogenicity of weak antigens; (iv) modulating antibody avidity, specificity, isotype, or subclass distribution; (v) promoting the induction of mucosal immunity; (vi) decreasing the dose of antigen in the vaccine to reduce costs; (vii) enhancing immune responses in immunologically immature, or senescent individuals; (viii) helping to overcome antigen competition in combination vaccines.

The mechanisms of action of adjuvants remains poorly understood. However, the identification of key receptors of the innate immune system made possible to achieve significant advances. Two broad groups can be distinguished based on their principal modes of action (Schinjs & T.O'Hagan, 2006), focusing on whether or not they have direct immunopotentiating effects on innate immune cells, or they function primarily as "delivery systems" to promote antigen uptake into antigen-presenting cells (APC). Liposomes are among these adjuvants.

(Page intentionally left blank)

Chapter 3

Methodologies

“The most exciting phrase to hear in science, the one that heralds new discoveries, is not
“Eureka!” (I found it!) but “That’s funny...” ”

Isaac Asimov (1920 – 1992)

(Page intentionally left blank)

3. CHAPTER 3 METHODOLOGIES

3.1. Materials

The synthetic peptide, CMLb2a2-25, with an aminated C-terminus (TVHSIPLTINKEEALQRPVASFEP-NH₂), with a purity of 96.10%, was purchased from Caslo (Denmark). Dioctadecyldimethylammonium chloride, DODAC, was purchased from Tokyo Kasei (Japan). 1-monooleoyl-rac-glycerol (MO) was purchased from Sigma-Aldrich (USA). Disposable polystyrene cuvettes were purchased from Sarstedt (Germany). Disposable Zeta DIP cells were purchased from Malvern (UK). Nucleopore Track-Etch Membrane filters (200 nm) were acquired from Whatman (UK), and Amicon Ultra-15 Centrifugal Filter Units (50 000 NMWL) were purchased from Milipore (USA).

Human THP-1 cell line was purchased from ATCC (USA). Coating mAb (TNF3/4), Detection mAb (TNF5-biotin) and Streptavidin-ALP included in ELISA KIT for human TNF- α , were purchased from Mabtech (Sweden). Albumin from bovine serum (BSA) and Alkaline Phosphatase Yellow (pNPP) liquid substrate system for ELISA were purchased from Sigma-Aldrich (USA). Tissue culture test plates were purchased from TPP (Switzerland).

3.2. BCR-ABL peptide analyses

A citrate-phosphate buffer (150 mM KCl; 10 mM KH₂PO₄; 10 mM H₃BO₄ and 10 mM Na-citrate) was used to prepare peptide solutions at different pH (4, 7.2 and 9). Citrate-phosphate buffer has a pH ranging from 3 to 10 which makes this a suitable buffer to study peptide or liposome behavior in acidic, neutral and alkaline environments without changing the buffer.

HEPES buffer, 4-(2-hydroxyethyl)-1-piperazineethanesulfonic acid, at pH=7.2 (10 mM) was also used for comparison. HEPES has a pH ranging from 6.8 to 8.2, therefore, it cannot be used to study BCR-ABL peptide in strongly acidic or alkaline conditions. Nevertheless, this buffer is largely used in cell culture because it is better at maintaining physiological pH despite changes in carbon dioxide concentration, and at pH=7.2 would be suitable to mimic body fluids such as human blood stream.

Three peptide concentrations (10 µg/mL, 20 µg/mL and 40 µg/mL) were analyzed through DLS assays described in section 3.4, before and after sonication which is also described below.

3.3. Nanoparticles preparation

Peptide/lipid nanoparticles were prepared according to the methods described in section 2.1.2. Specific experimental work is described below.

A) Lipid film hydration / sonication

(i) Direct insertion

The DODAC:MO (1:2) lipid film at different lipid concentrations was first obtained by pipetting the adequate volumes of DODAC and MO ethanolic solutions (20 mM), previously prepared, to different test tubes. The ethanol solvent of the preparations was evaporated under nitrogen stream to obtain a homogenous lipid film. Then, 5 mL of peptide solution at a concentration of 0,01 mg/mL was added to the test tubes to hydrate the lipid films, allowing the peptide encapsulation in newly formed DODAC:MO liposomes at different concentrations (Figure 3.1 B). Thus, it was studied the peptide encapsulation at different peptide/lipid ratios. The preparations were then submitted to 5 consecutive cycles of a process in which they were vigorously vortexed and the exposed to 30 seconds of sonication.

(ii) Post-insertion

For replicates preparation, the lipid film lipid film was hydrated with 2.5 mL of HEPES and submitted to vortex and sonication, as mentioned. These replicates were then incubated with 2,5 mL of a peptide solution (0.02 mg/mL), so that we could obtain solutions at a final concentration of 0.01 mg/mL (Figure 3.1 A). These samples were left at 50°C for an hour before being analyzed.

B) Ethanolic injection

(i) Direct-insertion

Defined volumes taken from previously prepared stock solutions of DODAC (20 mM) and MO (20 mM) in ethanol, were injected in 5 mL of peptide solution, preheated to 50°C, under vigorous vortexing (Figure 3.1 D). The organic solvent (ethanol) evaporates when it comes in

touch with the water due to the heat. The solutions obtained are mostly composed of multi-vesicular liposomes.

(ii) Post-insertion

Replicates were prepared in which the desired volume of lipid was injected in 2,5 mL of HEPES preheated to 50°C, under vigorous vortexing. After this, 2,5 mL of a peptide solution (0,02 mg/mL) was added, so that we obtained solutions at a final concentration of 0,01 mg/mL (Figure 3.1 C). These samples were incubated with the peptide solution for a few hours, at room temperature, before being analyzed.

C) Extrusion

All the solutions obtained from all methods were submitted to an extrusion process in a Northern Lipids Lipex Extruder. Under a 4-8 bar pressure, the liposomes were forced to pass through polycarbonate filters with a defined pore size. In this case, the liposomes were submitted to five passages through a filter with a pore size of 200nm, at a temperature of 50°C. Multi-lamellar vesicles were transformed in large uni-lamellar vesicles using methods A and B schematized in figure 3.1. When multi-vesicular vesicles prepared by methods C and D pass through an extrusion filter, their enclosed vesicles are released, however, smaller multi-vesicular vesicles are still in the extruded preparation.

3.3.1. Preparation of liposomes for hydration and injection method

When preparing liposomes with mixed lipid composition, the lipids must first be dissolved and/or mixed in an organic solvent to assure a homogeneous mixture of lipids. In this work, DODAC and MO are dissolved in ethanol, separately, properly sealed and stored at 4°C. Depending on the peptide/lipid ratio desired to be tested and considering the ratio DODAC/MO (1:2), the corresponding amount of DODAC and MO are mixed.

3.3.2. Preparation of nanoparticles by post-insertion and direct-insertion

Five different methodologies were tested in order to compare and decide which one is more suitable to the purpose of this work (Figure 3.1). This section aims to clarify the strategies adopted: post-insertion and direct insertion.

(i) Post-insertion and direct-insertion

Figure 3.1 shows a representation of the different methodologies applied in this work to attach peptide molecules to lipid vesicles.

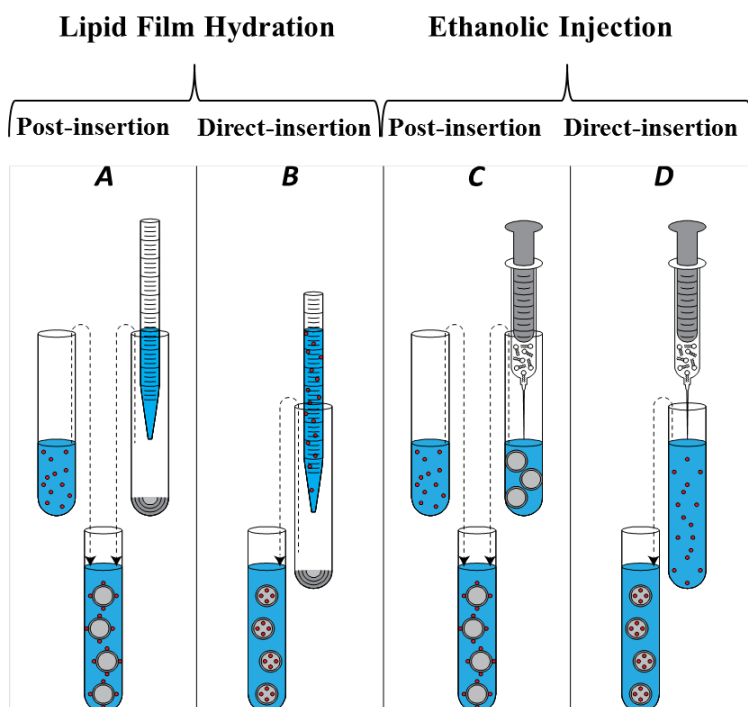


Figure 3.1 – Representation of the different methodologies applied in this work to encapsulate peptide molecules in lipid vesicles: A - Preparation of liposomes by lipid film hydration before adding peptide solution; B - Preparation of liposomes by lipid film hydration with peptide solution being added before lipid vesicles are formed; C - Preparation of liposomes by ethanolic injection before adding peptide solution; D - Preparation of liposomes by ethanolic injection hydration with peptide solution being added before lipid vesicles are formed (courtesy from João Neves - adapted).

Briefly, DODAC:MO (1:2) liposomes at different concentrations were prepared by lipid thin film hydration (Fig.3.1 A and B) and by ethanolic injection (Fig.3.1 C and D). In both methods, two different nanoparticles were obtained as the peptide solution could be added before or after lipid vesicles were formed, which may be referred as direct-insertion protocols (Fig.3.1 B and D) and post-insertion protocols (Fig. 3.1 A and C).

(ii) Effect of MLV liposomes and LUV liposomes in the final nanoparticle

Adding the peptide to the particles that were previously submitted to a process of extrusion is not the same as adding the peptide to liposomes that have not passed through extrusion. The extrusion process is known as being responsible for substances loss (Colletier, Chaize, Winterhalter, & Fournier, 2002; Xu, Costa, Khan, & Burgess, 2012). This motivated the inclusion of method E: liposomes prepared by lipid film hydration/extrusion followed by incubation with peptide after extrusion (Figure 3.2). At the left of figure 3.2 is represented one of the four methods described above, method A, and at the right is represented method E.

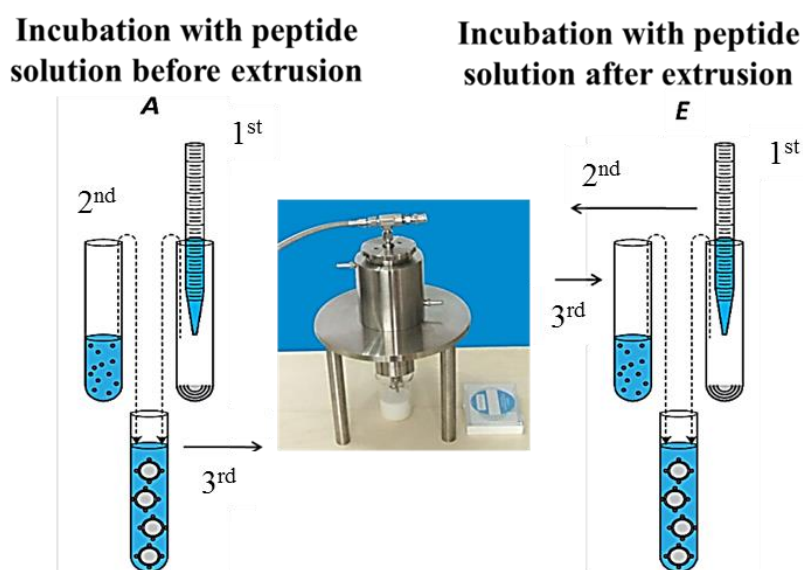


Figure 3.2 – Schematic representation of methods: A (left), preparation of liposomes by lipid film hydration (1st) before adding peptide solution (2nd) followed by extrusion (3rd); and method E (right), preparation of liposomes by lipid film hydration (1st) followed by extrusion (2nd) before adding peptide solution (3rd) (courtesy from João Neves – adapted).

Two peptide concentrations were tested (10 µg/mL and 20 µg/mL). By adding appropriate amounts of lipid from a stock solution of 20 mM of DODAC and MO concentration different peptide/lipid molar ratios were achieved and analyzed (Table 3.1).

Table 3.1 – Total lipid concentration (mM) peptide/lipid molar ratios, for 10 µg/mL and 20 µg/mL of peptide concentration.

10 µg/mL of peptide concentration	
[Lipid] (mM)	peptide-lipid molar ratio
1.75	1/500
1.05	1/300
0.875	1/250
0.7	1/200
0.35	1/100
20 µg/mL of peptide concentration	
[Lipid] (mM)	peptide-lipid molar ratio
1.75	1/250

3.4. Biophysical Characterization

3.4.1. Dynamic Light Scattering assays

The fate of intravenously injected liposomes is determined by a number of properties. Two of the most important are particle size and zeta potential. These techniques are described below.

“Dynamic light scattering” (DLS), also known as “photon correlation spectroscopy” (PCS) or “quasi-elastic light-scattering”, is a process that measures Brownian motion and relates this to the size of the particles (Pecora, 2000). Particles suspended in a liquid are never stationary. On the contrary, particles are constantly moving due to this Brownian motion, which correspond to the random collision with the molecules of the liquid that surrounds the particle. But what makes this useful is the fact that small particles move quickly and large particles move more slowly. Smaller particles are pushed further by the solvent molecules and move more rapidly. When a small particle is illuminated by a laser, it scatters the light in all

directions. This way, the laser illuminates the particles and the intensity fluctuations in the scattered light are analyzed. The Zetasizer Nano system is capable of measuring the rate of the intensity fluctuation and then uses this to calculate the size of the particles (Malvern, 2005).

The velocity of the Brownian motion is defined by a property known as the translational diffusion coefficient (usually given the symbol, D). The size of a particle, which is related to its speed due to Brownian motion, is calculated by using the Stokes-Einstein equation:

$$d(H) = kT / 3\pi\eta D \quad (3.1)$$

where:

$d(H)$ refers to the hydrodynamic diameter; D is the translational diffusion coefficient; k is the Boltzmann's constant; T is the absolute temperature and η represents viscosity.

A typical dynamic light scattering system comprises of six main components, has shown in Figure 3.3 ("Size theory," 2004). Firstly, a laser (1) provides a light source to illuminate the sample contained in a cell (2). For dilute concentrations, most of the laser beam passes through the sample, but some is scattered by the particles within the sample at all angles. A detector (3) is used to measure the scattered light. In the Zetasizer Nano series, the detector position will be at either 173° or 90° , depending upon the particular model.

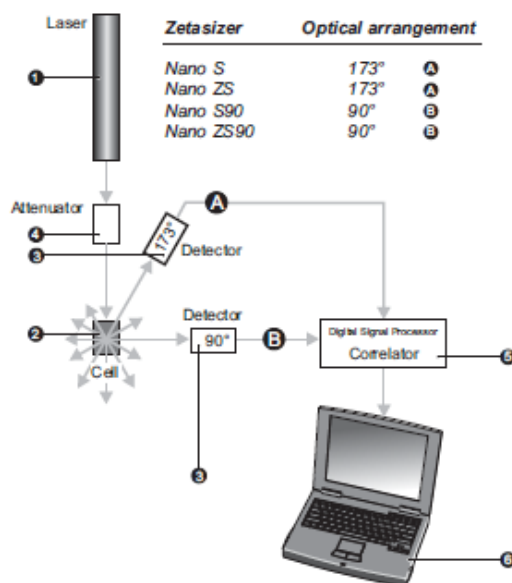


Figure 3.3 – Optical configurations of the Zetasizer Nano series for dynamic light scattering measurements (Malvern, 2005).

DLS is a convenient method to stability studies. Periodical DLS measurements of a sample can show the tendency to particles aggregation and sedimentation over time by seeing whether the hydrodynamic radius of the particle increases. If particles aggregate, there will be a larger population of particles with a larger radius (Schaffazick & Guterres, 2003).

3.4.2. Zeta (ζ) Potential assays

An efficient method to study the modification of particles surface is determining the zeta potential of nanoparticles in an aqueous environment. Briefly, the zeta potential is the overall charge a particle acquires in a particular medium. Both size and zeta potential can be measured on the same instrument that calculates the zeta potential by determining the Electrophoretic Mobility and then applying the Henry equation. The electrophoretic mobility is obtained by performing an electrophoresis experiment on the sample and measuring the velocity of the particles using Laser Doppler Velocimetry (LDV) (Malvern, 2005). Zeta potential measures the magnitude of the repulsion or attraction between particles charge. This measurement provides detailed information on dispersion and aggregation.

Knowledge of the zeta potential of a liposome preparation can help to predict the fate of liposomes *in vivo*. Any subsequent modification of the liposome surface can also be monitored by measurement of the zeta potential.

Due to their small size, the forces interacting on the surface of nanoparticles and in the dispersion liquid determine its behavior. Each particle may contain an electrical charge that can be positive or negative. If a particle is negative, it makes the positive ions in solution (called counter-ions, ions of opposite charge to that of the particle) to form a rigid layer around its adjacent surface; this layer of counter ions is known as Stern layer. Other positive ions may be attracted by the negative particle, but now they are repelled by the Stern layer. A dynamic equilibrium occurs and this results in the formation of a diffuse layer of counter-ions, which decrease with increasing distance from the surface of the particle. Thus an electrical double layer exists around each particle. Within the diffuse layer there is a notional boundary inside which the ions and particles form a stable entity. When a particle moves (e.g. due to gravity), ions within the boundary move with it, but any ions beyond the boundary do not travel with the particle. This boundary is called the surface of hydrodynamic shear or slipping plane, and the potential that exists at this boundary is known as the Zeta potential (Figure 3.4)(Malvern, 2005).

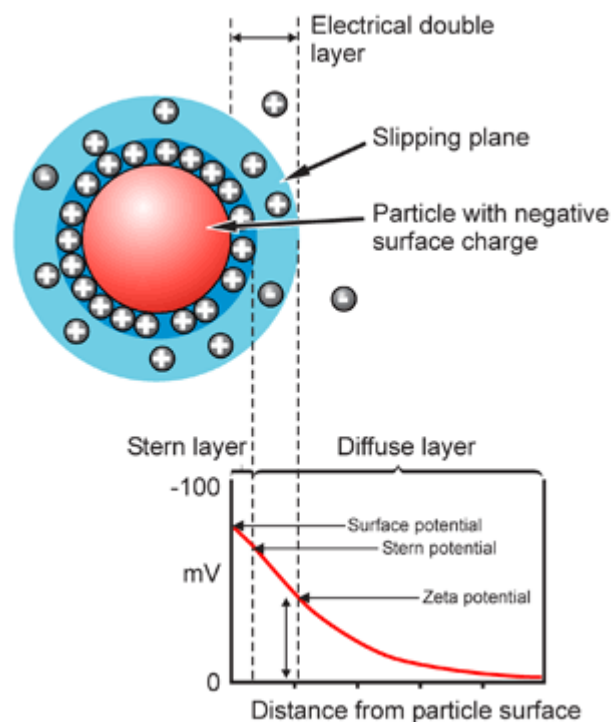


Figure 3.4 – Schematic representation of the double layer surrounding a particle in suspension (Malvern, 2005).

An individual particle and its associated ions move through the solution as a unit, and the potential at the border of the unit, Zeta potential can be measured in a simple manner, while the superficial charge cannot.

3.4.3. Electrophoresis and Electrophoretic Mobility

Electrophoresis consists on the migration of charged particles when an electric field is applied across an electrolyte. When this happens, charged particles suspended in the electrolyte are attracted towards the electrode of opposite charge. Viscous forces acting on the particles tend to oppose this movement (Figure 3.5). When equilibrium is reached between these two opposing forces, the particles move with constant velocity. This velocity is determined by the strength of electric field, the dielectric constant of and the viscosity of the medium, and by zeta potential. The light scattered at an angle of 17° is combined with the reference beam. This produces a fluctuating intensity signal where the rate of fluctuation is proportional to the speed of the particles. A digital signal processor is used to extract the characteristic frequencies in the scattered light (Malvern, 2005).

The velocity of a particle in an electric field is commonly referred to as its electrophoretic mobility. The zeta potential may then be determined using the Henry Equation:

$$U_E = \frac{2\varepsilon z f(ka)}{3\eta} \quad (3.2)$$

Where:

z refers to zeta potential; U_E is Electrophoretic mobility; ε is the dielectric constant; η is the viscosity; and $f(Ka)$ refers to Henrys function.

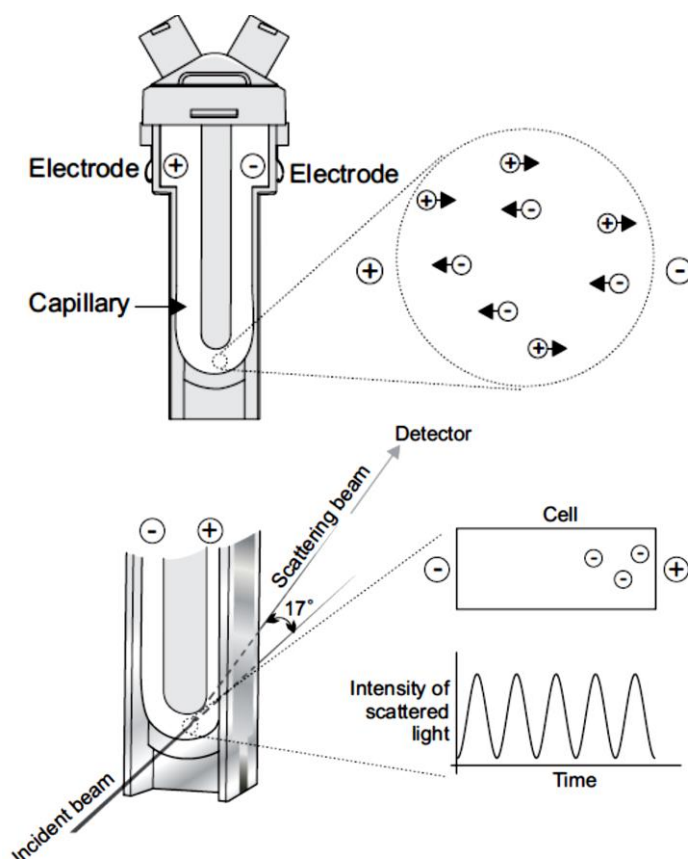


Figure 3.5 – The technique used to measure this velocity in Malvern’s Zetasizer Nano series (Malvern, 2005).

3.4.4. Mean diameter and zeta potential measurements

1 mL of each peptide-lipid samples was transferred to a 3 mL polystyrene disposable cuvette in order to determine the mean diameter of the nanoparticles. At least 5 measurements of each sample were considered to calculate the mean size (nm) average and respective standard deviation, in a Zetasizer Nano ZS equipment.

The same equipment was used to determine the superficial charge density of the peptide-lipid samples, and 1 mL of each was added to a 1 mL universal dip cell to measure ζ -potential value (mV).

If polydispersity is lower than 0,10, z-average values are reliable. On the other hand, if polydispersity is much higher than 0,10, the z-average is not trustworthy. Therefore, in these cases, the weighted mean size was calculated using the following formula:

$$\text{Weighted mean size} = \frac{\sum(\text{Population}_x \times \text{Mean size} \times \text{Population}_x\%)}{100} \quad (3.3)$$

3.5. Encapsulation Efficiency

A) Separation of encapsulated/non encapsulated peptide fractions by Amicon Centrifugation

To determine the encapsulation efficiency, it is necessary to separate liposomes from supernatant in order to quantify peptide amount in each of these two fractions. To do so, DODAC:MO (1:2) liposomes were centrifuged for 20 minutes, at 4500 g in 50 KDa amicons. Amicons are falcon-like tubes and were pre-washed with 5 mL of ultra-pure water on a centrifuge during 15 minutes at 4500g (4°C). These tubes have a filter unit that allows the separation of liposome-peptide complexes from the free peptide. The free peptide is so small that it is able to pass through the filter, and a peptide encapsulation fraction as well as a free peptide fraction can be obtained. After this, samples were frozen (-80°C) prior to lyophilization.

B) Liposome disruption

Triton-x (1%) was added to encapsulated fractions to disrupt liposomes, followed by vigorous vortexing in order to allow a quantification of encapsulated peptide. The lipid fraction was separated from the once encapsulated peptides after centrifugation during 20 minutes at 4500g. Samples were frozen (-80°C) prior to lyophilization. After lyophilization, samples were resuspended in a small volume before tricine gel separation, as described in the next section (section C).

C) Tricine–SDS-PAGE protocol and staining technique

The protocol used in this step is commonly used to separate proteins in the mass range 1–100 kDa (Schägger, 2006). It is the preferred electrophoretic system for the resolution of proteins smaller than 30 kDa. The peptide involved in this work is 2,4 kDa. The concentrations of acrylamide used in the gels are lower than in other electrophoretic systems. These lower concentrations facilitate electroblotting, which is particularly crucial for hydrophobic proteins. This protocol for Tricine–SDS-PAGE includes efficient methods for coomassie blue or silver staining.

After protocol described in paragraphs A and B above, three fractions for each sample were obtained: free peptide fraction; encapsulated peptide fraction; lipid fraction. On a first experiment, after lyophilization these fractions were dissolved in 100 μ L of water. It was then added 20 μ L of β .mercaptoethanol and 15 μ L of the total volume to each well. On a second experiment, these fractions were dissolved in 20 μ L of urea buffer (8 M), for lipid fraction and free peptide fraction, and in 50 μ L of urea buffer for encapsulated peptide fraction. It was then added 5 μ L of β .mercaptoethanol to samples dissolved in 20 μ L of urea and 10 μ L β .mercaptoethanol were added to samples dissolved in 50 μ L. After this, 35 μ L of each sample were loaded in each well. Finally, gels were stained with coomassie blue and with silver stain.

3.6. Delivery of antigenic BCR-ABL junctional peptide

Since this work aims to create an innovative system to treat chronic myeloid leukemia, combining lipid vesicles with a CML peptide, TNF- α quantification can be the proper approach to evaluate the system's ability to stimulate an immune response. Tumor Necrosis Factor-alpha (TNF- α) is a pro-inflammatory cytokine that mediates several chronic inflammatory diseases. It is produced and secreted primarily by macrophages and monocytes in response to a bacterial inflammation or a tumor. The overproduction of TNF- α is strongly involved in acute inflammation and chronic inflammatory diseases as it plays an important role in host defense and immunosurveillance.

Large amounts of TNF- α are released in response to lipopolysaccharide, LPS (Moreira-Tabaka et al., 2012; Pérez-Pérez, Shepherd, Morrow, & Blaser, 1995). Thus, LPS was

primarily tested to prove that the dose used is capable of inducing TNF- α production and that THP-1 cells are responsive to this lipopolysaccharide.

3.6.1. Cell Culture

Human THP-1 cells, cell line derived from the peripheral blood of a patient with acute monocytic leukemia, were grown in RPMI1640 supplemented with 20% of FBS, 1% of an antibiotic/antimycotic solution and 1% of L-glutamine, with 5 % CO₂ at 37 °C. This monocytic cell type is characterized by suspension growth. This cell line is used as a model for mimicking the function and regulation of monocytes and macrophages (Qin, 2012).

3.6.2. LPS Extraction assay

LPS was extracted from *E. coli* HB101 strain grown for 24h at 37°C with stirring, in lysogeny broth (LB) medium. Then 50 mL of cells were collected in a stationary phase with an optical density (660 nm) of approximately 0.8. Cells were washed twice with PBS (1x) and resuspended in 1 mL of RPMI medium without FBS. After this, cells were incubated at 100°C for 10 minutes to disrupt cells and release LPS, and filtered with a 0.2 μ m pore size filter. The filtrate fraction was applied to THP-1 cells.

3.6.3. LPS Activation assay

First, cells were centrifuged at 1100 rpm for 7 minutes (25°C). After obtaining the pellet, the supernatant was removed and 3mL of RPMI medium was added. To count cells a small volume was analyzed in Neubauer chamber. Then, each well of a 24-well culture plate was loaded with a volume of 500 μ L of THP-1 cells culture at a density of 0.5×10^6 cells/mL and 100 μ L of LPS at 0%, 25%, 50% and 100% were incubated with cells. Samples were collected to micro tubes and frozen after 4h, 12h and 24h of incubation. The response of stimulated THP-1 cells was assessed by determining the amount of TNF- α using an ELISA KIT for human TNF- α in a 96 well tissue culture plate.

3.6.4. Peptide and Peptide/DODAC:MO(1:2) Activation assay

The same protocol described for LPS activation assay was used in this step. To understand if BCR_ABL peptide used in this work could stimulate the production of TNF- α , six peptide concentrations dissolved in HEPES buffer were tested: 5, 10, 20, 50, 80 and 100 $\mu\text{g/mL}$. Samples were collected and frozen after 4h of incubation with cells, prior to TNF- α quantification with ELISA KIT.

Peptide/DODAC:MO(1:2) complexes were prepared by method E and C, as mentioned in section 1.2.1.1. Initially, 5 mL of samples at 1/300 and 1/500 molar ratio were produced. Then, samples were centrifuged for 20 minutes, at 4500 g in 50 KDa amicons and free peptide fraction was separated from peptide encapsulated fraction. This separation resulted in a volume of 2.1 mL for each encapsulated fraction which means that peptide and lipid concentrations were increased. Then, the same protocol for LPS and peptide activation was used to test peptide/DODAC:MO(1:2) formulations.

3.6.5. ELISA assay procedure

The Enzyme-Linked Immuno Sorbent Assay (ELISA) is a specific and highly sensitive method for quantitative measurements of cytokines or other analytes in solutions. This assay is suitable for the quantification of soluble mediator TNF- α . ELISA kit for human TNF- α is easy to conduct and commonly used in laboratory.

This assay is based on the use of a combination of two monoclonal coating antibodies, TNF3 and TNF4. The first monoclonal antibody (mAb) is coated on a microplate and is able to capture the cytokine of interest. The second antibody is used for detection as it binds to a different epitope on the cytokine. This detection antibody is, in turn, labeled with biotin, which allows subsequent binding of a Streptavidin-conjugated enzyme. Any unbound reagents are washed away. When substrate is added, a color reaction will develop that is proportional to the amount of cytokine bound. The concentration of cytokine is determined by comparison with a standard curve with known concentrations of cytokine ("Mabtech," 2013). Figure 3.6 illustrates the basic concept of the ELISA technique.

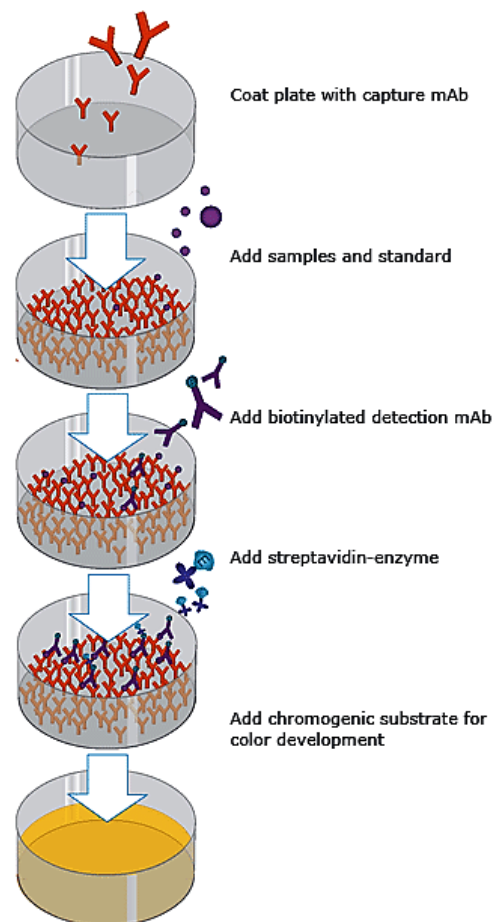


Figure 3.6 – The ELISA technique illustrated (“Mabtech,” 2013).

3.6.5.1. Experimental work

First, each microplate well is incubated with 100 μL of mAb TNF 3/4 overnight at 4-8°C. After washing with 200 μL of PBS twice, each well is incubated with 200 μL of incubation buffer (PBS (1x), 0.05% Tween and 0,1% BSA) for 1h at room temperature, after which wells are washed again five times with PBS containing 0.05% Tween. Then, 100 μL /well samples and TNF- α standards previously prepared are added and incubated for 2h at room temperature. After washing five times with incubation buffer, 100 μL of mAb biotin at 1 $\mu\text{g}/\text{mL}$ (in incubation buffer as well) were incubated for 1h at room temperature. After washing five times with incubation buffer again, 100 μL of Streptavidin-ALP diluted 1:1000

in incubation buffer were incubated for 1h at room temperature. After washing five times with incubation buffer for the last time, 100 μ L of pNPP substrate were added and optical density was measured (405 nm) in an ELISA reader after 15 minutes.

Chapter 4

Results and Discussion

“The important thing in science is not so much to obtain new facts as to discover new ways of thinking about them”

William Lawrence Bragg (1890 – 1971)

(Page intentionally left blank)

4. CHAPTER 4 RESULTS AND DISCUSSION

With this work we pretend to find the best methodology to produce a nanoparticle (peptide/liposomes) with the best physic-chemical properties (ex: size, surface charge and encapsulation efficiency) in order to test its potential to be used as liposomal vaccine.

DODAC:MO (1:2) liposomes were prepared using three different preparation methods: lipid film hydration (MLV), lipid film hydration/extrusion (SUV), ethanolic injection (MVV) and ethanolic injection/extrusion.

The nanoparticles (peptide/liposome) were prepared using five different protocol (A, B, C, D, E):

A – liposomes prepared by lipid film hydration (MLV) followed by peptide incubation;

B – liposomes prepared by lipid film hydration (lipid/peptide);

C – liposomes prepared by ethanolic injection (MVV) followed by peptide incubation;

D – liposomes prepared by ethanolic injection (lipid/peptide);

E – liposomes prepared by lipid film hydration/extrusion followed by peptide incubation.

Three different peptide concentration were studied, 10 µg/mL, 20 µg/mL and 40 µg/mL, and several total lipid concentration (0.35 mM, 0.7 mM, 1.05 mM, and 1.75 mM) were tested in order to get different peptide/lipid molar ratio (1/100, 1/200, 1/300, and 1/500).

The physicochemical properties of peptide/DODAC:MO (1:2) complexes were thoroughly analyzed by DLS assays (mean size and zeta-potential). Since DODAC and MO molar ratio are kept constant, it is expectable that all modifications observed in particles structure will be caused by the changes on peptide/lipid molar ratio due to the increase of lipid or peptide concentration and also preparation methodologies.

Zeta potential and mean diameter are two structural parameters that enabled the physicochemical characterization of the final peptide/lipid nanoparticle, and further evaluation of its applicability as liposome vaccine.

The z-average value giving by the Zetasizer Nano ZS equipment was carefully considered in the samples where the polydispersity index was superior to 0.10. If polydispersity is lower than 0.10 z-average values are reliable. On the other hand, if polydispersity is much higher than 0.10 the z-average cannot be used and we should analyze the population's distribution. The size distributions of the samples were analyzed individually and a new mean particle diameter was calculated through the weighted mean of the most representative size peaks of the samples.

4.1. Effect of pH, peptide concentration and sonication

Before studying the encapsulation efficiency of BCR-ABL peptide into the liposomes, the peptide behavior in buffer solutions at different pH was separately analyzed in terms of mean size and surface charge. These results may provide an insight of peptide structural conformation changes and its degree of aggregation in solution which may play an important role on peptide-liposomal membrane electrical attraction (Friede et al., 1993; Gregory Gregoriadis, 2007a; Ikonen, Murtomäki, & Kontturi, 2010; Strömstedt et al., 2010). Thus, this study emerges as an attempt to characterize and to know the most suitable pH condition to solubilize the peptide prior to liposome encapsulation.

At this point we would like to know if this peptide could resist to sonication, and if this procedure could induce some level of peptide disaggregation. Therefore, peptide behavior after sonication was thought important to study.

(A) pH effect

Three different concentrations of peptide (10 µg/mL, 20 µg/mL, 40 µg/mL) were solubilized in a citrate-phosphate buffer at pH 4, 7.2 and 9. Figure 4.1 shows the weighted mean size and z-potential values for three different peptide concentrations at different pH condition, before and after sonication.

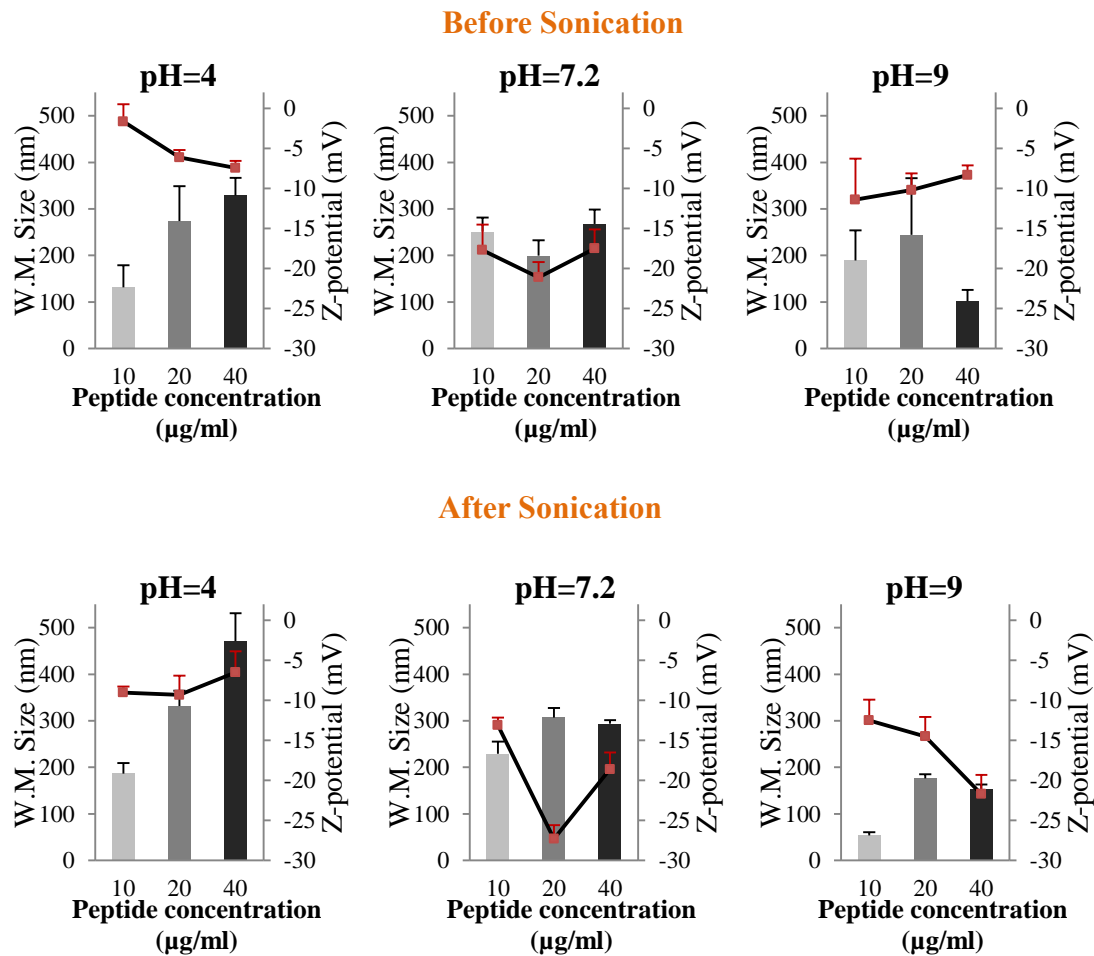


Figure 4.1 – Results of weighted mean size (nm) (bars - left axis) and z-potential (mV) (—■— - right axis) for preparations of 10 µg/mL, 20 µg/mL and 40 µg/mL of BCR-ABL peptide, in citrate-phosphate buffer at pH=4, 7.2 and 9, before and after sonication.

From Figure 4.1 we can observe that the peptide has a distinct behavior depending on pH conditions. Generally, before and after sonication the highest mean sizes were observed in acidic conditions, varying between 131.2 nm and 450 nm depending on the peptide concentration. On the contrary, the smaller mean sizes were noted in alkaline conditions (pH=9), varying from 50 nm and 244.3 nm. At neutral conditions (pH=7.2) the mean sizes are more similar and not so concentration dependent varying from 199.1 nm to 268 nm.

We can also observe that pH has also greater influence in the peptide surface charge. At pH=4, z-potential are the lowest being close to zero, while at pH=9 the peptide exhibited a

stronger negative charge. However, the highest z-potential values were observed at neutral pH.

From Figure 4.1 we can note that sonication was responsible for changes in mean sizes and z-potential at the three pH conditions, with the exception for the mean sizes at pH=7.2 that were not significantly changed.

Before sonication

(i) pH 7.2

At neutral conditions, with increasing peptide concentration, an increase in z-potential was first observed followed by a decrease: -17.7 mV (10 μ g/mL), -21.2 (20 μ g/mL) and -17.5 mV (40 μ g/mL).

The mean sizes of the three concentrations are similar: 251.3 nm (10 μ g/mL), 199.1 nm (20 μ g/mL), 268 nm (40 μ g/mL). Despite a decrease at 20 μ g/mL, mean sizes at neutral pH are not so concentration dependent.

At neutral pH, as H⁺ ions and HO⁻ ions are in equilibrium, it is expected a negative surface charge (z-potential) due to the balance between the four negative amino acid residues (one aspartic acid and three glutamic acids) and the two positive ones (arginine and lysine) that make up the BCR-ABL peptide (Table 2.1). Moreover, as most proteins at physiological pH, this peptide 's amino acids are above their isoelectric points, which results in a net negative charge (Mangino & Harper, 2007). From Figure 4.1 we can confirm that the BCR-ABL peptide is, in fact, characterized by an overall negative surface charge.

(ii) pH 4

At pH=4, the peptide has a different behavior depending on peptide concentration. Figure 4.1 shows that an increase in peptide concentration leads to an increase in negative surface charge: -1.6 mV (10 μ g/mL), -6.1 mV (20 μ g/mL) and -7.4 mV (40 μ g/mL). Nevertheless, in acidic condition, the peptide showed the negative surface charge more close to zero.

The weighted mean size follows the same trend as it increases with increasing peptide concentration: 131.2 nm (10 μ g/mL), 273.7 nm (20 μ g/mL) and 328.6 nm (40 μ g/mL). Generally, higher mean sizes were observed at pH=4 when compared to the neutral and alkaline conditions. This is in accordance to a reported study that reveals that an hydrophobic

peptide forms aggregates under acidic conditions (Do et al., 2013), which can explain the increase in mean size.

The pKa and pI values of the BCR-ABL peptide's amino acids (see section 2.2.2) explains that at lower pH the most (once negative) amino acids are more likely to have a surface charge close to zero while the positive ones remain positively charged. In fact, at pH=4, the pH is lowered far below the isoelectric point of most amino acids, the peptide will lose some negative charge and contain more positive charges which results in a net charge closer to zero. When pH is lowered far below the isoelectric point (pH=4), the peptide will lose its negative charge and contain more positive charges. The excess of H⁺ ions at acidic conditions, that neutralize negative amino acids, also play a role in the decrease of the surface charge observed at pH=4.

Results may suggest that the peptide has been denatured. A common misconception is that since a peptide is a short protein, it is as unstable as protein but the truth is that a peptide is much more stable than a protein because, for example, due to their short length most peptides do not have tertiary structure which is unstable because it is held together by non-covalent bonds such as electrostatic interaction. So, a peptide can only be damaged by covalent modification or break of peptide bonds and the term "denaturation" cannot be applied in this case. Because the secondary structures peptides are stabilized by weak, non-covalent interactions, these structures are easily disrupted by agents that disrupt these interactions, including changes in pH, among other parameters, which may end in loss of function.

Since the helices and sheets are held together by hydrogen bonds, any condition that may interfere with the formation of these bonds can disrupt and destroy the structure. High concentrations of H⁺ interfere with the formation of hydrogen bonds. Under these assumptions, results indicate that an acidic pH induces a change in the structure of the peptide resulting in a possible change of peptide activity. In fact, structural changes induced by denaturation under acidic conditions has been demonstrated by a number of techniques (López-Alonso et al., 2010).

(iii) pH 9

At alkaline conditions, the peptide has a different behavior depending on peptide concentration. An increase in peptide concentration leads to a decrease in negative surface charge: -11.4 mV (10 µg/mL), -10.2 mV (20 µg/mL) and -8.3 mV (40 µg/mL).

With increasing peptide concentration, the weighted mean size first suffers an increase followed by a decrease: 189.1 nm (10 μ g/mL), 244.3 nm (20 μ g/mL) and 101.7 nm (40 μ g/mL).

At alkaline pH positive amino acids may still be positive but close to zero, while negative amino acids remain negative and are in higher number. At pH=9 HO⁻ ions neutralize some peptide positive charges, which also contribute to the increase in negative surface charge when compared to acidic conditions.

The effects of high pH are analogous to those of low pH (Mangino & Harper, 2007) and can cause peptide damage. However, at alkaline pH the peptide obtained a stronger negative charge when compared to acidic conditions. This may be partially explained by the fact that pH=9 is largely above most amino acids isoelectric point, contrary to what happens at pH=4. Furthermore, the difference between pH=7.2 and pH=4 is 3.2, while the difference between pH=7.2 and pH=9 is much lower, 1.8. Thus, despite both acidic and alkaline conditions induce a change in peptide structure that leads to the decrease of z-potential when compared to the neutral condition, this change is also observed at pH=9, although, in less extension.

When pH is increased, at pH=9, mean sizes decreased when compared to neutral condition. In fact, it is visible the appearance of smaller populations (Appendix I), explaining the decrease in the weighted mean size. This suggests some level of disaggregation at this pH condition compared with the acidic and neutral conditions. Despite alkaline pH has a different effect in peptide mean sizes when compared to pH=4, a change in its structure is also suggested.

Both z-potential and mean size results suggested that a neutral pH is the proper condition to solubilize the peptide, maintaining its secondary structure and function. With a strong negative z-potential at pH=7.2, this peptide is expected to be attracted to cationic liposomes successfully (Friede et al., 1993; Gregory Gregoriadis, 2007a; Ikonen et al., 2010; Strömstedt et al., 2010). The three peptide concentrations tested are suitable to be used in the liposome encapsulation study.

After Sonication

Sonication, or ultrasound, is often utilized to disperse the substances. Although sonication cannot destroy covalent bond, it can have a profound influence on weak chemical bonds such as hydrogen, hydrophobic and ion bonds. Generally, after 10 seconds of sonication the samples presented higher negative surface charge for all pH conditions, however the

sonication procedure had greater impact either in mean size or z-potential values at alkaline conditions.

(i) pH 7.2

At neutral pH, z-potential values followed the same trend as before sonication, although they became more intense. With increasing peptide concentration, an increase in z-potential was first observed followed by a decrease: -13.1 mV (10 µg/mL), -27.5 mV (20 µg/mL) and -18.6 mV (40 µg/mL). A peculiar high z-potential is observed for 20µg/mL before and after sonication as well.

The mean sizes of the three concentrations generally increased when compared to mean sizes before sonication but the peptide concentration apparently did not induce significant changes as well: 229.5 nm (10 µg/mL), 306.9 nm (20 µg/mL), 294.1 nm (40 µg/mL). Despite a smaller value at 10µg/mL, mean sizes at neutral pH are still not so concentration dependent when compared to pH=4 and 9.

(ii) pH 4

At pH=4, after 10 seconds of sonication, mean sizes increased but followed the same trend as with increasing peptide concentration mean sizes increased: 186.4 nm (10 µg/mL), 331.4 nm (20 µg/mL) and 470.8 nm (40 µg/mL); similar to what was observed before sonication.

A significant change was observed in z-potential. After sonication, generally the three z-potential values increased and suffered an inversion, as it decreased with increasing peptide concentration this time: -9 mV (10 µg/mL), -9.3 mV (20 µg/mL) and -6.99 mV (40 µg/mL).

(iii) pH 9

At alkaline pH (pH=9), the sonication procedure had greater impact either in mean size or z-potential values. Mean sizes decreased and followed a different trend, while z-potential increased and followed a different trend as well.

Peptide surface charge increased with increasing peptide concentration: -12.5 mV (10 µg/mL), -14.5 mV (20 µg/mL) and -21.7 mV (40 µg/mL). While mean sizes first suffered an increase followed by a decrease: 53.7 nm (10 µg/mL), 175.1 nm (20 µg/mL), 153.2 nm (40 µg/mL).

An increase in negative charge after sonication suggests that negative amino acids are more exposed and, therefore, the peptide should be less aggregated. If peptides are dispersed rather than aggregated, its charge superficial density should be higher as well as its electrophoretic mobility, therefore, increasing the negativity of z-potential. However, the increase in most of the mean sizes after sonication is not in agreement with the disaggregation hypothesis. Somehow, sonication procedure is responsible for exposing more negative amino acids.

Circular dichroism would be useful to confirm, or not, changes in peptide structure (Purdie, Brittain, Towell, & Manning, 1994). However, has been shown that sonication procedure did not induce changes on a peptide's secondary structure using the same technique (Ruan, Luo, Zhang, & Xing, 2013). Nevertheless, results show a different peptide behavior before and after sonication.

Furthermore, sonication is, apparently, responsible for decreasing PDI values (Silva et al., 2008). The same was observed in this work for most of the samples while a few of them were kept constant (Appendix I).

Different trends were observed with increasing peptide concentration at acidic and alkaline pH before and after sonication. However, this was not so evident at neutral pH where the peptide is suggested to be more stable, which lead us to believe that the peptide integrity is more ashored at neutral conditions.

The behavior of different peptide concentrations vary from peptide to peptide, therefore, reported studies concerning this subject may be contradictory. Since information about this BCR-ABL peptide is hard to find, we present here, possibly, its first biophysical characterization under different pH conditions.

B) Buffer effect

Three different concentrations of peptide (10 µg/mL, 20 µg/mL, 40 µg/mL) were solubilized in a citrate-phosphate buffer and HEPES buffer at pH=7.2. Figure 4.2 shows z-potential and z-average results, before and after sonication.

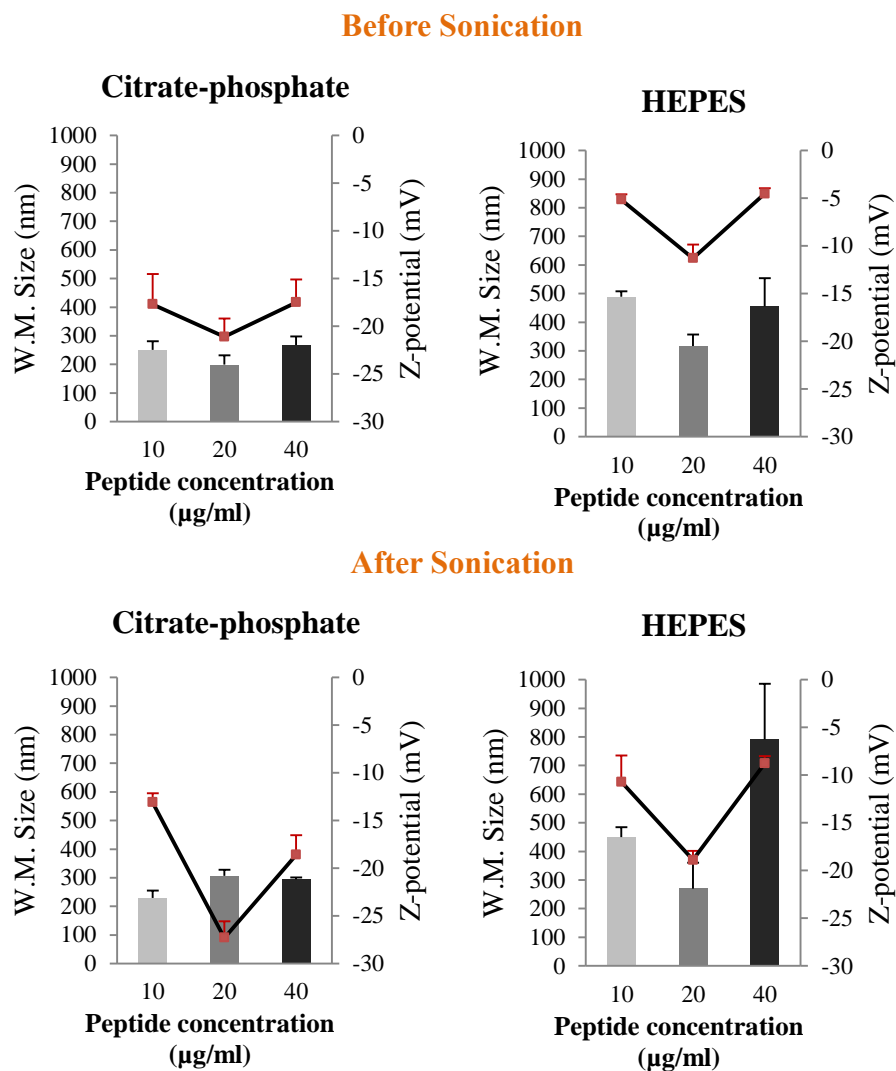


Figure 4.2 – Results of weighted mean size (nm) (bars - left axis) and z-potential (mV) (—■— - right axis) for preparations of 10 µg/mL, 20 µg/mL and 40 µg/mL of BCR-ABL peptide, in HEPES buffer and citrate-phosphate buffer at pH=7.2, before and after sonication.

From Figure 4.2 we can observe that when peptide is dissolved in HEPES (pH=7.2) instead of citrate-phosphate buffer at the same pH conditions, the weighed mean sizes are much higher and present less negative surface charge (before and after sonication). A peculiar increase in negative surface charge is observed at 20 µg/mL of peptide concentration for both buffers (before and after sonication), suggesting a concentration dependent behavior.

Citrate-phosphate buffer (150 mM KCl; 10 mM KH₂PO₄; 10 mM H₃BO₄ and 10 mM Na-citrate) is composed of significantly more salts than HEPES (10 mM). Therefore, these results

indicate that an increase in the amount of salts induce a change in the structure of the peptide so that a decrease in particles mean size is achieved. This suggests that peptide particles are more disaggregated in citrate-phosphate buffer. Higher z-potential values may be due to a higher exposition of negative amino acids that resulted from the particle disaggregation. However, the possibility that citrate-phosphate may be unfolding the peptide secondary structure cannot be confirmed and should be considered. High ionic strength that affect proteins and peptides may be achieved, among others, by high or low pH, but also by a high quantity of salts which can result in loss of function (Mangino & Harper, 2007). Electrostatic binding between peptides and liposomes may be salt sensitive as shown in other works (Colletier et al., 2002), which can affect the encapsulation efficiency of amphiphilic peptides, such as BCR-ABL peptide under study (Strömstedt et al., 2010).

After sonication, mean sizes do not vary significantly, with the exception for 40 μ g/mL of peptide concentration in HEPES buffer that increased significantly. However, a decrease in z-potential was observed for all peptide concentrations of both buffers. Apparently, sonication has influence on exposing more negative amino acids but a role on particle disaggregation cannot be confirmed.

The PDI values decreased in a few samples but were kept constant for most of them. Appendix I show further information, a detailed size distribution.

A peptide concentration of 10 μ g/mL was used in the subsequent work to obtain preliminary results about the most suitable lipid/peptide molar ratio and method of preparation. As peptide integrity was not accessed and particle disaggregation using sonication could not be confirmed, we decided to use a peptide solution without ultrasound treatment.

4.2. Incorporation of BCR_ABL peptide into DODAC:MO(1:2) liposomes

4.2.1. Citrate-phosphate versus HEPES

In a first attempt, peptide/liposomes nanoparticles were prepared in citrate-phosphate (pH=4, 7.2 and 9) and HEPES (pH=7.2) buffer. Not for a particular reason, method C (liposomes prepared by ethanolic injection followed by peptide incubation) and a 1/500 peptide /lipid molar ratio were chosen to be tested in the first place.

Figure 4.3 shows a photography of DODAC:MO(1:2) liposomes prepared by ethanolic injection in citrate-phosphate buffer at pH=9.



Figure 4.3 – Photography of DODAC:MO(1:2) liposomes prepared by ethanolic injection in citrate-phosphate buffer at pH=9.

Firstly, a volume of DODAC:MO was injected in a citrate-phosphate buffer solution (pH=9) but lipid precipitation was observed immediately (Figure 4.3), so incubation with a peptide citrate-phosphate solution was not necessary to be done.

Secondly, when liposomes were prepared in HEPES buffer precipitation was not observed. After incubating these liposomes with a peptide HEPES solution, precipitation was not detected as well.

As the previous results indicated that citrate-phosphate buffer provides peptide particles with higher z-potential, as an alternative, we intended to prepare liposomes in HEPES buffer prior to incubation with a peptide citrate phosphate solution (pH=9). DODAC:MO precipitation was not noted after injecting this lipid in an HEPES solution, however, it was observed after incubating these liposomes with a peptide citrate-phosphate solution. Although in less extension, the sample appearance was similar to what is shown in figure 4.3.

Lipid precipitation was also detected at pH=4 and 7.2 in citrate-phosphate, however, it was never observed when using HEPES (pH=7.2). As citrate-phosphate buffer contains significantly more salts than HEPES, this may explain the lipid precipitation. In fact, salts content is a critical issue and is responsible for inducing changes in liposomes (Gregory Gregoriadis, 2007b; Sabín, Prieto, Ruso, Hidalgo-Alvarez, & Sarmiento, 2006). The fact that a specific salt may be the cause for this can also be considered. However, further information about the interaction between DODAC and MO with the salts involved in this work is not available.

HEPES buffer resulted to be more appropriate. On the contrary, citrate-phosphate buffer is not appropriate to prepare liposomes at any pH condition. Taking in consideration that HEPES buffer mimics body fluids, such as human blood stream, and it is largely used in cell culture, due to the better performance on maintaining physiological pH despite changes in carbon dioxide concentration, this work was continued using HEPES buffer at a pH=7.2. Furthermore, HEPES has been used to prepare liposomes in a number of studies (Ikonen et al., 2010; Wattraint, Saadallah, Silva-Pires, Sonnet, & Sarazin, 2013; Xu, Costa, Khan, et al., 2012), as well as to prepare specifically DODAC liposomes (Feitosa, Alves, Castanheira, & Oliveira, 2009).

4.2.2. Incubation time

In order to know how much time it was necessary to incorporate the peptide in liposomes so that a stable nanoparticle could be achieved, a formulation of peptide/lipid molar ratio of 1/500 was prepared by post-insertion protocols: method A, liposomes prepared by lipid film hydration (MLV) followed by peptide incubation, and method C, liposomes prepared by ethanolic injection (MVV) followed by peptide incubation. The mean sizes and z-potential were measured after 1 and 5 hours of peptide incubation at a concentration of 10 μ g/mL.

Results for method A and C are presented in figure 4.4 and 4.5.

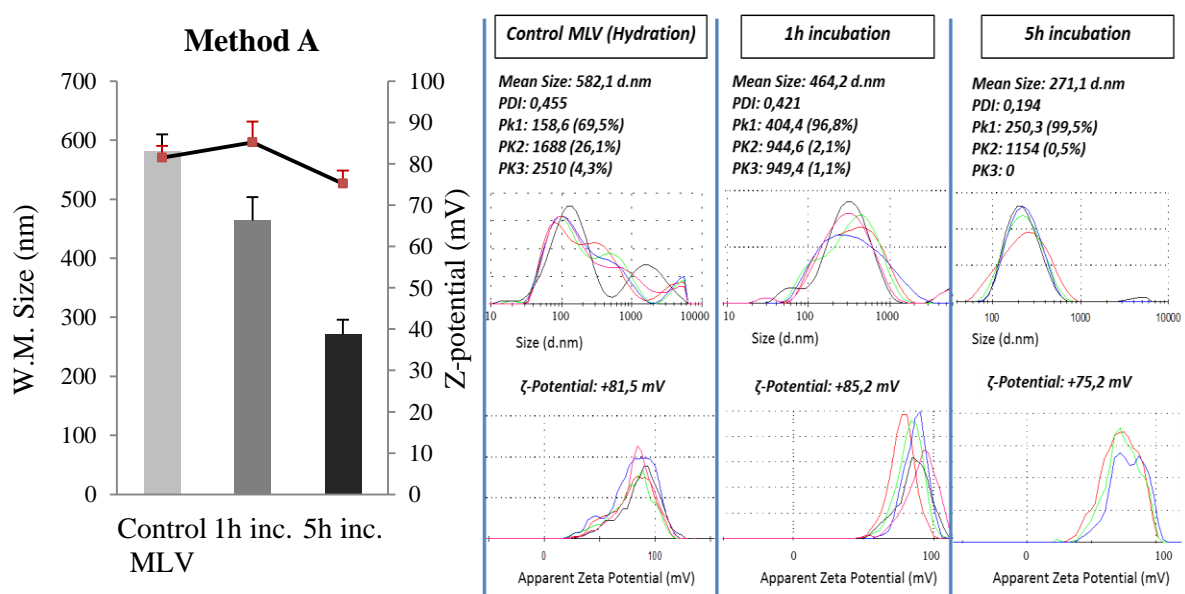


Figure 4.4 – At the left side are presented results of weighted mean size (nm) (bars - left axis) and z-potential (mV) (—■— - right axis) for lipid vesicles (control) and peptide/DODAC:MO nanoparticles prepared by method A at 1/500 molar ratio. At the right side are presented the distribution of intensity profiles of the respective mean size and z-potential.

Figure 4.4 shows that when nanoparticles are prepared by method A their weighted mean sizes decrease with increasing incubation time varying from 582.1nm to 271.1nm.

Z-potential values after 1h of incubation suffers a slight increase (from +81.5 mV to +85.2mV) decreasing after 5h of incubation (from +85.2 mV to +75.2 mV).

These results suggest that first we must have an electrostatic interaction between the positive charge of the liposome and the negative charge of the peptide, and after 5h of incubation more positive charge of liposome may be neutralized, resulting in a nanoparticle of smaller size and lower surface charge.

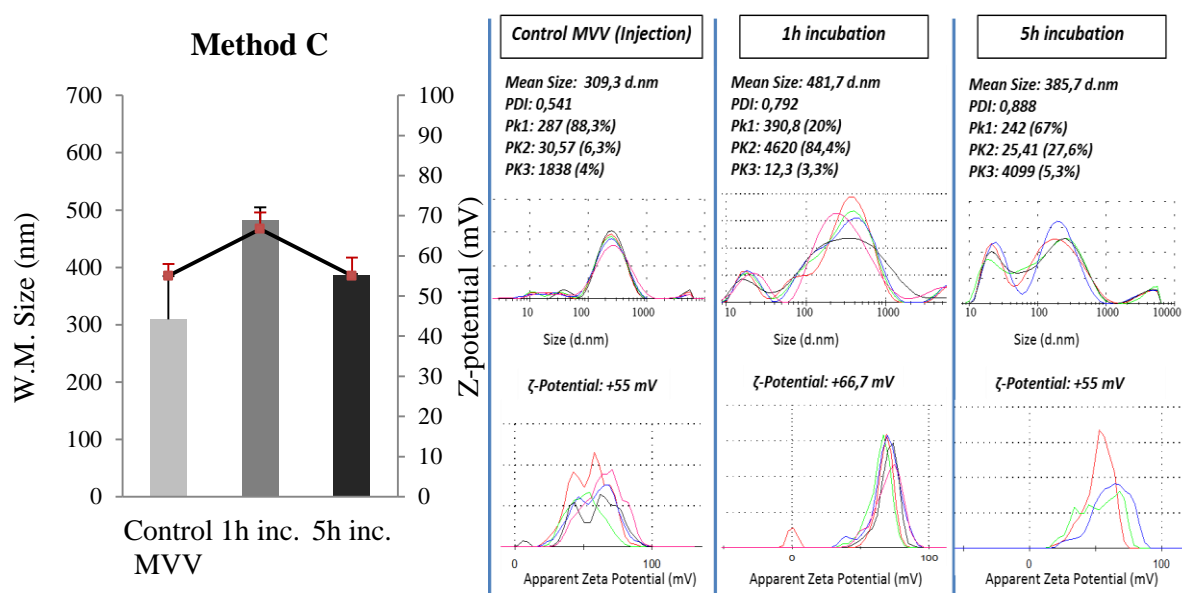


Figure 4.5 – At the left side are presented results of weighted mean size (nm) (bars - left axis) and z-potential (mV) (—■— - right axis) for lipid vesicles (control) and peptide/DODAC:MO nanoparticles prepared by method C at 1/500 molar ratio. At the right side are presented the distribution of intensity profiles of the respective mean size and z-potential.

Figure 4.5 shows that when nanoparticles are prepared by method C their weighted mean sizes increases after 1h of incubation, decreasing after 5h. Through the size distributing profile we can observe that the ethanolic injection method produces a more heterogeneous population of nanoparticles and a higher mean size compared with the control.

Z-potential values after 1h of incubation suffers a slight increase (+55 mV, +66.7 mV) decreasing after 5h of incubation (+55 mV, +55 mV).

These results suggest that lipid film hydration (MLV) produce different nanoparticles in terms of size and zeta-potential when compared with ethanolic injection (MVV), and the peptide incubation time influences the organization of the final nanoparticle. Nevertheless, 1h of incubation was thought sufficient to continue the subsequent work of this thesis. Direct-

insertion protocols, methods B and D, were not tested at this stage; however, samples prepared by these methods were chosen to be analyzed 1h after preparation as well as in the subsequent work.

The study from this section provides an insight on how much time is necessary to achieve charge neutralization (electrostatic interaction between liposomes and peptides) within one peptide/lipid molar ratio, as the same incubation time will be used in all nanoparticles characterized in this thesis. A detailed study about the exact time of incubation in which the final nanoparticle is the most properly organized would be valuable in future works after choosing the proper peptide/lipid formulation.

4.2.3. Effect of the preparation methods on nanoparticles behavior in solution

Four methodologies were used to encapsulate peptide molecules at 10 μ g/mL concentration using four different peptide/lipid molar ratios: 1/100; 1/200; 1/300 and 1/500 and the final nanoparticles were analyzed by DLS assays 1h after preparation/incubation, before and after extrusion.

(i) Lipid film hydration: Direct- insertion versus Post-insertion

Figures 4.6 to 4.9 show z-potential (mV) and weighted mean diameter (nm) values for formulations prepared by post-insertion protocol, method A (lipid hydration/peptide incubation), and direct-insertion protocol, method B (lipid hydration with peptide solution), after extrusion. Results for nanoparticles before extrusion are presented in Appendix II.

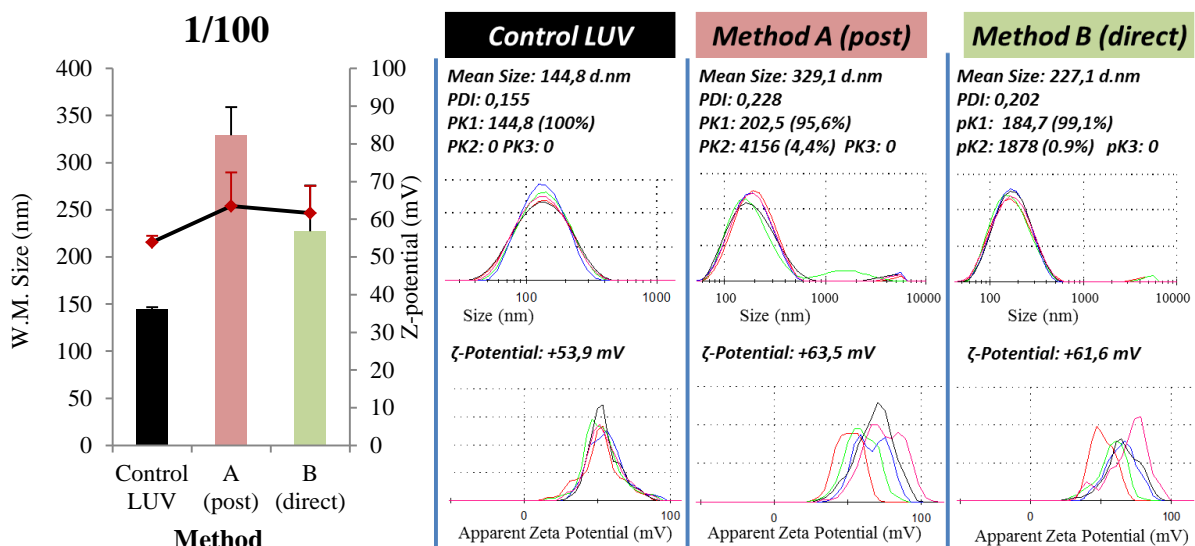


Figure 4.6 – At the left side are presented results of weighted mean size (nm) (bars - left axis) and z-potential (mV) (—■— - right axis) for peptide/DODAC:MO nanoparticles prepared by method A and B at 1/100 molar ratio, after extrusion. At the right side are presented the distribution of intensity profiles of the respective mean size and z-potential.

Figure 4.6 shows that nanoparticles prepared by method A and method B presented a higher weighted mean size, 329.1 nm (A) and 227.1 nm (B), when comparing with the control, 144.8nm. Z-potential followed the same trend, varying from +63.5 mV (A) to +61.6 mV (B) when comparing to +53.9 mV (LUV).

Direct-insertion method (B) is responsible for producing nanoparticles with smaller mean sizes and lower z-potential when compared with nanoparticles prepared by post-insertion protocol (A), suggesting a different conformational organization of the peptide within the nanoparticle.

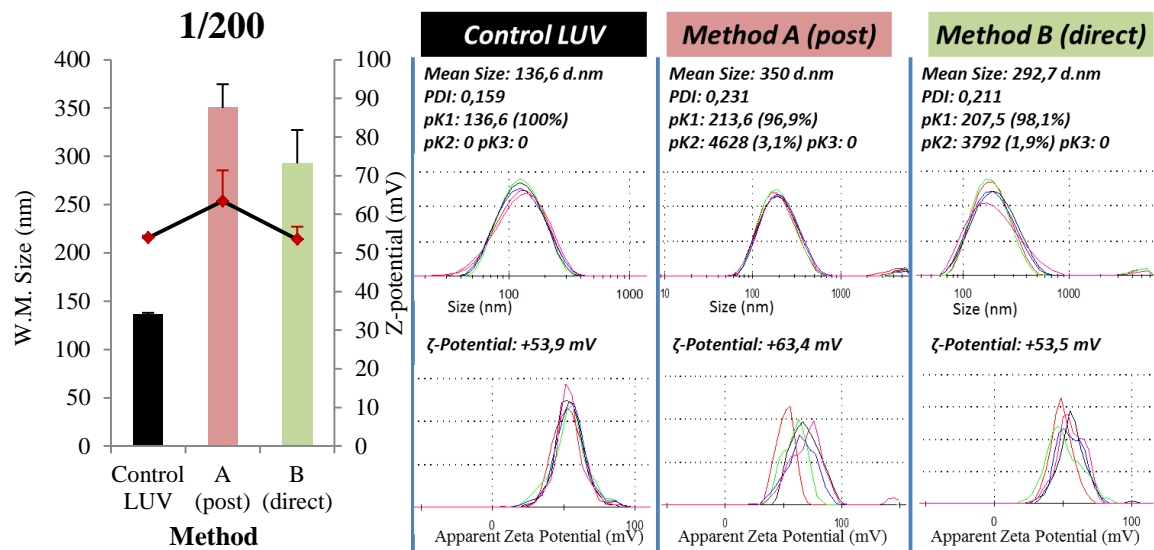


Figure 4.7 – At the left side are presented results of weighted mean size (nm) (bars -left axis) and z-potential (mV) (—■— - right axis) for peptide/DODAC:MO nanoparticles prepared by method A and B at 1/200 molar ratio, after extrusion. At the right side are presented the distribution of intensity profiles of the respective mean size and z-potential.

Figure 4.7 shows that nanoparticles at 1/200 molar ratio present a higher weighted mean size, 350 nm (post-insertion, A) and 292.7 nm (direct-insertion, B), when compared with LUV, 136.6 nm.

Z-potential presented some differences as well, varying from +63.4 mV (A) to +53.5 mV (B) comparing to +53.9 mV (LUV). It should be noted that nanoparticles prepared by direct insertion (B) show very similar z-potential values when comparing to the control.

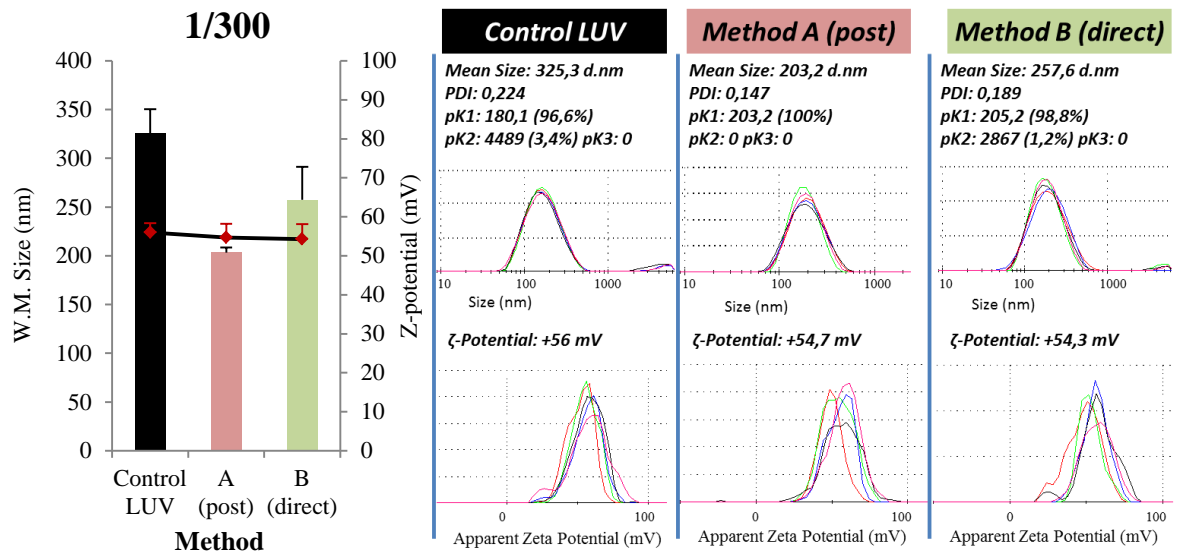


Figure 4.8 – At the left side are presented results of weighted mean size (nm) (bars - left axis) and z-potential (mV) (—■— - right axis) for peptide/DODAC:MO nanoparticles prepared by method A and B at 1/300 molar ratio, after extrusion. At the right side are presented the distribution of intensity profiles of the respective mean size and z-potential.

First, it is important to note that the control shows a mean size of 325.3 nm while the respective population 1 (pk1) demonstrate that 96.6% of the particles in suspension have a mean size of 180.1 nm. This is the value that is going to be considered as it is more trustworthy.

From figure 4.8 we can observe that nanoparticles at 1/300 molar ratio presented slightly higher mean sizes when compared to LUV, (180.1 nm), and direct-insertion method B produced nanoparticles with higher mean diameter (257.6 nm) than post-insertion method A (203.2 nm).

Z-potential values of peptide/lipid nanoparticles prepared by method A and B (+54.7 mV and +54.3 mV, respectively) are slightly lower than z-potential values of LUV (+56 mV).

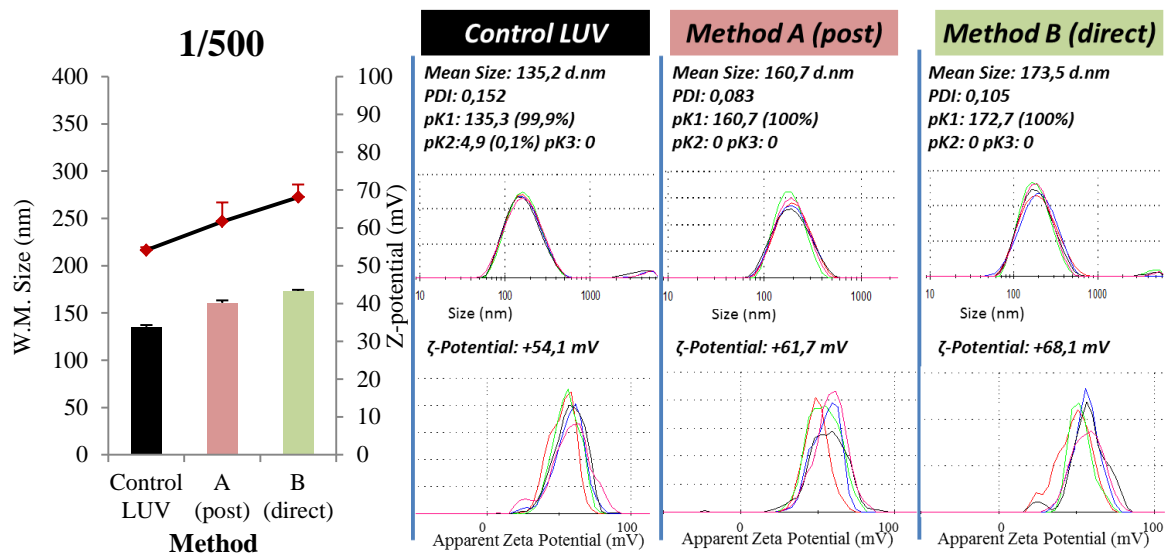


Figure 4.9 – At the left side are presented results of weighted mean size (nm) (bars - left axis) and z-potential (mV) (—■— - right axis) for peptide/DODAC:MO nanoparticles prepared by method A and B at 1/500 molar ratio, after extrusion. At the right side are presented the distribution of intensity profiles of the respective mean size and z-potential.

Results presented in Figure 4.9 show that lipid vesicles, LUV, have smaller mean sizes (135.2 nm) than peptide/liposomes nanoparticles at 1/500 molar ratio. Nanoparticles mean sizes are smaller when produced by post-insertion (A), 160.7 nm when compared to direct-insertion (B), 173.5 nm.

Z-potential followed the same trend as values are higher for nanoparticles, varying from +61.7 mV (A) to +68.1 mV (B), when compared to LUV (+54.1 mV). Post-insertion protocol (A) produced smaller nanoparticles than direct-insertion protocol (B).

From figure 4.6 to 4.9 we can observe that the negative charge of the peptide backbone has been neutralized by the addition of DODAC:MO (1:2) cationic aggregates in all formulations, suggesting that peptides were attached/incorporated into liposomes by electrostatic interaction attraction (Friede et al., 1993; Gregory Gregoriadis, 2007a; Ikonen et al., 2010; Strömstedt et al., 2010). However, different particle organizations were achieved according to the method of preparation and to the lipid content used to achieve different peptide/lipid molar ratios, which is in agreement with the literature (Gregory Gregoriadis, 2007b).

All nanoparticles showed higher mean sizes than the respective LUV (control). Peptides attached to liposomes membrane have been shown to produce higher mean size particles (Silva et al., 2008; Wattraint et al., 2013). Moreover, increasing sizes may be caused by liposome fusion induced by the negatively charged peptides attached to lipid vesicles (de Souza, Frisch, Duportail, & Schuber, 2002; Pecheur, Martin, Ruyschaert, Bienvenue, & Hoekstra, 1998).

Post-insertion protocol (A) seems to induce a greater change in LUV after peptide addition when compared to direct-insertion technique (B). At 1/300 and 1/500 molar ratio the higher lipid content was able to better organize the amount of peptide within the nanoparticles prepared by methods A and B as they produced more similar sizes. However, at 1/100 and 1/200 method A produced considerably higher nanoparticles. This may support the hypothesis that post-insertion protocol produces nanoparticles with higher amount of peptide attached to the outside of liposomal membrane rather than inside or attached to the inner side, which would be suitable for the aim of this thesis. In fact, it is known that peptides attached to the surface of liposomes are capable of inducing a stronger response (Gregory Gregoriadis, 2007a; Guan et al., 1998; Moreira, Ishida, Gaspar, & Allen, 2002; V. P. Torchilin, Rammohan, Weissig, & Levchenko, 2001).

Increasing lipid content is a critical parameter when preparing nanoparticles. Results show that nanoparticles prepared by lipid film hydration at 1/100 and 1/200 molar ratios are similar, suggesting that an increase in lipid content from 0.35 mM to 0.7 mM has not a great impact in the final nanoparticles. However, an increase from 0.7 mM (1/200 molar ratio) to 1.05 mM (1/300 molar ratio) leads to a considerable change. An increase in lipid concentration from 1.05 mM to 1.75 mM leads to another reorganization of the final nanoparticle.

In the distribution profiles from formulations 1/100 to 1/500, we can that the final nanoparticles become more homogeneous and compact. Generally, formulations with higher content of lipid, 1/300 (1.05 mM) and 1/500 (1.75 mM), showed more monodisperse populations and smaller sizes than 1/100 (0.35 mM) and 1/200 (0.7 mM) formulations. Higher lipid content produces considerably more lipid vesicles, thus, peptide particles per liposome should be significantly lower. In fact, a reported study presents a pore formation model induced by amphipathic peptides in liposomes that is based on the fact that when the vesicle size distribution is shifted towards smaller vesicles, there would be less of peptide molecules bound per liposome (Nir & Nieva, 2000). Thus, less negatively charged peptides attached to

each liposome induce less vesicle fusion, explaining the presence of smaller mean sizes at 1/300 and 1/500 molar ratios.

The results above suggest that an increase in lipid concentration leads to an increasingly better peptide-liposome organization, but also that there is a critical concentration below which there is too much peptide that cannot be properly incorporated (1.05 mM). Above this lipid concentration, an increase in mean size was observed for nanoparticles prepared by both methods A and B. In fact, 1 mM is the concentration at which DODAX vesicles have been typically produced ((Feitosa et al., 2009; Feitosa & Alves, 2008; Oliveira et al., 2012).

Z-potential values are generally higher, particularly when post-insertion protocol (A) was applied. These results are consistent with other studies in which an increase in the final nanoparticles surface charge was achieved after attaching cationic liposomes to negatively charged peptides by lipid film hydration (Silva et al., 2008). When direct-insertion protocol (B) was applied, a similar effect was observed although in less extension. On one hand, nanoparticles prepared by method B showed higher z-potential at 1/100 and 1/500 molar ratios. On the other hand, at 1/200 and 1/300 z-potential values were very close to LUV, showing even a very slight decrease (Figure 4.7 and 4.8).

Although both methods induced different conformational organizations, nanoparticles prepared by method B showed closer features to the control (LUV) when compared to method A. This reinforces that the post-insertion protocol has a strong influence in nanoparticle's mean size. This influence may be related to a higher peptide attachment to the surface of liposomes that, after inducing liposomes fusion and increasing vesicles size, a different surface charge rearrangement is also achieved. Distinct surface charge rearrangements were also observed with increasing lipid concentration.

(ii) Ethanolic injection: Direct- insertion versus Post-insertion

Figures 4.10 to 4.13 show z-potential (mV) and weighted mean diameter (nm) values for formulations prepared by post-insertion protocol, method C (ethanolic injection/incubation), and direct-insertion protocol, method D (ethanolic injection), after extrusion. A peptide concentration of 10 µg/mL was tested. The results for the nanoparticles before extrusion are presented in Appendix II.

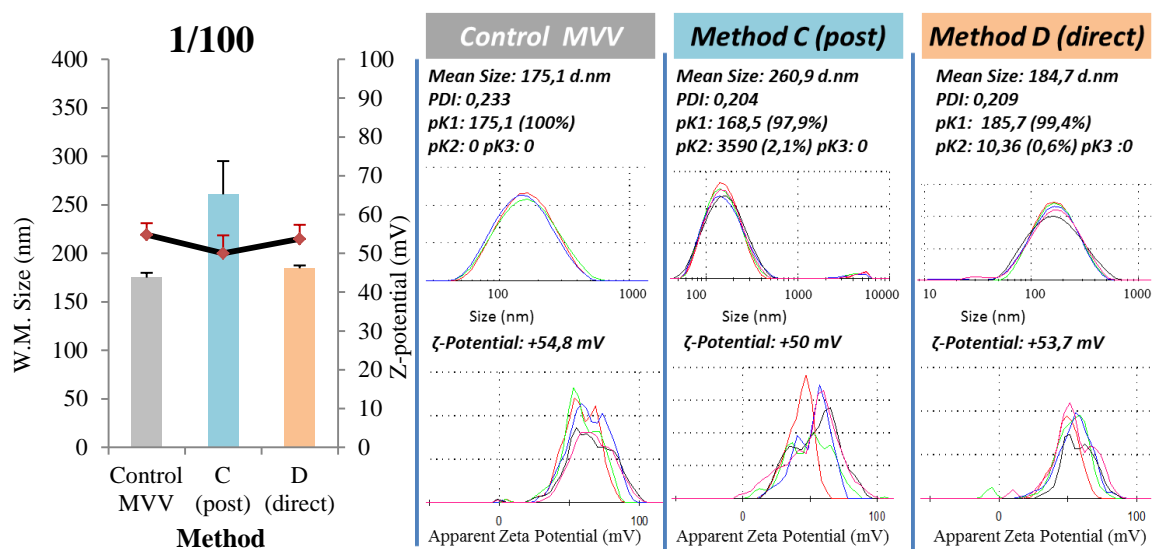


Figure 4.10 – At the left side are presented results of weighted mean size (nm) (bars - left axis) and z-potential (mV) (—■— - right axis) for peptide/DODAC:MO nanoparticles prepared by method C and D at 1/100 molar ratio, after extrusion. At the right side are presented the distribution of intensity profiles of the respective mean size and z-potential.

Figure 4.10 shows that weighted mean diameters are higher in nanoparticles at 1/100 molar ratio than in MVV. Peptide/lipid nanoparticles prepared by post-insertion (C) presented higher mean size, 260.9 nm, than nanoparticles produced by direct-insertion (D), 184.7 nm.

Z-potential follow the opposite tendency as nanoparticles prepared by method C and D have a lower surface charge (+50 mV and +53.7 mV, respectively) than the MVV control (+54.8 mV).

Nanoparticles prepared by method D are much more similar to the control than nanoparticles prepared by method C.

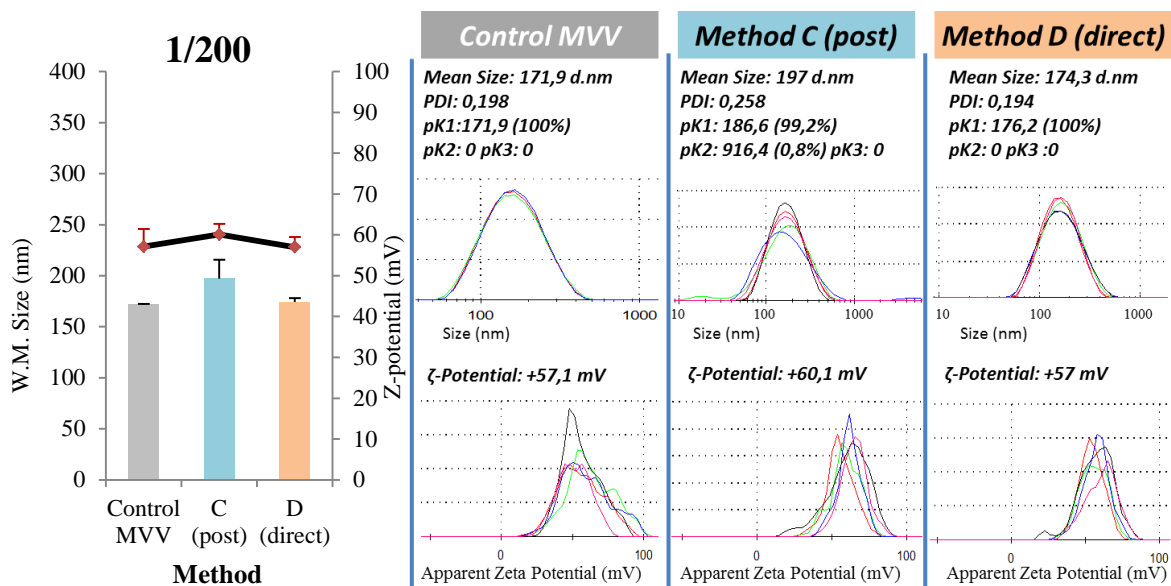


Figure 4.11 – At the left side are presented results of weighted mean size (nm) (bars - left axis) and z-potential (mV) (—■— - right axis) for peptide/DODAC:MO nanoparticles prepared by method C and D at 1/200 molar ratio, after extrusion. At the right side are presented the distribution of intensity profiles of the respective mean size and z-potential.

Figure 4.11 shows that weighted mean diameters of nanoparticles at 1/200 molar ratio prepared by post-insertion (C) and direct-insertion (D) are slightly higher compared to the control (MVV), and peptide/lipid nanoparticles prepared by method C (197 nm) have slightly higher mean sizes than nanoparticles produced by method D (174.3 nm).

Nanoparticles prepared by method C presented Z-potential values are slightly higher in (+60.1 mV) compared to nanoparticles prepared by method D (+57 mV) and also to the control (+57.1 mV). Post-insertion technique produced higher mean diameters than direct-insertion.

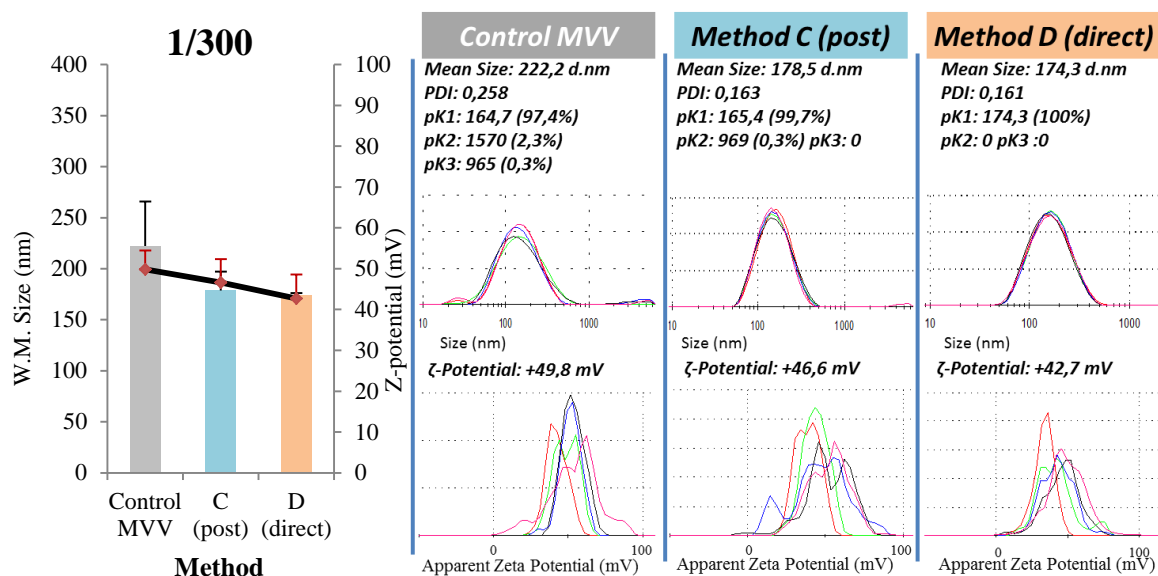


Figure 4.12 – At the left side are presented results of weighted mean size (nm) (bars - left axis) and z-potential (mV) (—■— - right axis) for peptide/DODAC:MO nanoparticles prepared by method C and D at 1/300 molar ratio, after extrusion. At the right side are presented the distribution of intensity profiles of the respective mean size and z-potential.

First, it is important to note that the control shows a mean size of 222.2 nm while the respective population 1 (pk1) demonstrates that 97.4% of the particles in suspension have a mean size of 164.7 nm. This is the value that is going to be considered for the control (MVV) as it is more trustworthy. A high PDI lead to a misleading mean size and it should be noted that the same happened in the control (LUV) prepared with the same lipid concentration, 1.05 mM (Figure 4.8).

Results presented in Figure 4.12 for 1/300 molar ratio show that control (MVV) have smaller mean sizes (164.7 nm) than peptide/liposomes nanoparticles. Method C produced slightly bigger nanoparticles (178.5 nm) than method D (174.3 nm).

Nanoparticles Z-potential followed the same tendency. The nanoparticles prepared by methods C and D are slightly less charged (+46.6 mV and +42.7 mV, respectively) than the control (+49.8 mV).

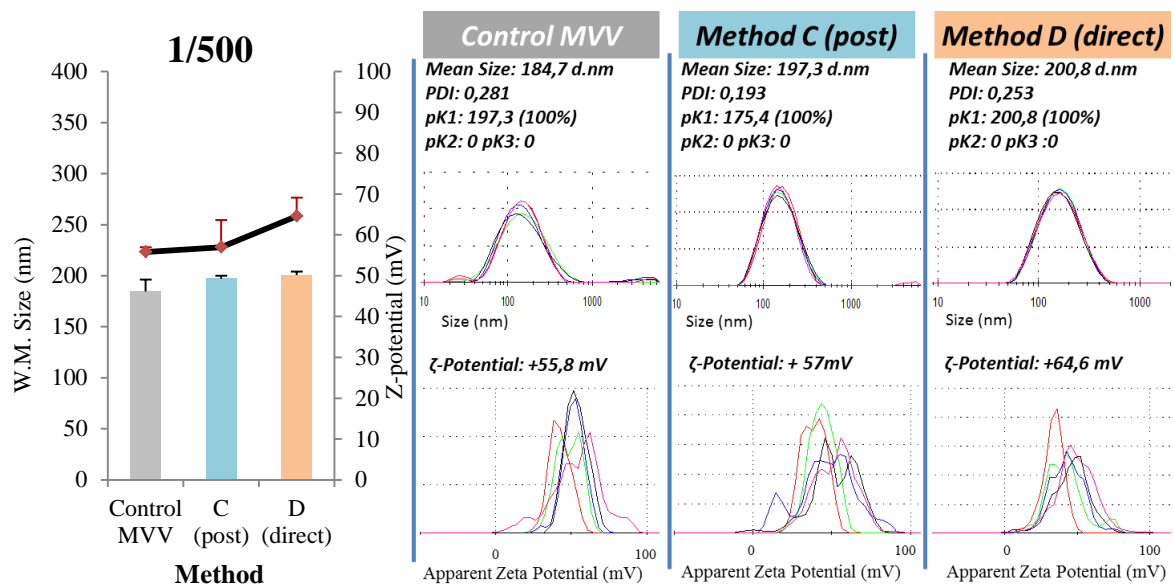


Figure 4.13 – At the left side are presented results of weighted mean size (nm) (bars - left axis) and z-potential (mV) (—■— - right axis) for peptide/DODAC:MO nanoparticles prepared by method C and D at 1/500 molar ratio, after extrusion. At the right side are presented the distribution of intensity profiles of the respective mean size and z-potential.

From results showed in Figure 4.13 for 1/500 molar ratio we can observe that MVV have smaller mean diameters than peptide/liposomes nanoparticles. However, from distribution by intensity profiles we can observe that PDI is high and pk1 comprises 100% of the populations. So, in this case, method C produces smaller nanoparticles (175.4 nm) than method D (MVV with 197.3 nm) considering both mean size and pk1.

The nanoparticles prepared by methods C and D presented slightly higher Z-potential values (+57 mV and +64.4 mV, respectively) compared with the control (MVV) (+55.8 mV). The nanoparticles prepared by method D presented the higher surface charge.

Results from figures to 4.10 to 4.13 suggest that peptides were incorporated into liposomes by electrostatic attraction using the ethanolic injection method, and the distinct methodologies adopted as well as the four peptide/lipid molar ratios produce different nanoparticles, similar to what happened with lipid film hydration method.

Generally, nanoparticles prepared by method C showed higher mean sizes than method D, with the exception for 1/500 formulation in which a slight smaller mean size was achieved. Z-potential followed the opposite trend as it is lower for method C.

Post-insertion protocol (C) apparently induces a greater change in MVV after peptide addition when compared to direct-insertion technique (D), an effect that is clearer at 1/100 and 1/200 molar ratios. This reinforces the hypothesis that post-insertion protocol produces nanoparticles with higher amount of peptide attached to the outside of liposomal membrane, inducing liposomes fusion and consequently creating higher nanoparticles.

The results above show that nanoparticles prepared by lipid film hydration at 1/100 and 1/200 molar ratios are similar, suggesting that an increase in lipid content from 0.35 mM to 0.7 mM has not a great impact in the final nanoparticles. However, an increase from 0.7 mM (1/200 molar ratio) to 1.05 mM (1/300 molar ratio) leads to a considerable change. An increase in lipid concentration from 1.05 mM to 1.75 mM leads to another reorganization of the final nanoparticle

At 1/300 and 1/500 molar ratios, considerable changes were observed in the final nanoparticles indicating a lipid concentration dependent effect. Higher lipid content was able to better organize the amount of peptide within the nanoparticles prepared by methods C and D and they produced more similar sizes between each other and comparing to the control. As a similar behavior was observed for lipid hydration methods, this reinforces that an increase in lipid concentration leads to a more proper peptide distribution through the lipid vesicles and that there is a critical lipid concentration, 1.05 mM. Above this lipid concentration, an increase in mean size was observed for nanoparticles prepared by both methods C and D, while the opposite was observed for methods A and B.

A) Lipid film hydration versus ethanolic injection

The four distinct protocols, as well as the four different peptide/lipid molar ratios, used in this study lead to the production of different nanoparticles in terms of its conformational organization. While lipid film hydration is a mechanical dispersion method, ethanol injection is a solvent dispersion method.

While weighted mean diameters of nanoparticles prepared by ethanolic injection methods, C and D, vary from 174.3 nm to 260.9 nm and PDI values vary from 0.161 to 0.250, nanoparticles prepared by lipid hydration methods, A and B, have higher mean sizes varying from 160.7 nm to 350 nm and smaller PDI that vary from 0.083 to 0.231. If we consider LUV and MVV preparations (controls), the same is observed for PDI values, but the opposite is observed for mean sizes as ethanolic injection produced higher mean size vesicles (175.1 nm; 171.9 nm; 164.7 nm (pK1); 197.3 nm (pK1)) than lipid film hydration (144.4 nm; 136.6 nm; 180.1 nm (pK1); 135.2 nm). Therefore, ethanolic injection is characterized by the production of more heterogeneous vesicles with a higher mean size when compared to lipid film hydration that produces more homogeneous populations and smaller mean sizes. When a negatively charged peptide is added to the preparations, mean sizes tendency is inverted.

Nanoparticles are more positively charged when prepared by lipid film hydration, varying from +55.3 mV to +85.2 mV, while ethanolic injection produce less positive particles, varying from +45.5 mV to +77.1 mV. This can be explained by the fact that nanoparticles prepared by ethanolic injection (MVV) followed by extrusion process are still MVV, although with less vesicles enclosed.

If all the particles in suspension have a large negative or positive z-potential then electrostatic repulsion between molecules will overlap Van der Waals interactions. Consequently, molecules will tend to repel each other and there is no tendency to flocculate – increasing stability. On the other hand, when zeta potential values are close to neutrality, the opposite happens and prominent Van der Waals interactions cause molecules aggregation as there is no force to prevent the particles coming together and flocculating. Particles with zeta potentials more positive than +30 mV or more negative than -30 mV are normally considered stable (“Zeta Potential theory,” 2004). Thus, all nanoparticles presented in figures 4.6 to 4.13 can be considered as stable, and differences between them should be attributed to the method of preparation and lipid concentration.

B) Post-insertion versus direct-insertion

Despite mean size and PDI differences, a similar behavior was observed for post-insertion protocols (A and C) using lipid film hydration and ethanolic injection methods with increasing lipid concentration. Likewise, direct-insertion protocols (B and D) showed

similarities in the behavior of nanoparticles prepared by those two methods. The same correlation may be extended to z-potential, excepting for 1/100 formulation.

As mentioned, results suggested that post-insertion protocols (A and C) produced nanoparticles with higher amount of peptides in the surface of liposomes. However, this outcome is stronger in nanoparticles prepared by lipid film hydration (A) rather than ethanolic injection. This is more evident at 1/100 and 1/200 molar ratios since nanoparticles prepared by method A showed mean sizes of 329.1 nm and 227.1, respectively (Figures 4.6 and 4.7), while nanoparticles prepared by method C showed mean sizes of 260.9 nm and 197.9 nm (Figures 4.10 and 4.11). The smaller size of peptide/lipid nanoparticles prepared by ethanolic injection can be caused by less peptide attached to the surface due to the morphological characteristics of vesicles produced by this method.

C) Extrusion versus non-extrusion methodology

It is important to refer that, previously, the extrusion process was undertaken with a filter of 400 nm pore size. However, results showed high PDI even after extrusion (data not shown). Studies already reported that DODAC naturally forms vesicles with mean sizes around 247 nm (Feitosa, Karlsson, & Edwards, 2006). Thus, a 200 nm pore size membrane was used instead. Using this pore size allows the production of the largest DODAC:MO(1:2) vesicles possible with low PDI, and higher mean size vesicles are more likely to be seen by the immune system. Furthermore, 200 nm vesicles have already been shown to be suitable for the immunological purpose of this thesis (V. P. Torchilin et al., 2001). Usually the optimal liposome size for administration is between 100 and 300 nm, because this size range of liposomes gives uniform and predictable drug-release rate and stability in the bloodstream (Gregory Gregoriadis, 2007b).

Unprocessed liposomes (e.g.: without extrusion) have limited uses in research because of their large diameters, size heterogeneity, multi internal compartments, low-trap volumes, and inconsistencies from preparation to preparation (Gregory Gregoriadis, 2007b). For example, approximately 10% of the total lipid in a typical MLV preparation is present in the outer monolayer of the external bilayer (Hope, Bally, Webb, & Cullis, 1985). When a single bilayer encloses an aqueous space to form a vesicle with a sufficiently large radius that approximately 50% of the total membrane lipids are present in the outer monolayer, a typical definition of a

LUV (Gregory Gregoriadis, 2007b). In fact, vesicles that did not undergo the extrusion treatment have rather polydisperse size distribution (Lasic, 1993) as we observed in this work (Appendix II).

By comparing results before extrusion with results after extrusion, it is clear that the extrusion procedure has great influence in the final nanoparticle. Mean sizes became more homogeneous and Z-potential values decreased, possibly due to the normal loss of lipid (Xu, Costa, Khan, et al., 2012). In lipid film hydration methods, A and B, nanoparticle's z-potential before extrusion varies from + 55.3 mV to +85.7 mV and after extrusion these values decreased varying from +53.5 mV to +68.1 mV. In ethanolic injection methods, C and D, z-potential vary from +45.5 mV to +77.1 mV before extrusion and vary from +42.7 mV to +64.6 mV after extrusion.

The extrusion process has more influence in decreasing z-potential and PDI of nanoparticles prepared by ethanolic injection, than in nanoparticles prepared by lipid film hydration. Yet, nanoparticles prepared by ethanolic injection have higher PDI before and after extrusion when compared to nanoparticles prepared by lipid film hydration. This may be explained by the morphological differences between MLV and MVV schematized in figure 2.3 (see section 2.1.2). The size distribution in a MVV preparation produced by ethanolic injection is more heterogeneous than is in MLV. Each MVV can form and enclosure a very wide range of liposomes sizes. When MVV particles pass through the extrusion filter, those enclosed vesicles are released, explaining the higher PDI even after extrusion. Extrusion effect will be further analysed in the next section of results (4.1.4).

D) Best methodology and formulation

Nanoparticles prepared by post-insertion technique, lipid film hydration (A) and ethanolic injection (C), suggested that peptides can be attached to the surface of liposomes by taking advantage of electrostatic attraction between particles of opposite charge. The amphiphilic character of the BCR-ABL peptide comprised of 48% of hydrophobic amino acids has also influence on the success of peptide incorporation into liposomes. They can be easily incorporated into liposomes noncovalently due to their lipid-like amphipathic properties with minimized activity loss or without laborious chemical functionalization steps (Sardan, Kilinc, Genc, Tekinay, & Guler, 2013).

Lipid film hydration has been recognized as one of the best methodologies to achieve higher rates of encapsulation (Frézard, 1999; Kirby & Gregoriadis, 1984). In the same line of works, a higher lipid content is associated with higher encapsulation efficiency (Xu, Costa, Khan, et al., 2012).

Until now method A is presented as the most encouraging nanoparticle preparation methodology as well as 1/300 and 1/500 peptide/lipid molar ratios, for the purpose of this thesis. However, as the extrusion process has been shown to be responsible for decreasing encapsulation due to peptide losses (Bhardwaj & Burgess, 2010; Colletier et al., 2002), it was though be benefic to this work a more detailed analyzes of the influence of the extrusion process in the final nanoparticle and adopt a strategy to avoid those losses.

4.2.4. Effect of MLV liposomes and LUV liposomes in the final nanoparticle – Method A versus method E

(i) Incorporation of 10 µg/mL peptide concentration

Formulations using 1/300 and 1/500 molar ratio showed the most encouraging results and will, therefore, be used in the subsequent work of encapsulation efficiency. An increase in lipid content induced more monodisperse nanoparticles.

At this stage, the work was focused on the comparison between two methods:

A - liposomes prepared by lipid film hydration (MLV) followed by peptide incubation and extrusion;

E - liposomes prepared by lipid film hydration/extrusion (LUV) followed by incubation with peptide.

As the lipid film hydration methods demonstrates more monodisperse populations than ethanolic injection methods, and as incubating peptide particles after lipid vesicle formation probably creates peptide/lipid complexes with more peptide particles attached to the outer membrane of liposomes rather than inside, method A was chosen to continue this work.

Hereupon, it was important to understand which effect has on the final nanoparticles adding the peptide molecules to MLV suspension (before extrusion) or to LUV suspension (after

extrusion). Therefore, method E was added to this work. In method A, peptide particles were incubated with DODAC:MO(1:2) multi-lamellar vesicles (MLV). In method E, peptide particles were incubated with DODAC:MO(1:2) large uni-lamellar vesicles (LUV).

Mean size and z-potential parameters were measured for methods A and E. Results are presented in figures 4.14 and 4.15. MVL and LUV control samples are presented as well. A peptide concentration of 10µg/mL and four peptide/lipid molar ratios were studied: 1/100; 1/200; 1/300 and 1/500.

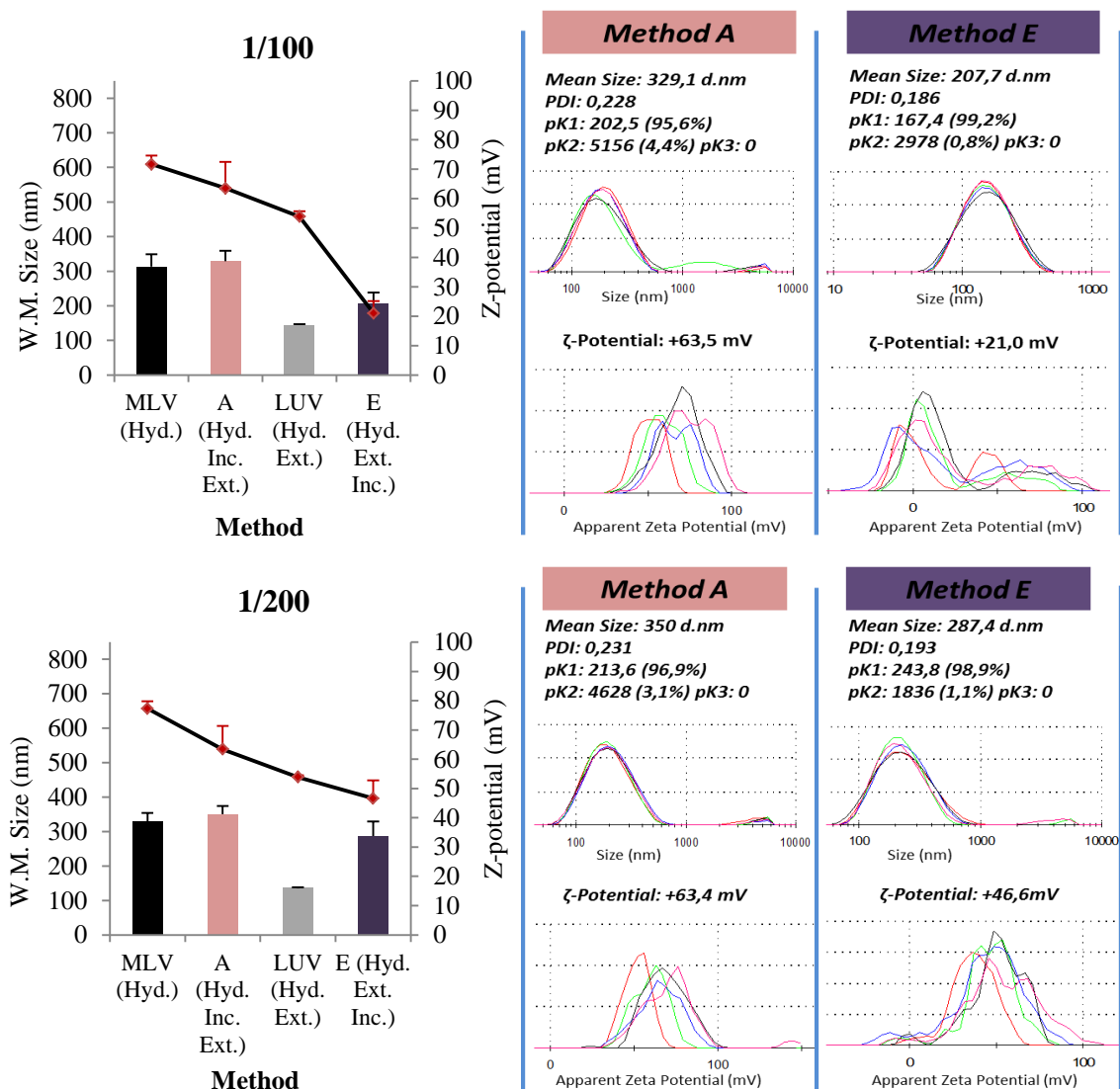


Figure 4.14 – At the left side are presented results of weighted mean size (nm) (bars - left axis) and z-potential (mV) (—■— - right axis) for nanoparticles prepared by method A and E at 1/100 (up) and 1/200 (bottom) molar ratio. At the right side are presented the distribution of intensity profiles of the respective mean size and z-potential.

From figure 4.14 we can observe that mean size values for 1/100 and 1/200 molar ratios follow the same tendency. Peptide/DODAC:MO nanoparticles prepared by method A presented higher mean sizes than LUV and slightly higher than MLV while nanoparticles prepared by method E presented higher mean sizes than LUV.

Peptide/lipid nanoparticles produced by method E showed smaller mean sizes than nanoparticles prepared by method A. When lipid concentration was increased from 0,35mM (1/100) to 0,7mM (1/200), nanoparticles produced by both methods showed an increase in mean sizes as well.

Z-potential values also follow the same trend for 1/100 and 1/200 molar ratios. MLV showed higher z-potential than nanoparticles prepared by method A. These, in turn, showed a higher surface charge than LUV. LUV presented higher surface charge than nanoparticles produced by method E.

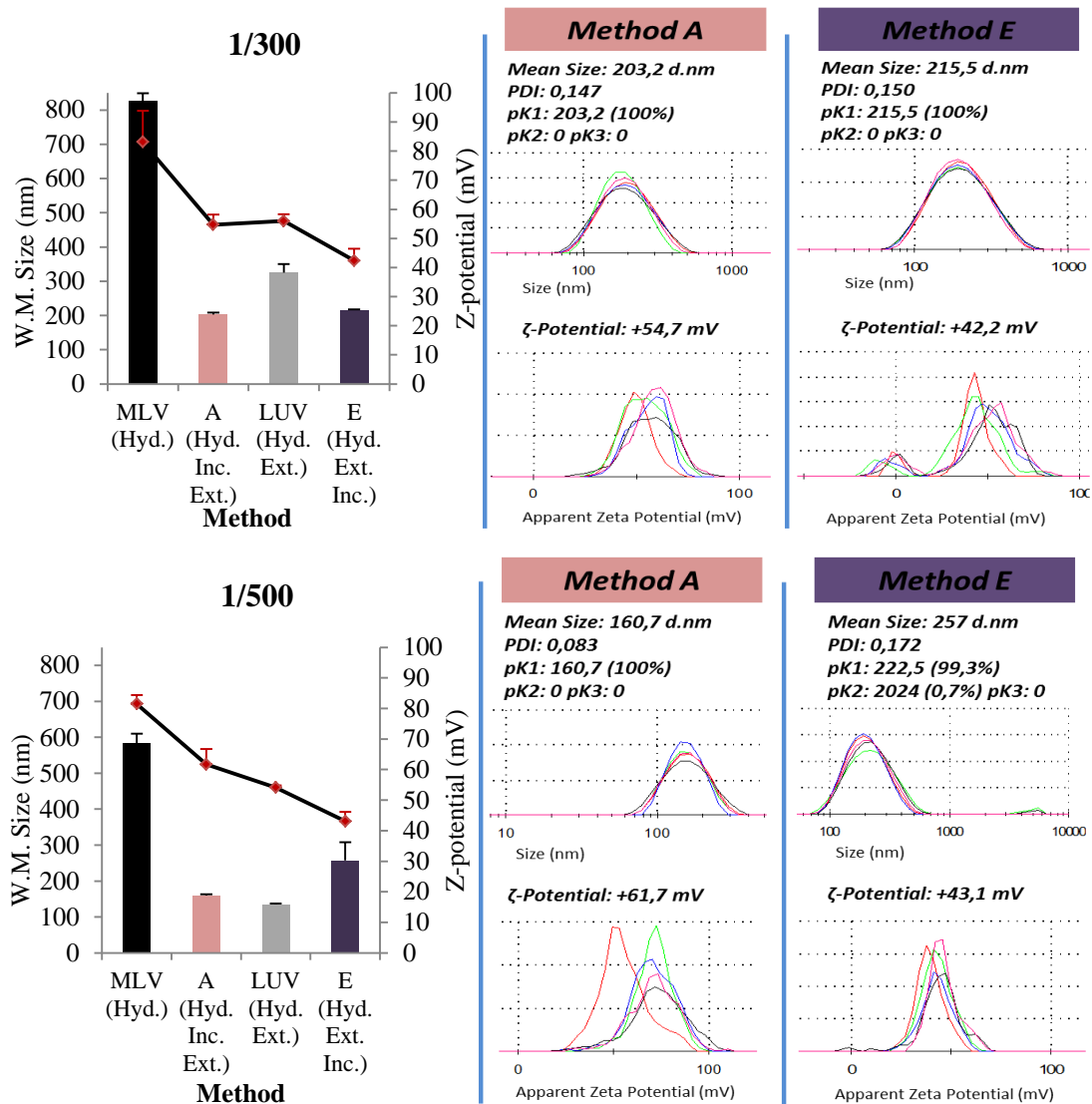


Figure 4.15 – At the left side are presented results of weighted mean size (nm) (bars - left axis) and z-potential (mV) (—■— - right axis) for nanoparticles prepared by method A and E at 1/300 (up) and 1/500 (bottom) molar ratio. At the right side are presented the distribution of intensity profiles of the respective mean size and z-potential.

Figure 4.15 shows that at 1/300 molar ratio, nanoparticles prepared by method A and E have smaller mean sizes than the control (LUV). Nanoparticles prepared by method E showed slightly higher mean diameter than nanoparticles prepared by method A. Nanoparticles prepared by methods A and E, presented lower Z-potential when compared with the control (LUV). Also nanoparticles prepared by method E showed lower z-potential than nanoparticles prepared by method A.

From figure 4.15 we can also observe that at 1/500 molar ratio, nanoparticles prepared by method A and E have higher mean sizes than LUV, and nanoparticles prepared by method E showed higher mean diameter than the one prepared by method A. In terms of surface charge, nanoparticles prepared by method E, present lower Z-potential compared to the control (LUV), while peptide/lipid particles prepared by method A showed higher z-potential than the control (LUV) and the nanoparticles prepared by method E.

Generally, nanoparticles prepared by method A and E presented different mean sizes and z-potential compared to the control (LUV). These results indicate that peptide particles are attached or incorporated into liposomes, producing different conformational organizations with nanoparticles with higher mean sizes and inducing a change in the surface charge of the nanoparticles.

When analyzing the distribution profiles we can observe that at 1/100, 1/200 and 1/300 molar ratio, nanoparticles prepared by method E show the presence of nanoparticles with negative z-potential this not being detected for nanoparticles prepared by method A. This may explain, partially, the smaller z-potential final values presented for nanoparticles produced by method E. The absent of negative particles may be due to loss of some peptide weakly linked to liposomes during extrusion in method A. Another possibility to take into consideration is that when the peptide-liposome conjugates pass through extrusion filter particles are rearranged and, therefore, the hypothesis that more peptide molecules may be hidden inside of the liposomes should be considered. In method E there are no peptide losses and they are not detached from liposomes membrane since the extrusion process is undertaken before peptide incubation.

At 1/500 molar ratio, nanoparticles prepared by both methods, A and E do not show the presence of particles with negative surface charge. Differently to what happened for 1/100, 1/200 and 1/300 molar ratios, at this 1/500 molar ratio nanoparticles produced by method E showed the absence of negative particles, indicating that the lipid content was enough to efficiently incorporate the peptides.

Peptide/lipid nanoparticles prepared by method E showed lower z-potential than nanoparticles prepared by method A. However, when the lipid content is doubled from 0,35mM (1/100 molar ratio) to 0,7mM (1/200 molar ratio), z-potential of nanoparticles prepared by method A is kept constant while z-potential of nanoparticles are prepared by method E increase. When

observing the distribution of intensity profiles of z-potential, nanoparticles prepared by method E (1/100 molar ratio) show the presence of some of more nanoparticle with negative surface charge, suggesting that a significant amount of peptide particles was not incorporated. A small lipid concentration (0,35mM) coupled to some lipid losses during the extrusion process, prior to peptide incubation, may lead to a critical total lipid content incapable of incorporating 10µg/mL of peptide concentration and achieving a stable final nanoparticle.

Results showed that 1/100 and 1/200 molar ratios show many similarities. However, when the lipid content is raised different particles organizations are achieved at 1/300 and 1/500 molar ratios. In fact, increasing lipid concentration leads to more stable nanoparticles and the formulation using 1,75mM (1/500 molar ratio) of lipid content showed the most promising results. When peptide particles are incubated with previously extruded liposomes (method E), nanoparticles conformal organizations are different from the nanoparticles in which peptide is added to cationic liposomes followed by extrusion of the overall nanoparticle (method A).

The addition of peptides to liposome after extrusion (method E) is apparently the suitable choice to produce nanoparticles with less antigen losses and with higher amount of peptide particles at the surface of the membrane of lipid vesicles.

Therefore, this method was chosen to continue the subsequent work instead of method A in which the final nanoparticles organization is influenced by peptide losses (Xu, Costa, Khan, et al., 2012).

The formulation consisting of 1/500 molar ratio prepared by method E showed encouraging results and the fact that it has the higher content of lipid, this opens the possibility of encapsulating a higher peptide concentration in future works (Xu, Costa, Khan, et al., 2012).

(ii) Incorporation of 10 µg/mol and 20 µg/mol peptide concentration

Nanoparticles were prepared by method E (liposomes prepared by lipid film hydration/extrusion (LUV) followed by incubation with peptide) using two distinct peptide concentrations, 10 µg/mL and 20 µg/mL, and one lipid concentration, 1.75 mM. Two peptide/lipid molar ratio were tested, 1/250 and 1/500.

Figure 4.16 presents the distribution of intensity profiles of mean size and z-potential for nanoparticles prepared at different peptide/lipid molar ratio.

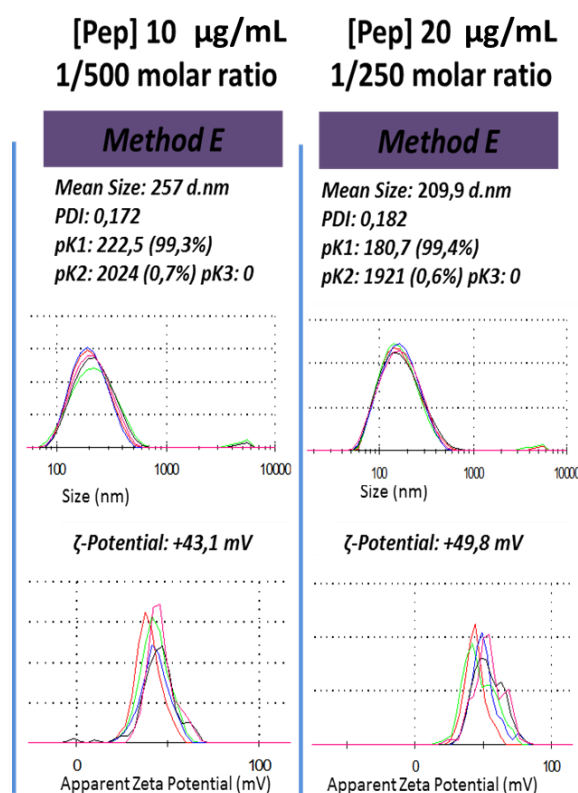


Figure 4.16 – Distribution of intensity profiles of the respective mean size (nm) and z-potential (mV) for peptide/DODAC:MO nanoparticles prepared by method E at 1/500 (left) and 1/250 (right) molar ratio.

From Figure 4.16 we can observe that nanoparticles prepared with 1,75 mM of lipid content and (1/500 molar ratio) present a mean size of 257 nm and a z-potential of +43.1 mV. When peptide concentration was increased to 20 µg/mL (1/250 molar ratio), nanoparticles mean size decreased to 209.9 nm and z-potential increased to +49.8 mV. Despite these differences, both

samples show very stable and homogeneous nanoparticles. Nevertheless, an increase in peptide concentration, apparently, leads to a more compact organization of the nanoparticle.

It should be noted that a peculiar high z-potential was observed for 20 $\mu\text{g/mL}$ at $\text{pH}=7.2$ in HEPES (see section 4.1.1- Effect of pH, peptide concentration and sonication). With a stronger negative charge, the peptide at this concentration would be attracted to the cationic liposomal membrane in a stronger manner compared to 10 $\mu\text{g/mL}$.

After the previous results had demonstrated that the lipid content is detrimental in nanoparticles preparation, these results show that peptide content is also responsible for changes in the final nanoparticle features (Wattraint et al., 2013). In fact, vesicles aggregation can be achieved by increasing lipid concentration (Rapaport, Peled, Nir, & Shai, 1996), choosing larger peptides and also by increasing peptides concentration (Nieva, Nir, & Wilschut, 2008). In this work, the opposite was observed for one of these aspects as a 20 $\mu\text{g/mL}$ induced a smaller mean size than 10 $\mu\text{g/mL}$. Microscopic observations have revealed that fusogenic peptides induce liposome shrinkage prior to membrane fusion, therefore, this may be an explanation for the occurred. These results indicated that the liposome membrane shrank slightly during the fusion, whereas the total volume increased slightly (Nomura et al., 2004). In any case, this may be understood as higher peptide concentrations may be encapsulated in 1.75 mM of total lipid content, opening the possibility of a detailed study in this subject.

4.3. Encapsulation efficiency

Choosing a peptide quantification assay was complicated by two factors: (i) the lack of information on how to efficiently separate the free peptide fraction from the encapsulated fraction; (ii) the lack of available assays capable of detecting such a low peptide concentration.

The methodology used in this work, therefore, serves as a new attempt to quantify low peptide concentrations as well as to know if the methodology used to separate peptide/liposome fraction from free peptide fraction was successful.

Encapsulation efficiency was studied using tricine-SDS-PAGE protocol as it is a suitable electrophoretic system for the resolution of proteins smaller than 30 kDa (Schägger, 2006). Considering a peptide concentration of 10 $\mu\text{g/mL}$, encapsulation efficiency was tested in the following samples:

- ▶ 1/300 peptide/lipid molar ratio prepared by method E;
- ▶ 1/500 peptide/lipid molar ratio prepared by method E;
- ▶ 1/300 peptide/lipid molar ratio prepared by method C;
- ▶ 1/500 peptide/lipid molar ratio prepared by method C.

In method E, liposomes are prepared by lipid film hydration/extrusion (LUV) followed by incubation with peptide. In method C liposomes are prepared by ethanolic injection followed by peptide incubation. These samples were chosen as both methods and both peptide/lipid molar ratios presented encouraging results, allowing the comparison between lipid film hydration and ethanolic injection methods, as well as a comparison between two different lipid contents.

Samples were produced in triplicate so that the same experiment could be optimized.

▶ **First Experiment**

Lyophilization was used to concentrate samples, expecting that peptide quantification would be better succeeded. After lyophilization and prior to gel analyses, samples were photographed. Figure 4.17 shows photographs of sample tubes from the first and second experiments. The third experiment presented similar results (not shown).

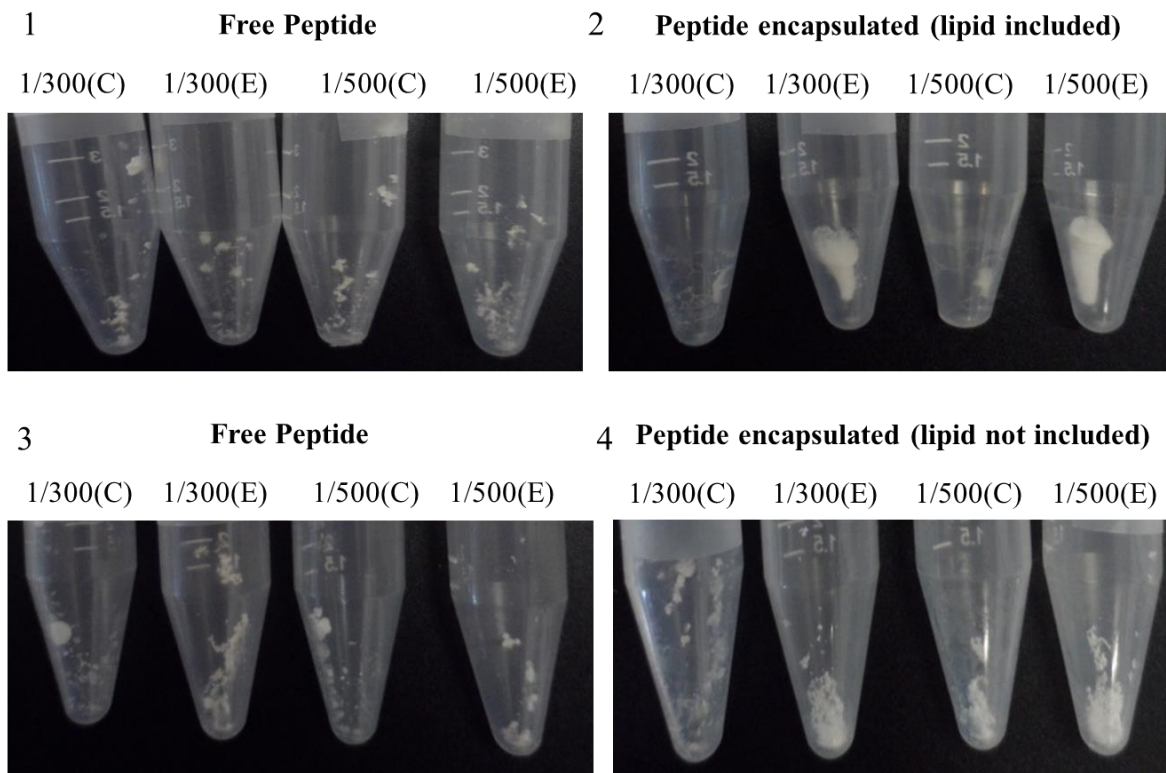


Figure 4.17 – Photography of sample tubes after lyophilization, containing: free peptide fraction (1) and peptide encapsulated fraction in which it lipid was not separated from peptide (2) – first experiment; free peptide fraction (3) and peptide encapsulated fraction after separation from lipid (4) – second experiment.

From Figure 4.17 we can distinguish some differences between samples. Free peptide was observed for all formulations (Figure 4.17 - 1 and 3). Yet, the encapsulated fractions presented higher peptide quantities (Figure 4.17 - 2 and 4).

Apparently, 1/500 formulation was able to enclosure slightly more peptide than 1/300 formulation in each method (Figure 4.17 - 4). However, despite smaller lipid content, 1/300 (method E) formulation was apparently able to encapsulate more peptide than 1/500 (method C) formulation. Samples prepared by lipid film hydration/extrusion, method E, demonstrated higher amount of encapsulated peptide than samples prepared by ethanolic injection, method C.

Firstly, coomassie blue staining was used to stain the gel but it was not sufficient to detect anything (not shown). Thus, silver staining was used afterwards, since it has a lower detection limit (Figure 4.18 and 4.19). Coomassie blue staining method allows the quantification of encapsulated peptide, yet, silver staining does not.

Figure 4.18 shows gels stained with silver. In this figure are presented free peptide fractions (1-4) and peptide encapsulated fractions (5-8). As the peptide used in this work has 2,4 KDa, the location of the band corresponding to 2 KDa is represented.

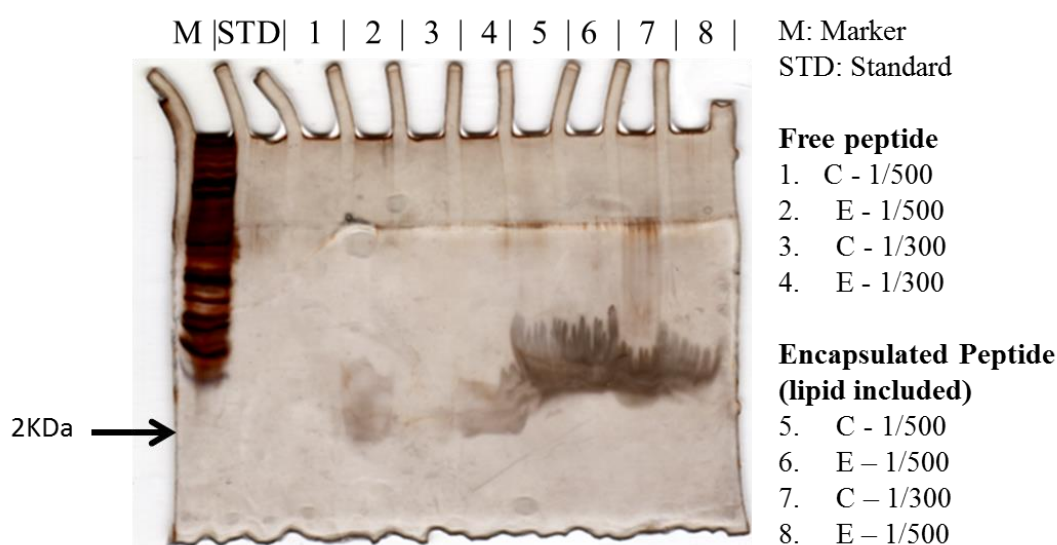


Figure 4.18 – Gel stained with silver staining. Samples showed correspond to method E and method C and to peptide/lipid molar ratios of 1/300 and 1/500.

Figure 4.18 shows the presence of free peptide in the samples 2 and 4, corresponding to 1/300 and 1/500 formulations prepared by method E. Free peptide was not detected in either formulations prepared by method C. Samples 5 to 8 correspond to the encapsulated fraction in which lipid was not separated from the peptide. These samples produced a smear effect probably due to the lipid molecules, and encapsulated peptide was not detected.

All peptide/lipid nanoparticles were prepared in 5 mL with a peptide concentration of 10 μ g/mL. Thus, all samples included a total 50 μ g of peptide before separation of free fraction and encapsulated fraction. A standard sample consisting of 45 μ g of peptide was used

as a control, the equivalent to 95% of encapsulation. Despite small quantities of free peptide being detected, in the standard sample it was not detectable any presence of it. This suggests that these results are not precise. Moreover, the 2KDa corresponding band does not appear in the gel, which indicates that the peptide did not run enough in the gel matrix, and reinforces that these results must be further confirmed.

► Second Experiment

Since results from the first experiment were not satisfactory, a second experiment with the same conditions was conducted. However, this time the encapsulated fraction was separated from the lipid content and both were analyzed separately.

Figure 4.19 shows gels stained with silver where it can be observed results from samples presented in photographs above (4.17 - 3 and 4). So, in this figure are presented free peptide fractions (wells 1 to 4), peptide encapsulated fractions previously separated from liposomes (wells 5 to 6) and, additionally, samples with the resulting lipid content (wells 9 to 11).

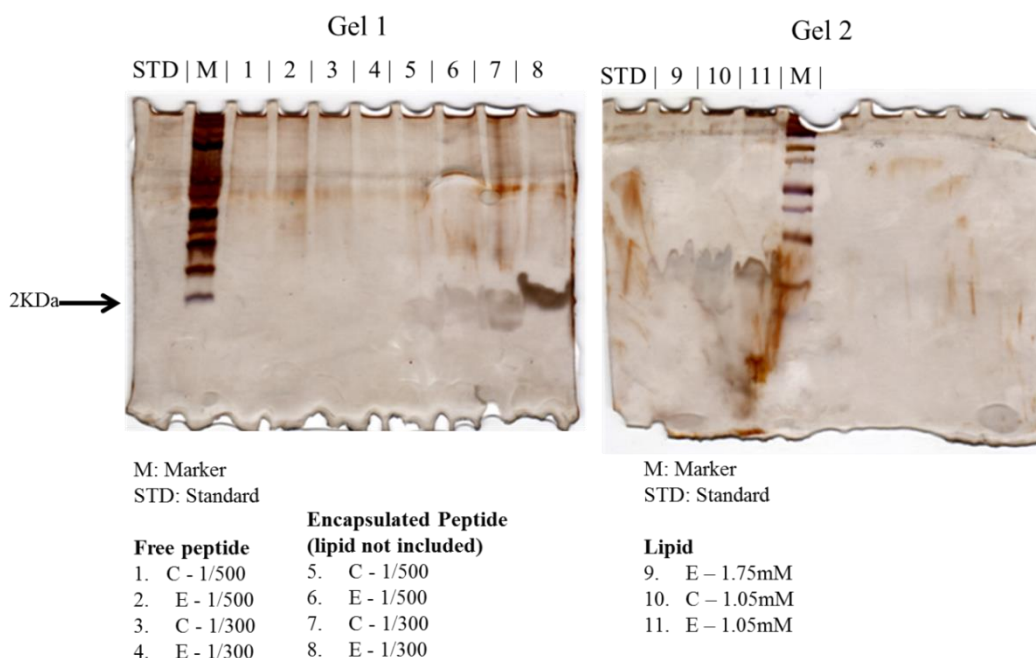


Figure 4.19 – Gels stained with silver staining. Samples showed correspond to method E and method C and to peptide/lipid molar ratios of 1/300 and 1/500.

From Figure 4.19 (Gel 1) we can observe that samples 1 to 4 show the absence of free peptide in all peptide/DODAC:MO formulations. On the other hand, wells 5 to 8 demonstrated the presence of the encapsulated peptide, especially in well 8 that corresponds to 1/300 formulation prepared by method E. A smear effect was not detected in gel 1.

Gel 2 includes the lipid fractions and a smear effect can be seen in 9 to 11 wells. Peptide presence was not detected. Therefore, it can be assumed that lipid molecules are responsible for this effect and it may be considered that the encapsulated peptide was successfully separated from liposomes.

In both gels depicted in Figure 4.19, the peptide was not detected in the standard sample as also shown in Figure 4.18. Results from both first and second experiments may be misleading probably due to two factors. Firstly, considering that each well can be loaded with only 15 μ L, peptide concentration may have not been high enough even considering that samples were dissolved in only 100 μ L of water prior to gel analyzes. Secondly, in small volumes of water is harder to solubilize this amphiphilic peptide. In fact, peptide precipitate was observed in the micro tubes. However, vigorous vortexing apparently dissolved it and the experience was continued.

► Third Experiment

In a third experiment, after lyophilization, samples were dissolved in smaller volumes (50 μ L) to increase peptide concentration, and the solvent used was urea buffer (8 M) in an attempt to increase the solubility of this amphiphilic peptide. Urea serves as an intermediate between water molecules and peptide molecules, which facilitates its hydration. A different gel preparation system was used as it allows the preparation of gels with deeper wells. These wells have a loading capacity of 35 μ L of sample volume instead of 15 μ L as in the previous experiments.

Figure 4.20 shows gels stained with coomassie blue staining. In this figure are presented free peptide fractions (wells 1 to 4), peptide encapsulated fractions previously separated from liposomes (wells 5 to 6) and, additionally, samples with the resulting lipid content (wells 9 to 12).

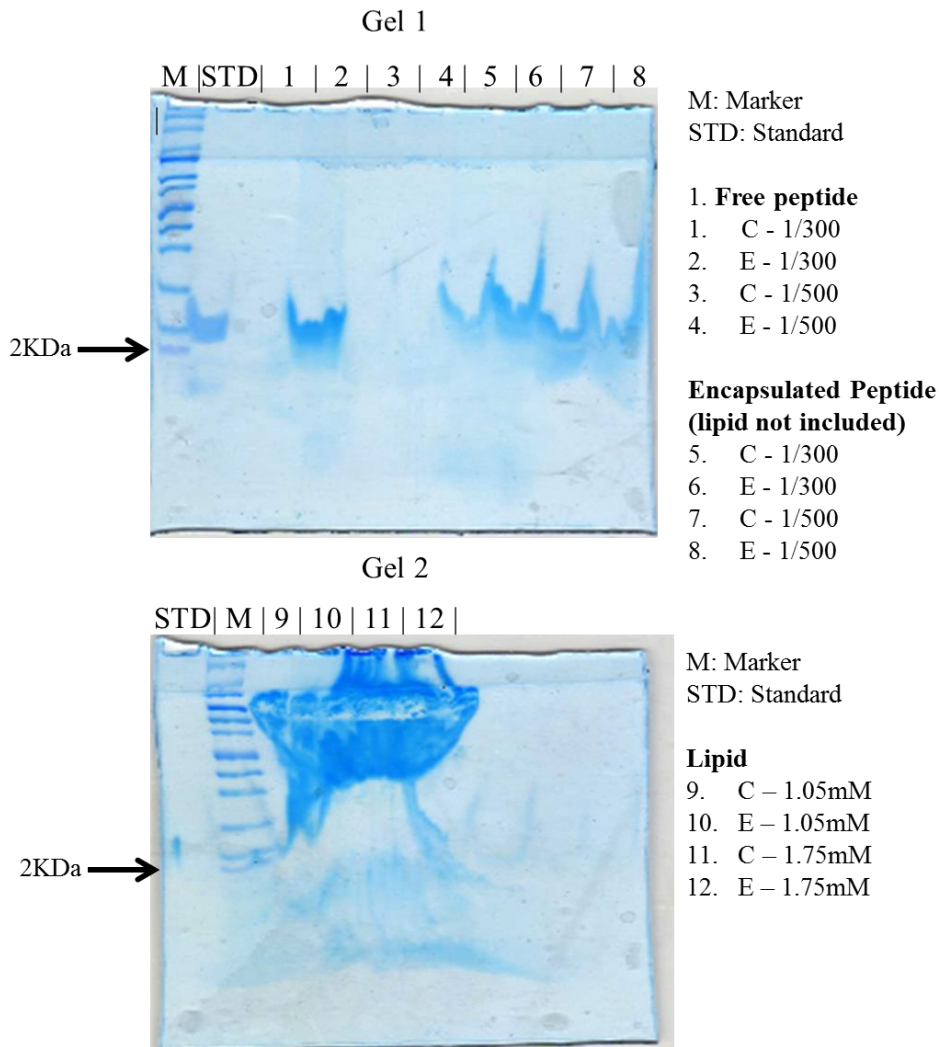


Figure 4.20 – Gels with comassie blue staining. Samples showed are relative to method E and method C and to peptide/lipid molar ratios of 1/300 and 1/500.

Gel 1 from Figure 4.20 shows a smear effect in wells 5 to 8, corresponding to peptide encapsulated fractions, probably due to the urea buffer salts or a too high peptide concentration. Because of this, peptide quantification was not possible. Although photographs from Figure 4.17 showed free peptide presence in all tubes, free peptide was detected only in the sample corresponding to 1/300 peptide/lipid molar ratio prepared by method E (well 2). Peptide may have not been pipetted properly into gel wells due to its low solubility, or this gel electrophoresis analyses is not sensitive enough to detect such small peptide quantities.

In gel 2, samples corresponded only to lipid fractions, in which significant haul can be seen again and peptide cannot.

Results from third experiment are more reliable than results from the first and second ones. Still, peptide low solubility and the low peptide concentration used in this work, 10 µg/mL, made peptide quantification by this method difficult. Nevertheless, peptide encapsulation was proven as free peptide was detected in much smaller quantities than encapsulated peptide.

In conclusion, the higher lipid content of 1.75 mM corresponding to 1/500 peptide/lipid molar ratio showed the highest encapsulation. This is consistent with reported results that indicate that higher lipid concentration is responsible, in part, for higher encapsulation efficiency (Colletier et al., 2002; Xu, Costa, Khan, et al., 2012). This was attributed to the positive impact on the total internal volume of liposomes and total vesicles number, resulting in higher entrapment volume (Xu, Costa, & Burgess, 2012; Xu, Khan, & Burgess, 2011, 2012a, 2012b).

It should be noted that 1/300 molar ratio prepared by method E showed higher encapsulation than the sample consisting of 1/500 molar ratio produced by method C. This reinforces that the lipid film hydration is a powerful method to achieve high encapsulation efficiencies (Frézard, 1999; Kirby & Gregoriadis, 1984). However, another variable should be considered, the extrusion process. In method E, the peptide is added to extruded MLV (LUV) while in method C the peptide is added to non-extruded MVV. As already mentioned, unprocessed liposomes have limited use due to heterogeneity. Before extrusion, MLV has 10% of the total lipid presented in the outer monolayer of the external bilayer, while after extrusion this value is raised to 50% (Gregory Gregoriadis, 2007b). The same explanation may serve for MVV and other unprocessed liposomes in general.

Several methods are available to evaluate the percentage of encapsulation (Zaia, Zaia, & Lichting, 1998). However, peptide concentration used in this work is so small that it was difficult to find a method capable to detect it. Nevertheless, efforts were made to understand which sample encapsulated more peptide.

4.4. Delivery of antigenic BCR-ABL junctional peptide

4.4.1. Optimization of the control LPS Activation

To evaluate the system's ability to stimulate an immune response an ELISA was conducted for the quantification of TNF- α . LPS was primarily tested to prove that THP-1 cells are responsive to this lipopolysaccharide and that activation translates into TNF- α production and secretion.

The formulations tested at this stage of the work are the same that were used in encapsulation efficiency tests, presented in the previous section of results.

Figure 4.21 shows the amount of TNF- α produced in pg/mL after incubating cells with four different LPS concentrations at three time points: 4h, 12h and 24h. The quantification assay was conducted at the final stage of the ELISA, 15 minutes after sample incubation with pNPP substrate. The optical density (405 nm) was measured on a suitable microplate reader and a calibration curve (Appendix III) was used to correlate O.D. measurements with TNF- α concentration (pg/mL).

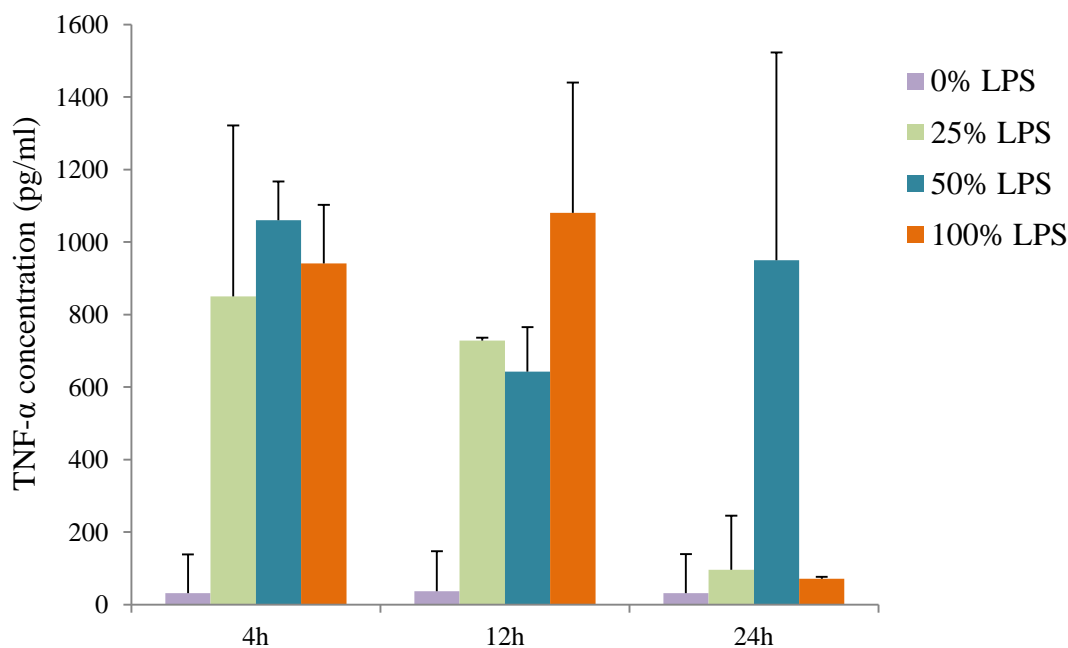


Figure 4.21 – Quantitative results for TNF- α (pg/mL) produced in response to 4h, 12h and 24h of incubation with four LPS conditions: 0%, 25%, 50% and 100%.

From Figure 4.21 we can observe that THP-1 cells are responsive to LPS. A residual quantity of TNF- α is naturally produced by these cells as it can be verified by samples to which LPS was not added (0% LPS). After 4h of incubation with LPS at 25%, 50% and 100%, TNF- α production is at its maximum when comparing to 12h and 24h, with minor exceptions. Other reported results have shown TNF- α production by THP-1 cells after 4h of incubation with LPS (Moreira-Tabaka et al., 2012). Therefore, 4h of incubation was chosen for subsequent work.

Although the maximum TNF- α concentration was induced by incubating cells with the highest amount of LPS, 100% (12h), standard deviations are generally high and increasing LPS dose does not necessarily lead to production of higher amounts of TNF- α . After 4h incubation, 25%, 50% and 100% of LPS conditions did not show significant differences as they led to detection of TNF- α concentrations of 850.3 pg/mL, 1060.2 pg/mL and 940.8 pg/mL, respectively.

After 24h of incubation TNF- α concentration decreased significantly in all conditions, with the exception for 50% LPS sample. This may be a sign of cells exhaustion or toxicity.

4.4.2. Peptide Activation assay

To ensure that BCR-ABL peptide used in this work can stimulate the production of TNF- α , six peptide concentrations dissolved in HEPES buffer were tested: 5, 10, 20, 50, 80 and 100 μ g/mL. Samples were collected and frozen after 4h of incubation with cells, prior to TNF- α quantification.

Figure 4.22 shows TNF- α concentration produced by THP-1 cells with increasing peptide concentrations, after 4h of incubation. Using an ELISA kit, the optical density (405nm) was measured after 15 minutes incubation with pNPP substrate and a calibration curve (Appendix III Figure 2) was used to convert O.D. measures in TNF- α concentration (pg/mL).

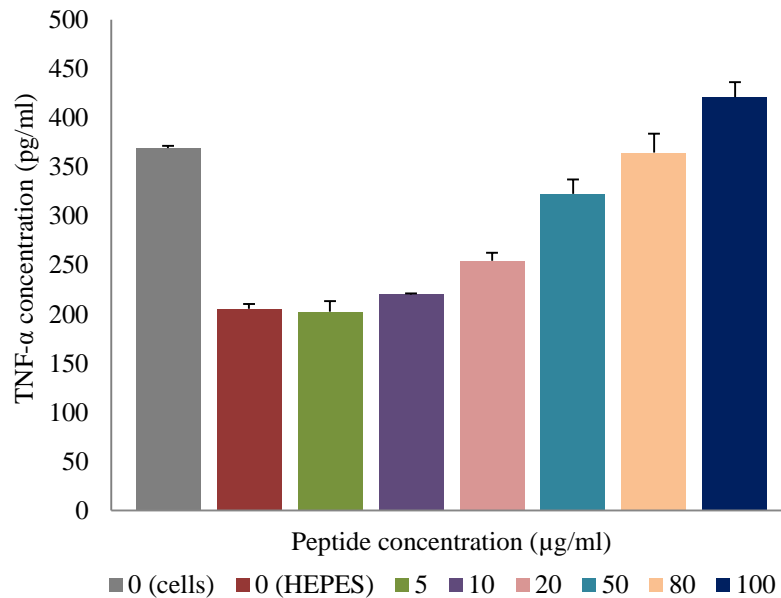


Figure 4.22 – Quantitative results for TNF- α (pg/mL) produced by THP-1 cells in response to 4h of incubation with increasing peptide concentrations: 0 (cells control), 0 (HEPES control), 5, 10, 20, 50, 80 and 100 $\mu\text{g/mL}$.

Although the sample that contains only cells (control) demonstrated a high concentration of TNF- α , Figure 4.22 clearly shows an increasing TNF- α production with increasing peptide concentration. Cells control sample odd result may be due to culture medium interference as it did not happen in the other experiences.

Cells were also incubated with HEPES buffer which also resulted in some TNF- α production. This sample demonstrated a result similar to the sample that was incubated with the lowest peptide concentration, 5 $\mu\text{g/mL}$. From 10 $\mu\text{g/mL}$ upwards, BCR-ABL peptide is capable of inducing a concentration dependent overexpression of TNF- α . The overproduction of TNF- α is strongly involved in acute inflammation and chronic inflammatory diseases as it plays an important role in host defense and immunosurveillance.

4.4.3. Peptide/DODAC:MO(1:2) Activation assay

To evaluate if DODAC:MO (1:2) system can stimulate the production of TNF- α , peptide/DODAC:MO(1:2) nanoparticles prepared by method E (liposomes prepared by lipid film hydration/extrusion (LUV) followed by incubation with peptide) and C (liposomes prepared by ethanolic injection followed by peptide incubation) were tested:

- ▶ 10 μ g/mL [peptido] and 1.75 mM [lipid] (1/500 molar ratio) - method E
- ▶ 10 μ g/mL [peptido] and 1.05 mM [lipid] (1/300 molar ratio) - method E
- ▶ 10 μ g/mL [peptido] and 1.75 mM [lipid] (1/500 molar ratio) - method C
- ▶ 10 μ g/mL [peptido] and 1.05 mM [lipid] (1/300 molar ratio) - method C

Samples were submitted to a previous amicon separation so that free peptide molecules could be excluded from analyses and the samples could be concentrated to boost the response by THP-1 cells. The intent was to increase peptide concentration as 10 μ g/mL did not induce significantly high TNF- α concentrations (Figure 4.22) and detailed study about encapsulation of higher peptide concentrations had not been conducted. Therefore, the real peptide concentration came to be 23.8 μ g/mL instead of 10 μ g/mL and lipid concentration became to 4.17 mM and 2.5 mM instead of 1.75 mM and 1.05 mM, respectively.

Figure 4.23 presents TNF- α concentration produced by THP-1 cells after 4h of incubation with DODAC:MO (1:2) lipid vesicles (controls) and peptide/DODAC:MO(1:2) nanoparticles. The optical density (405 nm) was measured after 15 minutes of incubation with pNPP substrate and a calibration curve (Appendix III) was used to convert O.D. measures in TNF- α concentration (pg/mL).

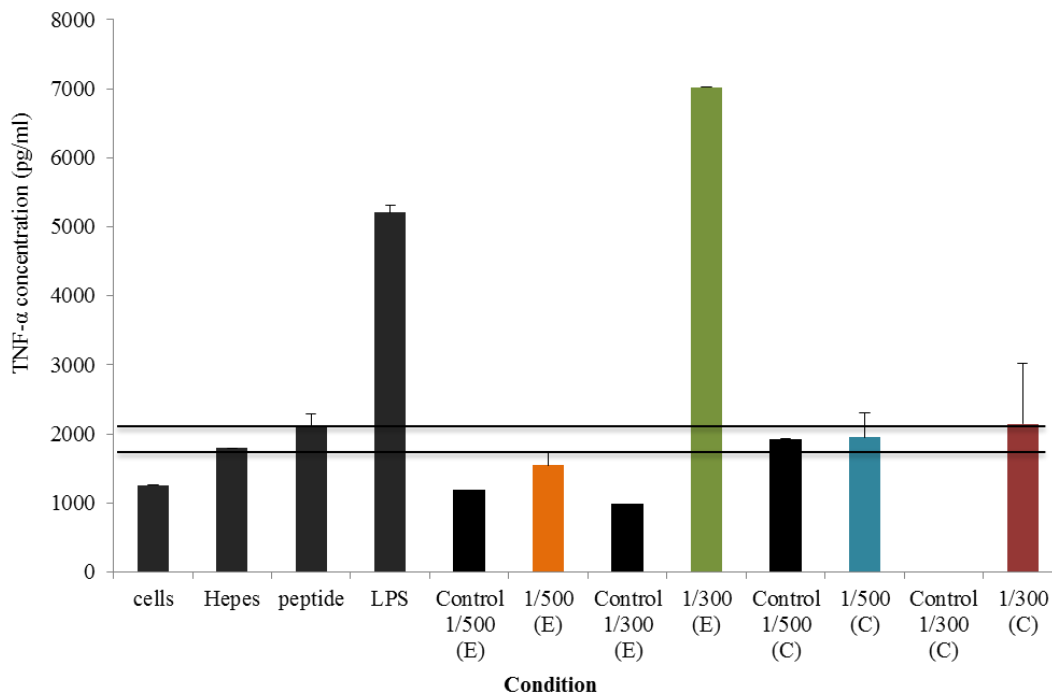


Figure 4.23 – Quantitative results for TNF- α (pg/mL) produced by THP-1 cells in response to 4h of incubation with DODAC:MO (1:2) vesicles and peptide/DODAC:MO(1:2) nanoparticles. Cells without any treatment, HEPES at 10 mM, LPS at 100% and peptide at 23.8 μ g/mL were used as controls.

From Figure 4.23 we can observe that THP-1 cells naturally produced a small quantity of TNF- α , 1256 pg/mL, as expected. The production of this pro-inflammatory cytokine was higher when cells were incubated with HEPES buffer (10 mM), 1795 pg/mL. Peptide at a concentration of 23.8 μ g/ml was able to induce a higher response than cells and HEPES controls. LPS showed a very high production of a TNF- α concentration, 5205.5 pg/mL, as expected.

Generally, lipid vesicles (controls) showed lower results when compared to peptide or HEPES samples, which means that the presence of lipid is not responsible for TNF- α overproduction.

On one hand, vesicles produced by method C induced a slightly higher response at both molar ratios tested (1/300 and 1/500). On the other hand, vesicles prepared by method E induced an extremely strong response at only one peptide/lipid molar ratio (1/300). These findings support that liposomes as delivery vehicles are capable of increasing the index of a peptide or a drug as already reported in other studies (Gregory Gregoriadis, 2007a; Guan et al., 1998).

This will improve peptide biological effect and will allow decreasing the dose to be administrated.

Despite having less lipid, 1/300 formulations showed a higher effect than 1/500 formulations. This indicates that the formulation that is capable of achieving the highest encapsulation efficiency is not necessarily the most effective in inducing an immune response.

It is also important to refer that the data obtained from the ELISA reader showed gaps in some values (Appendix III). This is responsible for the result obtained for the lipid vesicles prepared by method C (control), with a total lipid content that correspond to the peptide/lipid 1/300 molar ratio, as well as it may be disguising other results from Figure 4.23. Nevertheless, the lack of values for TNF- α production was observed for the smaller absorbance values, meaning for the samples that induced the weakest responses.

Figures 4.24 and 4.25 show the most representative microscope images that focus the different outcomes of the distinct conditions. These pictures were taken using an inverted fluorescence microscope (Olympus IX71).

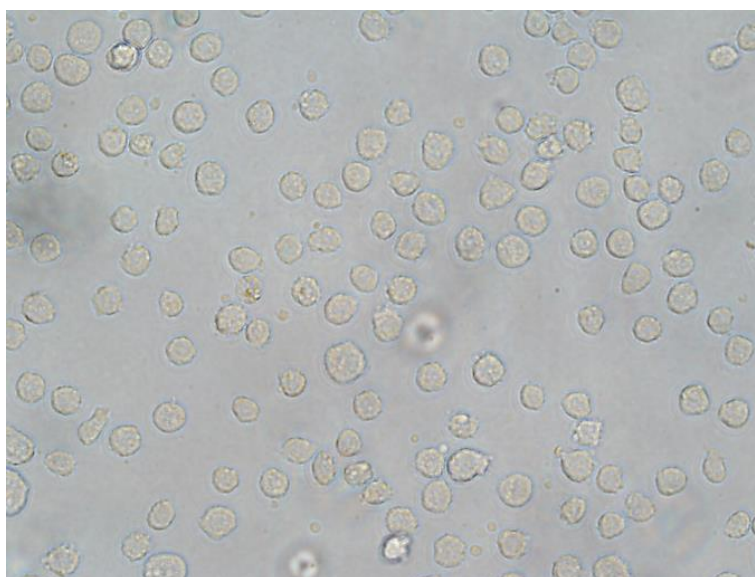


Figure 4.24 – THP-1 cells after 4h, without any treatment (40x magnification).

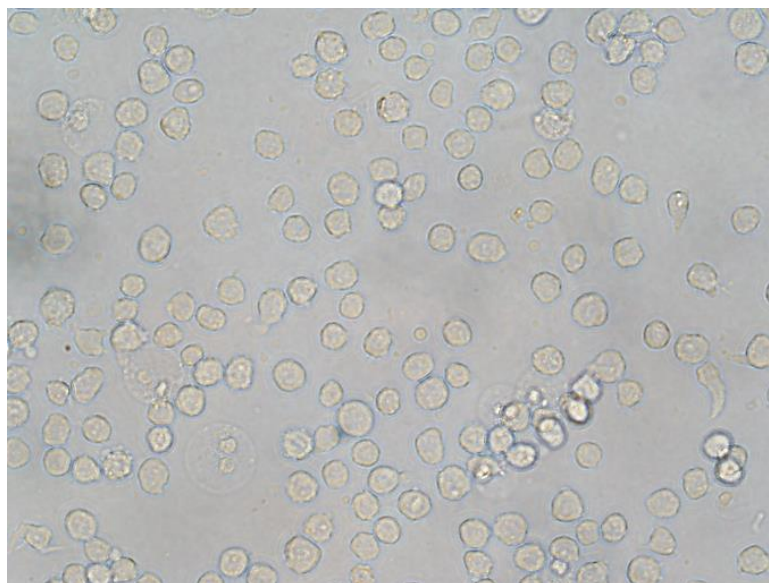


Figure 4.25 – THP-1 cells after 4h of incubation with a peptide concentration of 100 µg/mL (40x magnification).

Figure 4.24 shows that THP-1 cells have a cylindrical shape. Figure 4.25 shows that a peptide concentration of 100 µg/mL, after 4h of incubation, induced a change in very few cells.

Nanoparticles produced a peculiar effect on THP-1 cells after 4h of incubation. This behavior was detected in all nanoparticles as well as in the respective controls. Several aggregates were visible at the naked eye at this time point of the experiment (images not shown). These peculiar outcomes may be due to a high lipid concentration as samples had to be concentrated prior to this analyzes in order to raise the probabilities of obtaining results with such a low peptide concentration. Nevertheless, there is no sign that this behavior is harmful to cells.

(Page intentionally left blank)

Chapter 5

Conclusions and Future Directions

(Page intentionally left blank)

5. CHAPTER 5 CONCLUSIONS AND FUTURE DIRECTION

5.1. Conclusions

A neutral pH is a suitable condition to solubilize BCR-ABL peptide. Results suggested that acidic and alkaline conditions may induce changes in peptide's secondary structure, possibly leading to its loss of function as well.

In spite of citrate-phosphate buffer showed more desirable peptide features at acidic and alkaline conditions than HEPES buffer, HEPES was more adequate to produce nanoparticles at neutral conditions.

DLS results (Zeta potential and mean diameter) showed that the nanoparticles produced depend on the protocol used and also on the peptide/lipid molar ratio. However, results suggested that the peptides were attached / incorporated into liposomes for all the different protocols.

The four distinct protocols, as well as the four different peptide/lipid molar ratios, used in this study led to the production of different nanoparticles in terms of its conformational organization. The mean size and z-potential of the final nanoparticles are dependent or affected by lipid concentration, mode of preparation and peptide concentration.

Increasing lipid concentration leads to a higher number of lipid vesicles, consequently decreasing the number of peptides per liposome and ultimately decreasing liposomes fusion. Results suggested that an increase in lipid concentration leads to an increasingly better peptide-liposome organization, but also that there is a critical concentration below which there is too much peptide that cannot be properly incorporated (1.05 mM).

Lipid film hydration method produces more homogeneous nanoparticles than ethanolic injection.

Nanoparticles prepared by post-insertion protocol leads to a higher peptide amount at the surface of vesicles when compared to direct-insertion technique. These peptides at the surface of liposomes induce membrane fusion, increasing nanoparticle's mean size.

The use of the extrusion process before or after peptide addition to liposomes preparation is a detrimental factor to achieve higher peptide encapsulation as this size-reducing process is

responsible for peptide loss. The distribution of intensity profiles showed that only at 1/500 molar ratio formulation all the negative particles were neutralized when peptides were added after extrusion (method E).

Lipid film hydration, method A, demonstrated higher encapsulation efficiency than ethanolic injection, method C. Higher lipid concentration showed higher peptide encapsulation, however, a lower lipid concentration was able to induce a stronger response by THP-1 cells.

Gel electrophoresis technique using tricine was valuable to detect peptide presence/absence among the different samples, as well as to show that the methodology used to separate the free fraction from the encapsulated peptide fraction was successful.

Peptide/DODAC:MO(1:2) nanoparticles were capable of inducing a stronger cells response than the peptide by itself. The most encouraging results were observed for 1/300 molar ratio (10 µg/mL of peptide concentration and 1.75 mM of lipid concentration) prepared by lipid film hydration and using the post-insertion protocol.

The optimization of the control using LPS was successfully conducted and THP-1 cells worked as a suitable cell model. Nanoparticles produced a peculiar aggregation effect on THP-1 cells possibly due to a high lipid concentration. Cytotoxicity studies were not conducted; however, there is no morphological sign that this aggregation behavior is harmful to cells. In fact, based on previous studies, there are reasons to believe that this lipid content does not cause any harmful effect.

Despite the cytotoxicity issues around cationic liposomes, it has been shown that they promote a much higher humoral and cytotoxic T lymphocyte immune response against the antigen (Chen & Huang, 2005).

This thesis addressed the characterization of the cationic system DODAC/Monoolein (1:2) and emphasized its potential in the development of an immunoprotective treatment for chronic myeloid leukemia.

After the preliminary results described in this thesis, encapsulation and delivery of the BCR-ABL peptide can be optimized in future works.

Potentiated biological activity of the system should be repeated for confirmation and ideally evaluated in *in vivo* models.

5.2. Future work

In the next couple of years, consolidation therapy for myeloid leukemia will be more immune based. Antigen discovery associated to novel nanotechnology approaches will potentiate the development of vaccines targeting peptides that are highly specific to myeloid leukemia cells. Such discoveries will revolutionize survival perspectives of CML patients.

Based on the preliminary results obtained in this study future developments can be made in the following research lines:

- It would be valuable to test the incorporation of increasing peptide concentrations into DODAC:MO (1:2) lipid vesicles to elicit the most potent, yet highly leukemia-specific, immune responses.
- Fluorescence anisotropy would be an excellent tool for the study of molecular interactions, since it provides important information about the location of the peptide within the liposome. Using fluorescently (e.g. FITC) labeled molecules would be helpful to quantify the incorporation of antigenic peptide.
- It would be important to confirm the structural integrity of the peptides after their incorporation into liposomes. Circular Dichroism (CD) spectroscopy as one of the most sensitive methods for detecting changes in protein structure, would be useful to determine the structure of antigenic peptide when incorporated in the liposomal formulations
- Other microscopic techniques to visualize particle's features, as confocal fluorescence microscopy (CFM) using appropriate fluorophores, atomic force microscopy (AFM) or even scanning electron microscope (SEM), can represent powerful tools in this research field.
- Imaging at high resolution is extremely useful both when characterizing biophysically the liposomes and when monitoring the uptake of nano-delivery systems by target cells. Incorporation of antigenic peptide and PEG-folate to be quantified by Confocal Raman microscopy (CRM) in order to obtain sub-micrometer resolved images of chemical components in the liposomes.

- With further understanding of the processes involved in immune response regarding CML, it will be possible to more accurately determine the optimal timing for the application of liposomal vaccine therapies to elicit the most potent immune responses. With exhaustive laboratory and animal data supporting leukemia liposomal vaccines, studies will be moving rapidly into the clinical setting.

(Page intentionally left blank)

REFERENCES

- Alving, C. R. (1991). Liposomes as carriers of antigens and adjuvants. *Journal of immunological methods*, *140*(1), 1–13. Retrieved from <http://www.ncbi.nlm.nih.gov/pubmed/1712030>
- Audibert, F. (2003). Adjuvants for vaccines, a quest. *International Immunopharmacology*, *3*, 1187–1193.
- Bangham, A. D., Standish, M. M., & Watkins, J. C. (1965). Diffusion of univalent ions across the lamellae of swollen phospholipids. *Journal of Molecular Biology*, *13*(1), 238–52.
- Bergantini, A. P. F., Castro, F. A., Souza, A. M., & Fett-conte, A. C. (2005). Leucemia mielóide crônica e o sistema Fas-FasL. *Rev. bras. hematol. hemoter*, *27*(2), 120–25.
- Bessalle, R., Gorea, A., Shalit, I., Metzger, J. W., Dass, C., Desiderio, D. M., & Fridkin, M. (1993). Structure-function studies of amphiphilic antibacterial peptides. *Journal of Medicinal Chemistry*, *36*(9), 1203–1209. doi:10.1021/jm00061a011
- Bhardwaj, U., & Burgess, D. J. (2010). Physicochemical properties of extruded and non-extruded liposomes containing the hydrophobic drug dexamethasone. *International journal of pharmaceutics*, *388*(1-2), 181–9. doi:10.1016/j.ijpharm.2010.01.003
- Bitounis, D., Fanciullino, R., Iliadis, A., & Ciccolini, J. (2012). Optimizing Druggability through Liposomal Formulations: New Approaches to an Old Concept. *ISRN pharmaceutics*, *2012*, 738432. doi:10.5402/2012/738432
- Bocchia, M., Defina, M., & Aprile, L. (2010). Complete molecular response in CML after p210 BCR–ABL1-derived peptide vaccination. *Nature Reviews*, *7*, 600–3. Retrieved from <http://www.nature.com/nrclinonc/journal/vaop/ncurrent/full/nrclinonc.2010.141.html>
- Chikh, G. G., Kong, S., Bally, M. B., Meunier, J. C., & Schutze-Redelmeier, M. P. (2001). Efficient delivery of Antennapedia homeodomain fused to CTL epitope with liposomes into dendritic cells results in the activation of CD8+ T cells. *Journal of immunology*, *167*(11), 6462–70. Retrieved from <http://www.ncbi.nlm.nih.gov/pubmed/11714813>
- Colletier, J.-P., Chaize, B., Winterhalter, M., & Fournier, D. (2002). Protein encapsulation in liposomes: efficiency depends on interactions between protein and phospholipid bilayer. *BMC biotechnology*, *2*, 9. Retrieved from <http://www.pubmedcentral.nih.gov/articlerender.fcgi?artid=113741&tool=pmcentrez&rendertype=abstract>
- Copland, M. J., Baird, M. A., Rades, T., McKenzie, J. L., Becker, B., Reck, F., ... Davies, N. M. (2003). Liposomal delivery of antigens to human dendritic cells. *Vaccine*, *21*, 883–890.
- Dao, T., & Scheinberg, D. a. (2008). Peptide vaccines for myeloid leukaemias. *Best practice & research. Clinical haematology*, *21*(3), 391–404. doi:10.1016/j.beha.2008.05.001

- De Souza, D. L., Frisch, B., Duportail, G., & Schuber, F. (2002). Membrane-active properties of alpha-MSH analogs: aggregation and fusion of liposomes triggered by surface-conjugated peptides. *Biochimica et biophysica acta*, *1558*(2), 222–37. Retrieved from <http://www.ncbi.nlm.nih.gov/pubmed/11779571>
- Do, T. D., Lapointe, N. E., Economou, N. J., Buratto, S. K., Feinstein, S. C., Shea, J.-E., & Bowers, M. T. (2013). Effects of pH and Charge State on Peptide Assembly: The YVIFL Model System. *The journal of physical chemistry. B*, *117*(37), 10759–10768. doi:10.1021/jp406066d
- Druker, B. J., Talpaz, M., Resta, D. J., Peng, B., Buchdunger, E., & J.M. Ford, et al. (2001). Efficacy and safety of a specific inhibitor of the BCR-ABL tyrosine kinase in chronic myeloid leukemia. *N Engl J Med*, *344*(14), 1031–37.
- Drummond, D. C., Meyer, O., Hong, K., Kirpotin, D. B., & Papahadjopoulos, D. (1999). Optimizing Liposomes for Delivery of Chemotherapeutic Agents to Solid Tumors. *Pharmacol. Rev.*, *51*(4), 691–744. Retrieved from <http://pharmrev.aspetjournals.org/content/51/4/691.full>
- Falkenburg, J. H. F., Smit, W. M., & Willemze, R. (1997). Cytotoxic T-lymphocyte (CTL) responses against acute or chronic myeloid leukemia. *Immunological Reviews*, (157), 223–230.
- Feitosa, E., & Alves, F. R. (2008). The role of counterion on the thermotropic phase behavior of DODAB and DODAC vesicles. *Chemistry and physics of lipids*, *156*(1-2), 13–6. doi:10.1016/j.chemphyslip.2008.08.001
- Feitosa, E., Alves, F. R., Castanheira, E. M. S., & Oliveira, M. E. C. D. R. (2009). DODAB and DODAC bilayer-like aggregates in the micromolar surfactant concentration domain. *Colloid and Polymer Science*, *287*(5), 591–599. doi:10.1007/s00396-009-2008-1
- Feitosa, E., Karlsson, G., & Edwards, K. (2006). Unilamellar vesicles obtained by simply mixing dioctadecyldimethylammonium chloride and bromide with water. *Chemistry and Physics of Lipids*, *140*(1-2), 66–74.
- Fifis, T., Gamvrellis, A., Crimeen-Irwin, B., Pietersz, G. a, Li, J., Mottram, P. L., ... Plebanski, M. (2004). Size-dependent immunogenicity: therapeutic and protective properties of nano-vaccines against tumors. *Journal of immunology (Baltimore, Md. : 1950)*, *173*(5), 3148–54. Retrieved from <http://www.ncbi.nlm.nih.gov/pubmed/15322175>
- Frézard, F. (1999). Liposomes: from biophysics to the design of peptide vaccines. *Brazilian journal of medical and biological research*, *32*(2), 181–189. Retrieved from <http://www.ncbi.nlm.nih.gov/pubmed/10347753>
- Friede, M., Vanregenmortel, M. H. V., & Schuber, F. (1993). Lyophilized Liposomes as Shelf Items for the Preparation of Immunogenic Liposome-Peptide Conjugates. *Analytical Biochemistry*, *211*(1), 117–122. Retrieved from <http://www.sciencedirect.com/science/article/pii/S0003269783712418>

- Gregoriadis, G., Florence, A. T., & Patel, H. M. (1993). *Liposomes in Drug Delivery*. Switzerland: Harwood Academic.
- Gregoriadis, Gregory. (1990). Immunological adjuvants: a role for liposomes. *Immunology Today*, 11, 89–97. doi:10.1016/0167-5699(90)90034-7
- Gregoriadis, Gregory. (2007a). *Liposome Technology: Entrapment of drugs and other materials into liposomes*. Retrieved from http://books.google.pt/books/about/Liposome_Technology_Entrapment_of_drugs.html?id=pA5tAAAAMAAJ&pgis=1
- Gregoriadis, Gregory. (2007b). *Liposome Technology. Liposome Preparation and Related Techniques. Volume I*. (3rd ed.). London.
- Guan, H. H., Budzynski, W., Koganty, R. R., Krantz, M. J., Reddish, M. A., Rogers, J. A., ... Samuel, J. (1998). Liposomal formulations of synthetic MUC1 peptides: effects of encapsulation versus surface display of peptides on immune responses. *Bioconjug Chem*, 9(4), 451–8.
- Guilhot, F., Roy, L., Saulnier, P.-J., Guilhot, J., Barra, A., Gombert, J.-M., & Turhan, A. (2008). Immunotherapeutic approaches in chronic myelogenous leukemia. *Leukemia & lymphoma*, 49(4), 629–34. doi:10.1080/10428190801927510
- Hambly, A. (2013). Proteins - Amino Acids. Retrieved October 10, 2013, from <http://www.whitetigernaturalmedicine.com/nutrition/proteins-amino-acids>
- Hashizume, H., Baluk, P., Morikawa, S., McLean, J. W., Thurston, G., Roberge, S., ... McDonald, D. M. (2000). Openings between defective endothelial cells explain tumor vessel leakiness. *The American journal of pathology*, 156(4), 1363–80. doi:10.1016/S0002-9440(10)65006-7
- Hope, M. J., Bally, M. B., Webb, G., & Cullis, P. R. (1985). Production of large unilamellar vesicles by a rapid extrusion procedure. Characterization of size distribution, trapped volume and ability to maintain a membrane potential. *Biochimica et Biophysica Acta (BBA) - Biomembranes*, 812(1), 55–65. Retrieved from <http://www.sciencedirect.com/science/article/pii/0005273685905218>
- HubPages, I. (2013). Notes on Standard Twenty Amino Acids. Retrieved October 15, 2013, from <http://nalinimarquez.hubpages.com/hub/Notes-on-Amino-Acids>
- Ikonen, M., Murtomäki, L., & Kontturi, K. (2010). Microcalorimetric and zeta potential study on binding of drugs on liposomes. *Colloids and surfaces. B, Biointerfaces*, 78(2), 275–82. doi:10.1016/j.colsurfb.2010.03.017
- Jain, R. K. (1987). Transport of Molecules in the Tumor Interstitium : A Review Transport of Molecules in the Tumor Interstitium : A Review. *Cancer Res*, 47, 3039–3051.
- Kersten, G. F., & Crommelin, D. J. (1995). Liposomes and ISCOMS as vaccine formulations. *Biochimica et biophysica acta*, 1241(2), 117–38. Retrieved from <http://www.ncbi.nlm.nih.gov/pubmed/7640293>

- Kirby, C., & Gregoriadis, G. (1984). Dehydration-Rehydration Vesicles: A Simple Method for High Yield Drug Entrapment in Liposomes. *Bio/Technology*, 2(11), 979–984. doi:10.1038/nbt1184-979
- Kulkarni, C. V, Wachter, W., Iglesias-Salto, G., Engelskirchen, S., & Ahualli, S. (2011). Monoolein: a magic lipid? *Physical chemistry chemical physics : PCCP*, 13(8), 3004–21. doi:10.1039/c0cp01539c
- Laouini, a., Jaafar-Maalej, C., Limayem-Blouza, I., Sfar, S., Charcosset, C., & Fessi, H. (2012). Preparation, Characterization and Applications of Liposomes: State of the Art. *Journal of Colloid Science and Biotechnology*, 1(2), 147–168. doi:10.1166/jcsb.2012.1020
- Lasic, D. D. (1993). *Liposomes: From Physics to Applications* (p. 575). Elsevier Science Ltd. Retrieved from <http://www.amazon.com/Liposomes-Applications-Danilo-D-Lasic/dp/0444895485>
- Lee, T., Wu, H., Tseng, Y., & Lin, C. (2004). A Novel Peptide Specifically Binding to Nasopharyngeal Carcinoma For Targeted Drug Delivery A Novel Peptide Specifically Binding to Nasopharyngeal Carcinoma For Targeted Drug Delivery. *Cancer Res*, 64, 8002–8008.
- Lee, T.-Y., Lin, C.-T., Kuo, S.-Y., Chang, D.-K., & Wu, H.-C. (2007). Peptide-mediated targeting to tumor blood vessels of lung cancer for drug delivery. *Cancer research*, 67(22), 10958–65. doi:10.1158/0008-5472.CAN-07-2233
- Lo, A., Lin, C.-T., & Wu, H.-C. (2008). Hepatocellular carcinoma cell-specific peptide ligand for targeted drug delivery. *Molecular cancer therapeutics*, 7(3), 579–89. doi:10.1158/1535-7163.MCT-07-2359
- López-Alonso, J. P., Bruix, M., Font, J., Ribó, M., Vilanova, M., Jiménez, M. A., ... Laurents, D. V. (2010). NMR spectroscopy reveals that RNase A is chiefly denatured in 40% acetic acid: implications for oligomer formation by 3D domain swapping. *Journal of the American Chemical Society*, 132(5), 1621–30. doi:10.1021/ja9081638
- Ludewig, B., Barchiesi, F., Pericin, M., Zinkernagel, R. M., Hengartner, H., & Schwendener, R. A. (2000). In vivo antigen loading and activation of dendritic cells via a Liposomal peptide vaccine mediates protective antiviral and anti-tumour immunity. *Vaccine*, 19(1), 23–32.
- Mabtech. (2013). Retrieved October 26, 2013, from <http://www.mabtech.com/main/Page.asp?PageId=28>
- Malvern. (2005). Zetasizer Nano Series User Manual. *Malvern Instruments Ltd.*
- Mangino, M., & Harper, J. (2007). Protein Denaturation. Retrieved October 25, 2013, from <http://class.fst.ohio-state.edu/FST822/lectures/Denat.htm>

- Masuda, K., Horie, K., Suzuki, R., Yoshikawa, T., & Hirano, K. (2002). Oral delivery of antigens in liposomes with some lipid compositions modulates oral tolerance to the antigens. *Microbiol Immunol.*, *46*(1), 55–8.
- Matsumura, Y., & Maeda, H. (1986). A new concept for macromolecular therapeutics in cancer chemotherapy: mechanism of tumorotropic accumulation of proteins and the antitumor agent smancs. *Cancer research*, *46*(12 Pt 1), 6387–92. Retrieved from <http://www.ncbi.nlm.nih.gov/pubmed/2946403>
- Melief, C., & Kast, V. (1995). T-cell immunotherapy of tumours by adoptive transfer of cytotoxic T lymphocytes and by vaccination with minimal essential epitopes. *Immunological Reviews*, (145), 167–177.
- Melo, J. V. (1996). The diversity of BCR-ABL fusion proteins and their relationship to leukemia phenotype. *Blood*, (88), 2375–2384.
- Morein, B., Villacrés-Eriksson, M., Sjölander, A., & Bengtsson, K. L. (1996). Novel adjuvants and vaccine delivery systems. *Veterinary immunology and immunopathology*, *54*(1-4), 373–84. Retrieved from <http://www.ncbi.nlm.nih.gov/pubmed/8988882>
- Moreira, J. N., Ishida, T., Gaspar, R., & Allen, T. M. (2002). Use of the post-insertion technique to insert peptide ligands into pre-formed stealth liposomes with retention of binding activity and cytotoxicity. *Pharmaceutical research*, *19*(3), 265–9. Retrieved from <http://www.ncbi.nlm.nih.gov/pubmed/11934232>
- Moreira-Tabaka, H., Peluso, J., Vonesch, J.-L., Hentsch, D., Kessler, P., Reimund, J.-M., ... Muller, C. D. (2012). Unlike for human monocytes after LPS activation, release of TNF- α by THP-1 cells is produced by a TACE catalytically different from constitutive TACE. *PloS one*, *7*(3), e34184. doi:10.1371/journal.pone.0034184
- Mottram, P. L., Leong, D., Crimeen-Irwin, B. S. G., Xiang, S. D., Meanger, J., Ghildyal, R., ... Plebanski, M. (2007). Type 1 and 2 Immunity Following Vaccination Is Influenced by Nanoparticle Size: Formulation of a Model Vaccine for Respiratory Syncytial Virus. *Molecular Pharmaceutics*, *4*(1), 73–84.
- Nieva, J. L., Nir, S., & Wilschut, J. (2008). Destabilization and Fusion of Zwitterionic Large Unilamellar Lipid Vesicles Induced by a β -Type Structure of the Hiv-1 Fusion Peptide. Retrieved from <http://informahealthcare.com/doi/abs/10.3109/08982109809035524>
- Nir, S., & Nieva, J. L. (2000, March). Interactions of peptides with liposomes: pore formation and fusion. *Progress in lipid research*. Retrieved from <http://www.ncbi.nlm.nih.gov/pubmed/10775764>
- Nomura, F., Inaba, T., Ishikawa, S., Nagata, M., Takahashi, S., Hotani, H., & Takiguchi, K. (2004). Microscopic observations reveal that fusogenic peptides induce liposome shrinkage prior to membrane fusion. *Proceedings of the National Academy of Sciences of the United States of America*, *101*(10), 3420–5. doi:10.1073/pnas.0304660101
- Northfelt, D. W., Martin, F. J., Working, P., Volberding, P. A., Russell, J., Newman, M., ... Kaplan, L. D. (1996). Doxorubicin encapsulated in liposomes containing surface-bound

- polyethylene glycol: pharmacokinetics, tumor localization, and safety in patients with AIDS-related Kaposi's sarcoma. *Journal of Clinical Pharmacology*, 36(1), 55–63.
- Oliveira, I. M. S. C., Silva, J. P. N., Feitosa, E., Marques, E. F., Castanheira, E. M. S., & Real Oliveira, M. E. C. D. (2012). Aggregation behavior of aqueous dioctadecyldimethylammonium bromide/monoolein mixtures: a multitechnique investigation on the influence of composition and temperature. *Journal of colloid and interface science*, 374(1), 206–17. doi:10.1016/j.jcis.2012.01.053
- Orlowski, R. Z., Nagler, A., Sonneveld, P., Bladé, J., Hajek, R., Spencer, A., ... Harousseau, J.-L. (2007). Randomized phase III study of pegylated liposomal doxorubicin plus bortezomib compared with bortezomib alone in relapsed or refractory multiple myeloma: combination therapy improves time to progression. *Journal of clinical oncology : official journal of the American Society of Clinical Oncology*, 25(25), 3892–901. doi:10.1200/JCO.2006.10.5460
- Pecheur, E. I., Martin, I., Ruyschaert, J. M., Bienvenue, A., & Hoekstra, D. (1998). Membrane Fusion Induced by 11-mer Anionic and Cationic Peptides : A Structure - Function Study. *Biochemistry*, 37(8), 2361–71. doi:10.1021/bi972697f
- Pecora, R. (2000). Dynamic light scattering measurement of nanometer particles in liquids. *Journal of Nanoparticle Research*, 2(2), 123–131.
- Pérez-Pérez, G. I., Shepherd, V. L., Morrow, J. D., & Blaser, M. J. (1995). Activation of human THP-1 cells and rat bone marrow-derived macrophages by *Helicobacter pylori* lipopolysaccharide. *Infection and immunity*, 63(4), 1183–7. Retrieved from <http://www.pubmedcentral.nih.gov/articlerender.fcgi?artid=173132&tool=pmcentrez&rendertype=abstract>
- Philippot, J. R., & Schuber, F. (1995). *Liposomes as Tools in Basic Research and Industry*. Boca Raton: CRC Press.
- Pinilla-Ibarz, J., Cathcart, K., Korontsvit, T., Soignet, S., Bocchia, M., Caggiano, J., ... Scheinberg, D. a. (2000). Vaccination of patients with chronic myelogenous leukemia with bcr-abl oncogene breakpoint fusion peptides generates specific immune responses. *Blood*, 95(5), 1781–7. Retrieved from <http://www.ncbi.nlm.nih.gov/pubmed/10688838>
- Publishing, W. B. (2013). pH and pKa. Retrieved October 20, 2013, from <http://www.web-books.com/MoBio/Free/Ch2A4.htm>
- Purdie, N., Brittain, H. G., Towell, J. F., & Manning, M. C. (1994). Chapter 6 Analysis of protein structure by circular dichroism spectroscopy. *Techniques and Instrumentation in Analytical Chemistry*, 14, 175–205. Retrieved from <http://www.sciencedirect.com/science/article/pii/S0167924408701793>
- Qin, Z. (2012). The use of THP-1 cells as a model for mimicking the function and regulation of monocytes and macrophages in the vasculature. *Atherosclerosis*, 221(1), 2–11. doi:10.1016/j.atherosclerosis.2011.09.003

- Quintás-Cardama, A., & Cortes, J. (2009, February 19). Molecular biology of bcr-abl1-positive chronic myeloid leukemia. *Blood*. doi:10.1182/blood-2008-03-144790
- Ramon, G. (1924). Sur la toxine et surranatoxine diphtheriques. *Ann. Inst. Pasteur*, 38, 1.
- Rao, M., & Alving, C. R. (2000). Delivery of lipids and liposomal proteins to the cytoplasm and Golgi of antigen-presenting cells. *Adv Drug Deliv Rev.*, 41(2), 171–88.
- Rapaport, D., Peled, R., Nir, S., & Shai, Y. (1996). Reversible surface aggregation in pore formation by pardaxin. *Biophysical journal*, 70(6), 2502–12. doi:10.1016/S0006-3495(96)79822-3
- Ruan, L., Luo, H., Zhang, H., & Xing, Z. (2013). Effect of sonication on a novel designed peptide. *Journal of Wuhan University of Technology-Mater. Sci. Ed.*, 28(3), 622–626. doi:10.1007/s11595-013-0741-2
- Ryhänen, S. (2006). Biophysical Studies on Cationic Liposomes : Implications for Self-assembly and Mechanism of Lipofection. Helsingfors universitet. Retrieved from <https://helda.helsinki.fi/handle/10138/20213>
- Sabín, J., Prieto, G., Ruso, J. M., Hidalgo-Alvarez, R., & Sarmiento, F. (2006). Size and stability of liposomes: a possible role of hydration and osmotic forces. *The European physical journal. E, Soft matter*, 20(4), 401–8. doi:10.1140/epje/i2006-10029-9
- Sardan, M., Kilinc, M., Genc, R., Tekinay, A. B., & Guler, M. O. (2013). Cell penetrating peptide amphiphile integrated liposomal systems for enhanced delivery of anticancer drugs to tumor cells. *Faraday Discussions*. doi:10.1039/c3fd00058c
- Schaffazick, S. R., & Guterres, S. A. (2003). Caracterização e estabilidade físico-química de sistemas poliméricos nanoparticulados para administração de fármacos. *Quimica Nova*, 26(5), 726–737.
- Schägger, H. (2006). Tricine–SDS-PAGE. *Nature Protocols*, 1(1), 16–22.
- Schijns, V. E. (2000). Immunological concepts of vaccine adjuvant activity. *Current opinion in immunology*, 12(4), 456–63. Retrieved from <http://www.ncbi.nlm.nih.gov/pubmed/10899018>
- Schinjs, V. E. J. C., & T.O’Hagan, D. (2006). *Immunopotentiators in Modern Vaccines*. *Immunopotentiators in Modern Vaccines* (pp. 125–128).
- Shtivelman, E., Lifshitz, B., Gale, R. P., Roe, B. A., & Canaani, E. (1986). Alternative splicing of RNAs transcribed from the human abl gene and from the bcr-abl fused gene. *Cell*, 47(2), 277–284.
- Silva, R., Little, C., Ferreira, H., & Cavaco-Paulo, A. (2008). Incorporation of Peptides in Phospholipid Aggregates using Ultrasound. *Ultrasonics Sonochemistry*, 1026–1032.

- Singer, S. J., & Nicolson, G. L. (1972). The fluid mosaic model of the structure of cell membranes. *Science (New York, N.Y.)*, 175(4023), 720–31. Retrieved from <http://www.ncbi.nlm.nih.gov/pubmed/4333397>
- Size theory. (2004). In *Zetasizer Nano Series User Manual*. England.
- Smahel, M. (2011). Antigens in chronic myeloid leukemia: implications for vaccine development. *Cancer immunology immunotherapy*, 60(12), 1655–68. doi:10.1007/s00262-011-1126-z
- Strömstedt, A. a., Ringstad, L., Schmidtchen, A., & Malmsten, M. (2010). Interaction between amphiphilic peptides and phospholipid membranes. *Current Opinion in Colloid & Interface Science*, 15(6), 467–478. doi:10.1016/j.cocis.2010.05.006
- Taneichi, M., Ishida, H., Kajino, K., Ogasawara, K., Tanaka, Y., Kasai, M., ... Uchida, T. (2006). Antigen Chemically Coupled to the Surface of Liposomes Are Cross-Presented to CD8 + T Cells and Induce Potent Antitumor Immunity. *Journal of immunology*, 177(4), 2324–30. Retrieved from <http://www.ncbi.nlm.nih.gov/pubmed/16887993>
- Thiele, L., Merkle, H. P., & Walter, E. (2003). Phagocytosis and phagosomal fate of surface-modified microparticles in dendritic cells and macrophages. *Pharmaceutical research*, 20(2), 221–8. Retrieved from <http://www.ncbi.nlm.nih.gov/pubmed/12636160>
- Torchilin, V. (2003). *Liposomes: A Practical Approach*. (V. Torchilin, Ed.) (2nd editio., p. 424). Oxford University Press, USA. Retrieved from <http://www.amazon.com/Liposomes-Practical-Approach-Vladimir-Torchilin/dp/0199636540>
- Torchilin, V. P., Rammohan, R., Weissig, V., & Levchenko, T. S. (2001). TAT peptide on the surface of liposomes affords their efficient intracellular delivery even at low temperature and in the presence of metabolic inhibitors. *Proceedings of the National Academy of Sciences of the United States of America*, 98(15), 8786–91. doi:10.1073/pnas.151247498
- Volpe, G., Cignetti, A., Panuzzo, C., Kuka, M., Vitaggio, K., Brancaccio, M., ... Saglio, G. (2007). Alternative BCR/ABL splice variants in Philadelphia chromosome-positive leukemias result in novel tumor-specific fusion proteins that may represent potential targets for immunotherapy approaches. *Cancer research*, 67(11), 5300–7. doi:10.1158/0008-5472.CAN-06-3737
- Watraine, O., Saadallah, I., Silva-Pires, V., Sonnet, P., & Sarazin, C. (2013). Influence of the insertion of a cationic peptide on the size and shape of nanoliposomes: a light scattering investigation. *International journal of pharmaceutics*, 454(2), 621–4. doi:10.1016/j.ijpharm.2013.05.008
- Wimmer, R., Andersen, K. K., Vad, B., Davidsen, M., Mølgaard, S., Nesgaard, L. W., ... Otzen, D. E. (2006). Versatile interactions of the antimicrobial peptide novispirin with detergents and lipids. *Biochemistry*, 45(2), 481–97. doi:10.1021/bi051876r

- Wu, H.-C., & Chang, D.-K. (2010). Peptide-mediated liposomal drug delivery system targeting tumor blood vessels in anticancer therapy. *Journal of oncology*, 2010, 723–798. doi:10.1155/2010/723798
- Xu, X., Costa, A., & Burgess, D. J. (2012). Protein encapsulation in unilamellar liposomes: high encapsulation efficiency and a novel technique to assess lipid-protein interaction. *Pharmaceutical research*, 29(7), 1919–31. doi:10.1007/s11095-012-0720-x
- Xu, X., Costa, A. P., Khan, M. a, & Burgess, D. J. (2012). Application of quality by design to formulation and processing of protein liposomes. *International journal of pharmaceutics*, 434(1-2), 349–59. doi:10.1016/j.ijpharm.2012.06.002
- Xu, X., Khan, M. A., & Burgess, D. J. (2011). A quality by design (QbD) case study on liposomes containing hydrophilic API: I. Formulation, processing design and risk assessment. *International journal of pharmaceutics*, 419(1-2), 52–9. doi:10.1016/j.ijpharm.2011.07.012
- Xu, X., Khan, M. A., & Burgess, D. J. (2012a). A quality by design (QbD) case study on liposomes containing hydrophilic API: II. Screening of critical variables, and establishment of design space at laboratory scale. *International journal of pharmaceutics*, 423(2), 543–53. doi:10.1016/j.ijpharm.2011.11.036
- Xu, X., Khan, M. A., & Burgess, D. J. (2012b). Predicting hydrophilic drug encapsulation inside unilamellar liposomes. *International journal of pharmaceutics*, 423(2), 410–8. doi:10.1016/j.ijpharm.2011.12.019
- Zaia, D., Zaia, C., & Lichting, J. (1998). Determinação de Proteínas Totais Via Espectrofotometria: Vantagens e Desvantagens dos Métodos Existentes. *Química Nova*, 21(6), 787–793.
- Zeta Potential theory. (2004). In *Zetasizer Nano Series User Manual*. England.

(Page intentionally left blank)

APPENDIX I

(Page intentionally left blank)

Table 1 – Results of mean diameter (nm) of 10 µg/mL, 20 µg/mL and 40 µg/mL of BCR-ABL peptide, in citrate-phosphate buffer at pH=4, 7.2 and 9, before and after sonication.

pH	Condition	[peptide] (µg/m)	Z-Ave (nm)	PDI	Pk 1 (nm)	Pk 2 (nm)	Pk 3 (nm)	Pk 1 (%)	Pk 2 (%)	Pk 3 (%)	Weighted Mean (nm)
4	before sonication	10	2264,0	1,0	136,6	0,3	0,0	97,6	2,4	0,0	131,3
		20	1336,0	0,8	273,7	0,0	0,0	100,0	0,0	0,0	273,7
		40	1240,0	0,8	328,7	0,0	0,0	100,0	0,0	0,0	328,7
	after sonication	10	3212,0	1,0	193,1	0,3	0,0	96,9	3,1	0,0	186,4
		20	979,4	0,7	331,4	0,0	0,0	100,0	0,0	0,0	331,4
		40	1406,0	0,8	480,9	0,2	0,0	97,6	2,4	0,0	470,9
7,2	before sonication	10	848,8	0,8	256,1	0,3	0,0	98,3	1,7	0,0	251,3
		20	773,9	0,7	159,3	413,6	0,0	86,6	13,4	0,0	199,3
		40	507,0	0,6	268,0	0,0	0,0	100,0	0,0	0,0	268,0
	after sonication	10	1110,0	0,8	229,5	0,0	0,0	100,0	0,0	0,0	229,5
		20	341,7	0,3	306,9	0,0	0,0	100,0	0,0	0,0	306,9
		40	699,2	0,6	299,1	17,2	0,0	98,1	1,9	0,0	294,1
9	before sonication	10	1630,0	0,8	204,2	0,4	19,7	94,7	2,9	2,4	189,1
		20	1206,3	0,8	224,0	17,1	1853,3	87,9	11,3	0,8	244,3
		40	485,5	0,5	139,6	29,7	0,6	74,1	22,2	3,7	101,7
	after sonication	10	382,4	0,4	59,9	12,3	0,0	87,4	12,6	0,0	53,7
		20	290,4	0,4	216,3	132,1	0,0	52,5	47,5	0,0	176,1
		40	402,5	0,4	159,2	23,5	0,0	95,6	4,4	0,0	153,2

Table 2 – Results of mean diameter (nm) of 10 µg/mL, 20 µg/mL and 40 µg/mL of BCR-ABL peptide, in citrate-phosphate (CP) and HEPES at pH=7.2, before and after sonication.

Buffer	Condition	[peptide] (µg/mL)	Z-Ave (nm)	PDI	Pk 1 (nm)	Pk 2 (nm)	Pk 3 (nm)	Pk 1 (%)	Pk 2 (%)	Pk 3 (%)	Weighted Mean (nm)
CP	before sonication	10,0	848,8	0,8	256,1	0,3	0,0	98,3	1,7	0,0	251,3
		20,0	773,9	0,7	159,3	413,6	0,0	86,6	13,4	0,0	199,3
		40,0	507,0	0,6	268,0	0,0	0,0	100,0	0,0	0,0	268,0
	after sonication	10,0	1110,0	0,8	229,5	0,0	0,0	100,0	0,0	0,0	229,5
		20,0	341,7	0,3	306,9	0,0	0,0	100,0	0,0	0,0	306,9
		40,0	699,2	0,6	299,1	17,2	0,0	98,1	1,9	0,0	294,1
HEPES	before sonication	10,0	598,9	0,6	544,0	93,7	0,0	87,8	12,2	0,0	489,0
		20,0	1275,0	0,9	390,5	37,6	1,0	80,4	13,9	5,7	317,0
		40,0	706,5	0,5	464,7	19,0	0,0	98,2	1,8	0,0	455,8
	after sonication	10,0	656,5	0,6	486,4	90,1	0,0	90,8	9,2	0,0	450,1
		20,0	973,8	0,8	383,0	67,6	0,0	82,9	17,0	0,0	269,9
		40,0	916,2	0,6	858,0	131,0	1853,0	88,6	10,8	0,6	791,1

(Page intentionally left blank)

APPENDIX II

(Page intentionally left blank)

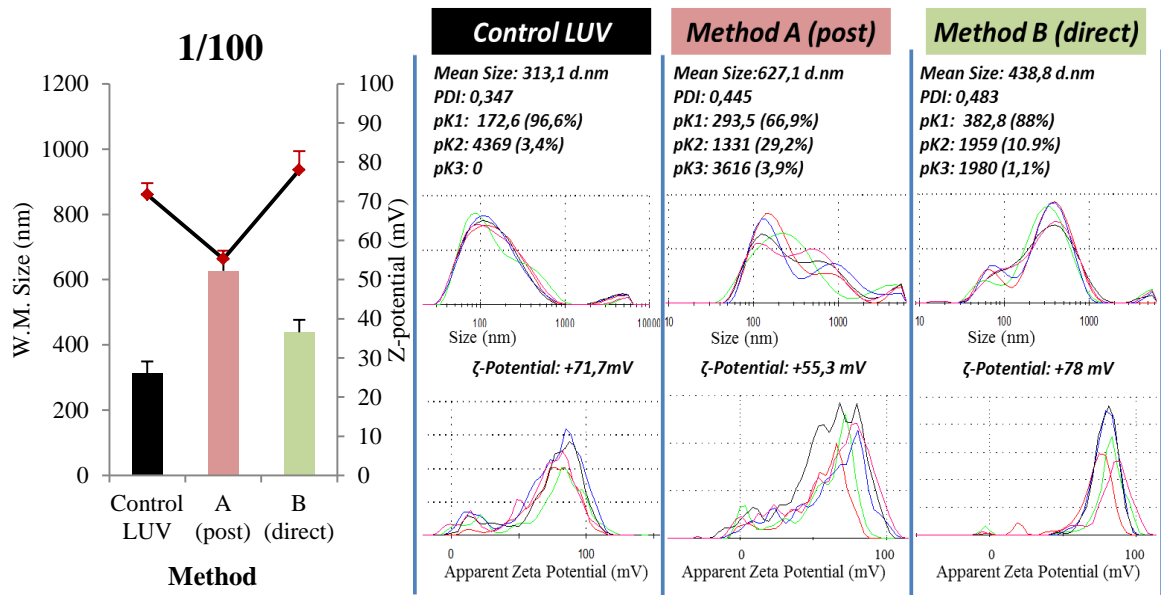


Figure 1 – At the left side are presented results of weighted mean size (nm) (bars - left axis) and z-potential (mV) (—■— - right axis) for peptide/DODAC:MO nanoparticles prepared by method A and B at 1/100 molar ratio, after extrusion. At the right side are presented the distribution of intensity profiles of the respective mean size and z-potential.

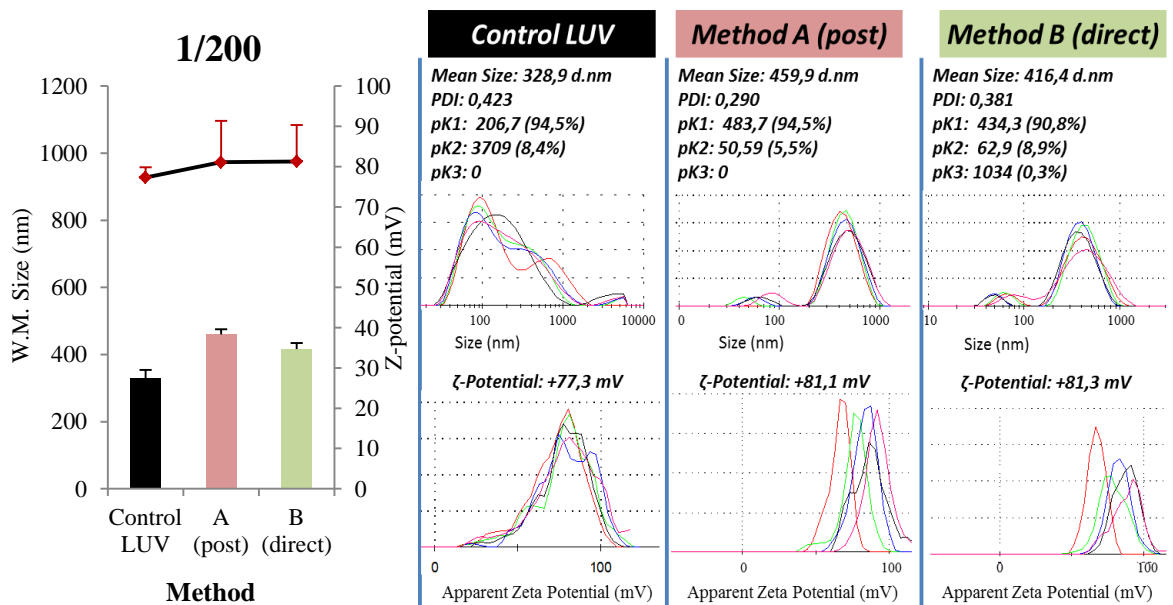


Figure 2 – At the left side are presented results of weighted mean size (nm) (bars - left axis) and z-potential (mV) (—■— - right axis) for peptide/DODAC:MO nanoparticles prepared by method A and B at 1/200 molar ratio, after extrusion. At the right side are presented the distribution of intensity profiles of the respective mean size and z-potential.

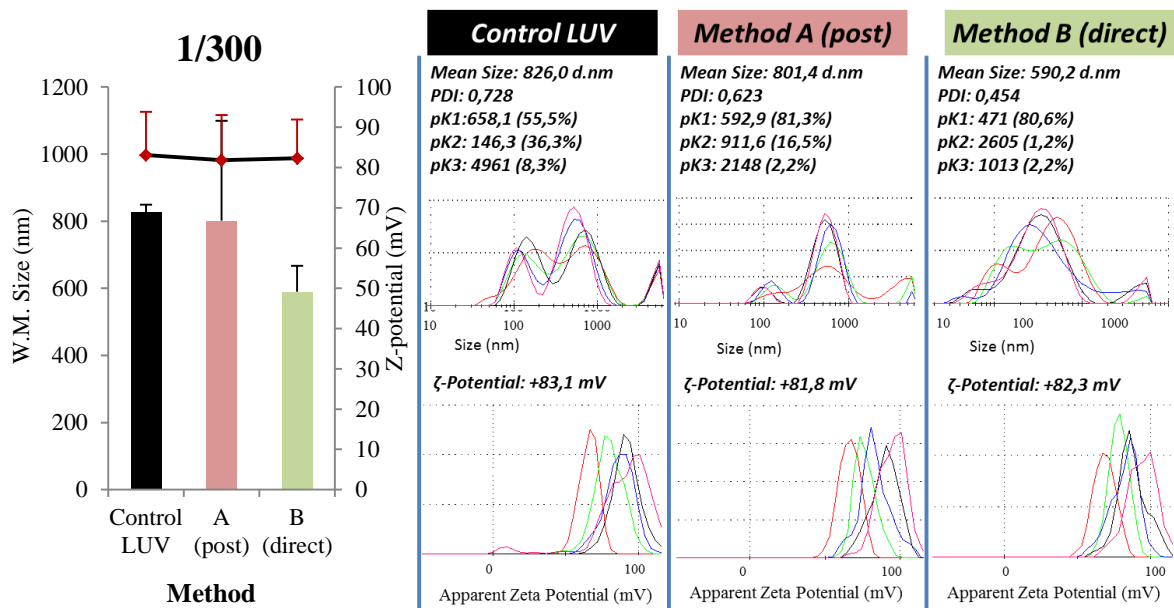


Figure 3 – At the left side are presented results of weighted mean size (nm) (bars - left axis) and z-potential (mV) (—■— - right axis) for peptide/DODAC:MO nanoparticles prepared by method A and B at 1/300 molar ratio, after extrusion. At the right side are presented the distribution of intensity profiles of the respective mean size and z-potential.

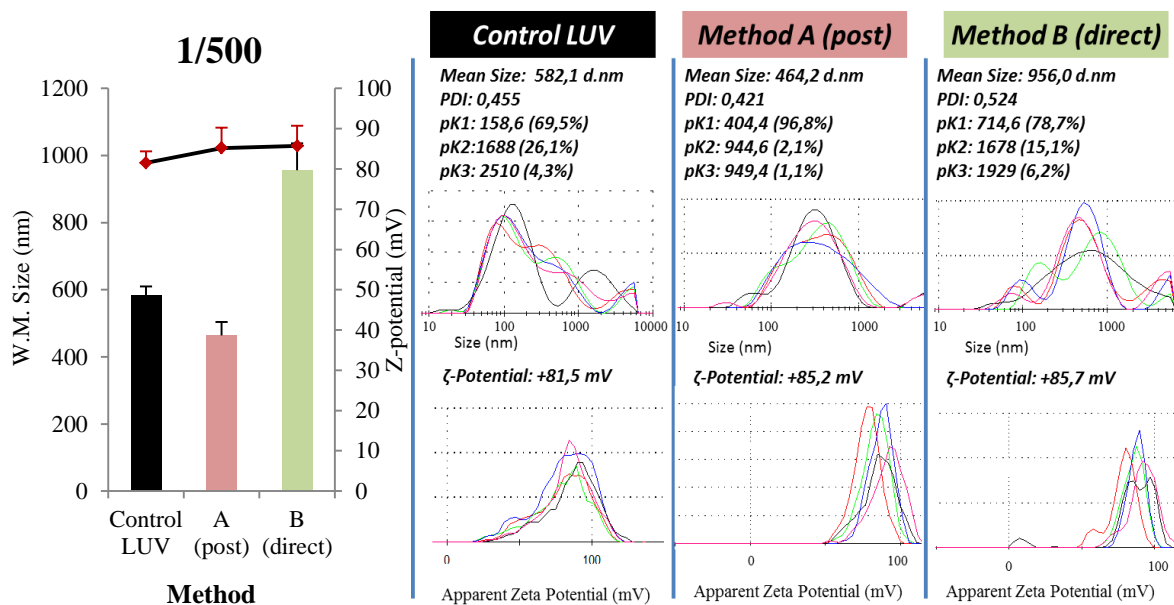


Figure 4 – At the left side are presented results of weighted mean size (nm) (bars - left axis) and z-potential (mV) (—■— - right axis) for peptide/DODAC:MO nanoparticles prepared by method A and B at 1/500 molar ratio, after extrusion. At the right side are presented the distribution of intensity profiles of the respective mean size and z-potential.

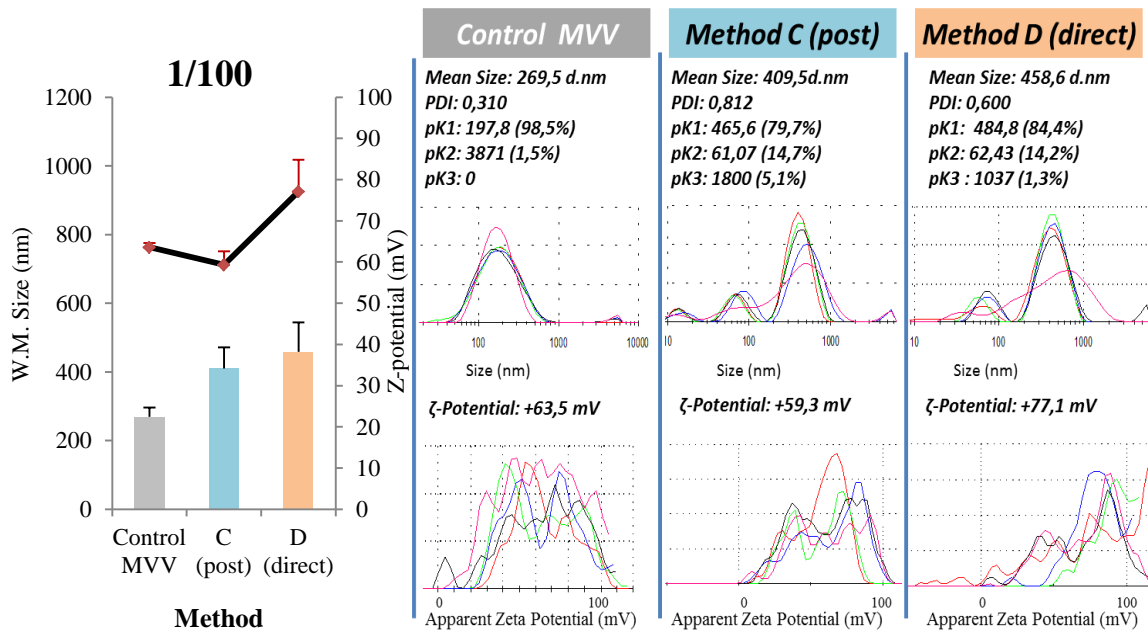


Figure 5 – At the left side are presented results of weighted mean size (nm) (bars - left axis) and z-potential (mV) (—■— - right axis) for peptide/DODAC:MO nanoparticles prepared by method C and D at 1/100 molar ratio, after extrusion. At the right side are presented the distribution of intensity profiles of the respective mean size and z-potential.

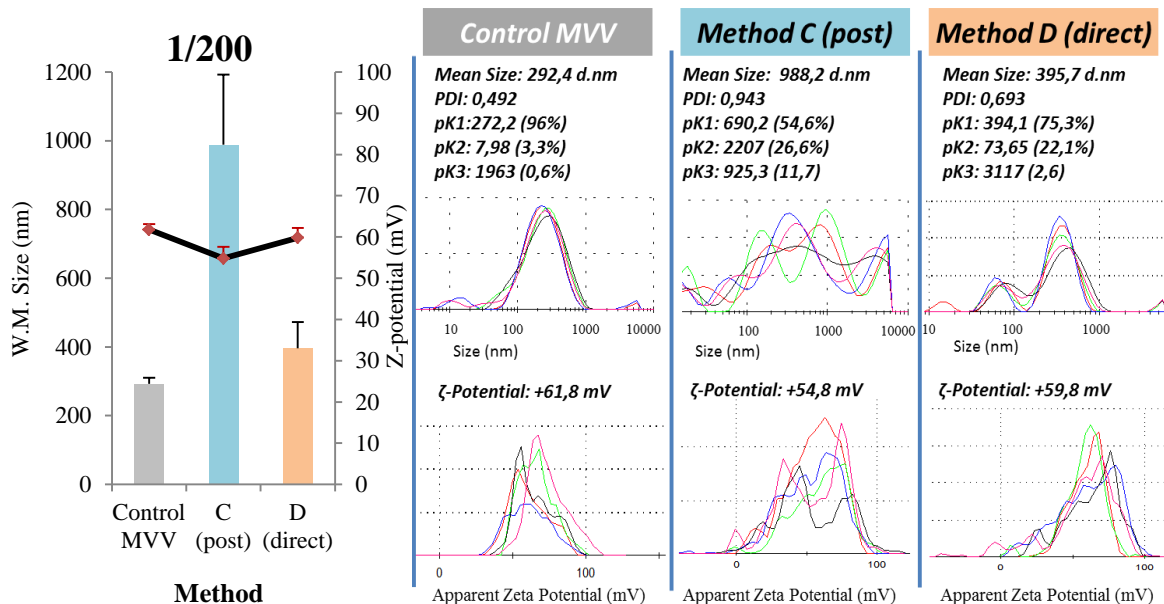


Figure 6 – At the left side are presented results of weighted mean size (nm) (bars - left axis) and z-potential (mV) (—■— - right axis) for peptide/DODAC:MO nanoparticles prepared by method C and D at 1/200 molar ratio, after extrusion. At the right side are presented the distribution of intensity profiles of the respective mean size and z-potential.

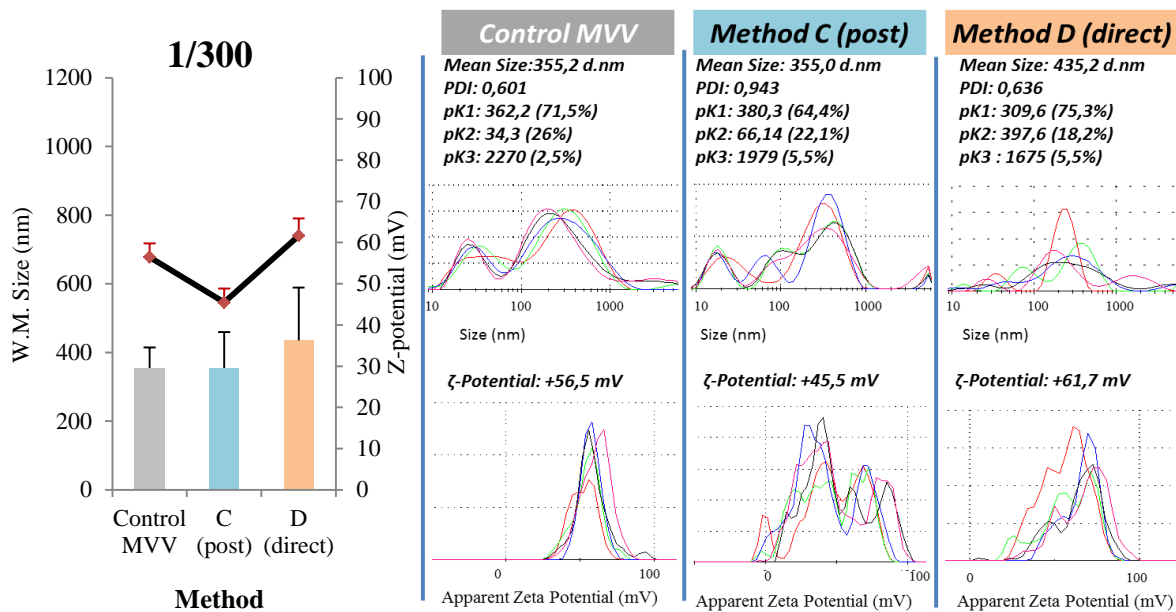


Figure 7 – At the left side are presented results of weighted mean size (nm) (bars - left axis) and z-potential (mV) (—■— - right axis) for peptide/DODAC:MO nanoparticles prepared by method C and D at 1/100 molar ratio, after extrusion. At the right side are presented the distribution of intensity profiles of the respective mean size and z-potential.

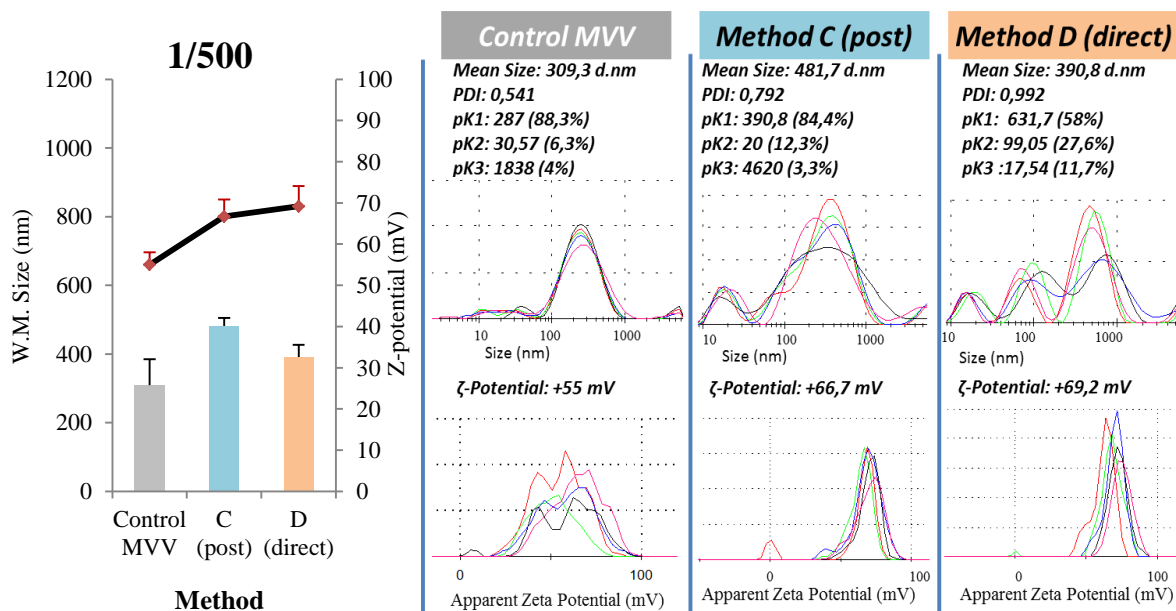


Figure 8 – At the left side are presented results of weighted mean size (nm) (bars - left axis) and z-potential (mV) (—■— right axis) for peptide/DODAC:MO nanoparticles prepared by method C and D at 1/100 molar ratio, after extrusion. At the right side are presented the distribution of intensity profiles of the respective mean size and z-potential.

APPENDIX III

(Page intentionally left blank)

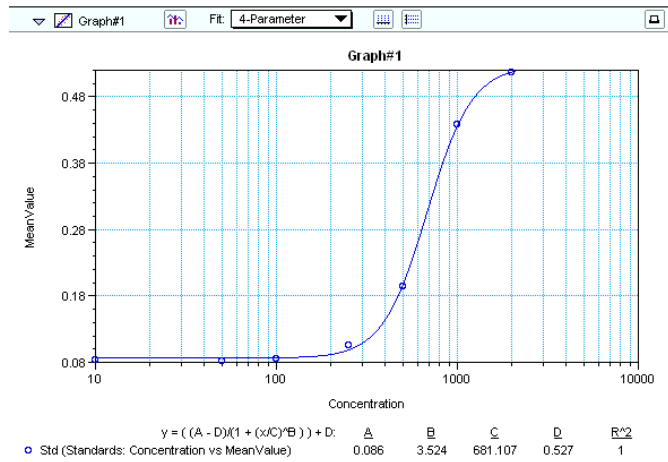


Figure 1 – Calibration curve for the optimization of the control LPS activation.

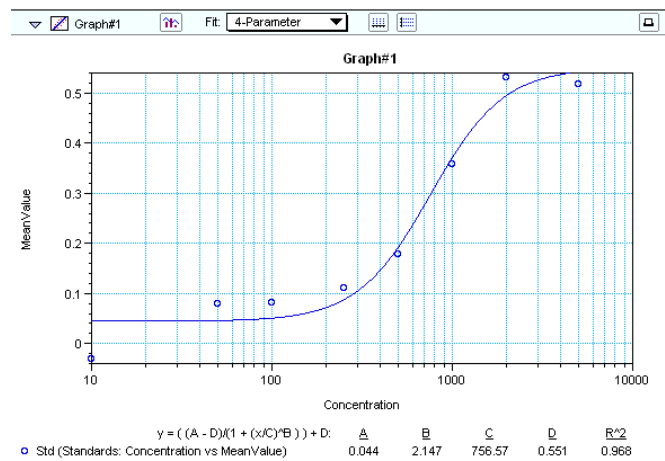


Figure 2 – Calibration curve for peptide activation assay.

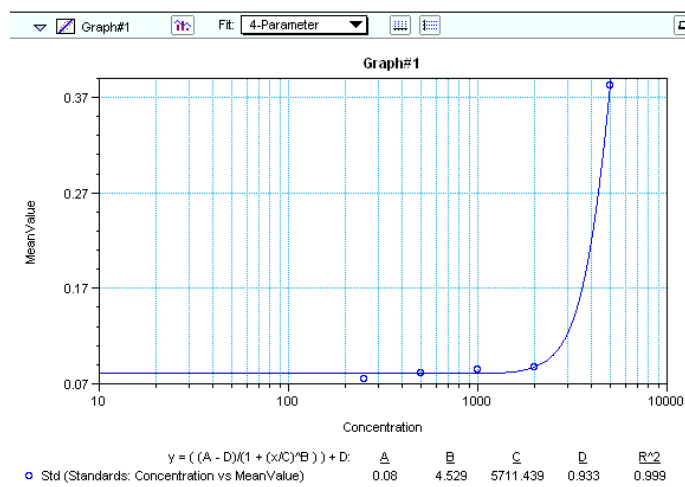


Figure 3 – Calibration curve for peptide/DODAC:MO(1:2) formulations activation assay.

Table 1 – Results optical density (O.D.) and TNF- α concentration calculated from calibration curve obtained in an ELISA reader for different conditions tested in THP-1 cells after 15 minutes of substrate incubation.

Sample	O.D.	Outliers	TNF- α (pg/mL)
Cells	0,079		Range?
	0,081		1255,98
LPS	0,419	Outlier	5209,637
Peptide	0,088		2006,068
	0,092		2234,897
E 1.75mM	0,082		1465,187
E 1.75mM	0,08		895,872
E 1.75mM	0,093		2263,481
E 1.75mM	0,079		Range?
E 1.75mM (Control)	0,078		Range?
E 1.75mM (Control)	0,074	Outlier	Range?
E 1.75mM (Control)	0,08		Range?
E 1.75mM (Control)	0,081		1187,586
E 1.05mM	0,078		Range?
E 1.05mM	0,693	Outlier	7023,044
E 1.05mM	0,077		Range?
E 1.05mM	0,078		Range?
E 1.05mM (Control)	0,078		Range?
E 1.05mM (Control)	0,08		Range?
E 1.05mM (Control)	0,071	Outlier	Range?
E 1.05mM (Control)	0,081		982,17
C 1.75mM	0,099		2481,182
C 1.75mM	0,084		1719,4
C 1.75mM	0,083		1653,145
C 1.75mM	0,079		Range?
C 1.75mM (Control)	0,075	Outlier	Range?
C 1.75mM (Control)	0,086		1928,535
C 1.75mM (Control)	0,079		Range?
C 1.75mM (Control)	0,074	Outlier	Range?
C 1.05mM	0,087		1948,934
C 1.05mM	0,211		3915,682
C 1.05mM	0,08		895,872
C 1.05mM	0,085		1804,633
C 1.05mM (Control)	0,076		Range?
C 1.05mM (Control)	0,073	Outlier	Range?
C 1.05mM (Control)	0,074	Outlier	Range?
C 1.05mM (Control)	0,079		Range?